UNIVERSITY OF
BIRMINGHAM

DIFFUSION OF BIOACTIVE MOLECULES

by

YULAN ZHANG

A thesis submitted to the
University of Birmingham
for the degree of

DOCTOR OF PHILOSOPHY

School of Chemical Engineering

The University of Birmingham

September 2012

Abstract

An artificial liposome membrane system has been employed for *in vitro* screening of the human absorption of biologically active molecules for applications in nutrition and drug treatments. Initial work with molecules having small permeabilities demonstrated that they could not be measured using the technique since they were absorbed by the membrane. A critical innovation was to pre-treat the membrane by equilibrating it with the molecule of interest since this avoids the absorption problem but required more complex data analysis. Bioactive molecules with strong antioxidant and anti-cancer activity extracted from green tea showed a strong affinity to the membrane, which suggests that this significantly limits bioavailability. Ethanol but not dimethyl sulfoxide (DMSO) was found to enhance the diffusion of paracetamol, theophylline, acyclovir, nadolol and amphotericin B. The potential synergistic effect on the diffusion of paracetamol in the presence of caffeine was investigated but it was shown to have a detrimental effect. Finally, an effective protection of Epigallocatechin-3-gallate (EGCG) from the environment was achieved by the preparation of beeswax microspheres as a carrier.

Acknowledgements

Firstly, I would like to show my deepest gratitude to my supervisors Prof. Mike Adams and Prof. Zhibing Zhang for their outstanding guidance and constant support. It is their valuable advice and inspiration that made certain that my work was to maintain a consistent standard and it is their remarkable patience that kept me motivated and encouraged when facing challenges.

I give my great thanks to Dr. James Bowen for his excellent technical supports and useful discussions which I benefit a lot, and who is always being an excellent example of a scientific researcher to me.

I would also like to give my sincere thanks to Dr. Shiping Zhu and Dr. Guoping Lian from Unilever for giving me an unforgettable industrial experience, and my gratitude extends to The School of Chemical Engineering at The University of Birmingham, Unilever, Colworth, China Scholarship Council who have provided me the precious opportunity and financial support.

I give my great thanks to Dr. Ruben Mercade-Prieto, my fellow members of my research group and the excellent staff in The School of Chemical Engineering including Hazel Jennings, Elaine Mitchell, Lynn Draper, and Kathleen Hynes for their countless help and efforts.

I would thank for my dear grandma and my parents for always being understanding and encouraging throughout my difficult time in my studies. I would also thank my boyfriend Kai Lee for his constant encouragement and his help on the MATLAB, who himself is an excellent PhD student.

TABLE OF CONTENTS

LIST OF FIGURES

LIST OF TABLES

NOMENCLATURE

A	Area cm^2
A_{UV}	UV aborbance
c	Concentration of the absorbing species mg/mL
C_0	Initial concentration, mg/mL
C_A	Concentration in the acceptor solution, mg/mL
C_D	Concentration in the donor solution, mg/mL
C_s	Saturation solubility in the matrix, mg/mL
$C_{x,0}$	Boundary concentration at $x = 0$
$C_{x,h}$	Boundary concentration at $x = h$
D	Diffusion coefficient, cm^2/s
f_2	Similarity factor
F	The oral drug bioavailability in human, %
F_a	Human absorption fraction, %
F_g	The fraction that escapes metabolism, %
F_h	The fraction that escapes first pass hepatic metabolism, %
EE	Encapsulation efficiency, %
h	Thickness, cm
I	Intensity of the transmitted light
I_0	Intensity of the incident light
k_a	Absorption constant, min^{-1}
k_r	Release constant, s^{-1}
K	Partition coefficient
K_{oct}	Partition coefficient between *n*-octanol and water
$K_{oct\text{-}alk}$	Partition coefficient of *n*-octanol and water minus alkane and water
L	Pathlength, cm

m	Mass absorbed in the membrane, mg
m'	Mass in the donor solution in the absorption experiment, mg
M_t	Amount of released drug at time t, mol
n	Number of moles
P	Permeability, cm/s
P_{app}	Apparent permeability, cm/s
t	Time, s
V	Volume of the membrane, mL
V_A	Volume of the acceptor chamber, mL
V_D	Volume of the donor chamber, mL
V'	Volume of the donor solution in the absorption experiment, mL
ε	Absorptivity
λ_{max}	Maximum absorption wavelength, nm

Abbreviations

AFM	Atomic Force Microscopy
AI	Active Ingredient
ATP	Adenosine Triphosphate
CS	Chitosan-tripolyphosphate
EC	Epicatechin
ECG	(-)-epicatechin-3-gallate
EGC	(-)-epigallocatechin
EGCG	Epigallocatechin-3-gallate
ESEM	Environmental Scanning Electron Microscopy
DLS	Dynamic Light Scattering

DMSO	Dimethyl Sulfoxide
GI	Gastrointestinal
GTC	Green Tea Catechin
HPLC	High Performance Liquid Chromatography
HPPS	High Performance Particle Sizer
MW	Molecular Weight
PAMPA	Parallel Artificial Membrane Permeation Assay
PBS	Phosphate Buffer Solution
PSA	Polar Surface Area
PSD	Particle Size Distribution
SEM	Scanning Electron Microscopy
TP	Tea Polyphenols

CHAPTER 1: INTRODUCTION

1.1 PROJECT TOPIC AND BACKGROUND

The bioavailability of a potentially active ingredient (AI) is a major concern during the design and development of products especially for the food and pharmaceutical sectors. In general, bioavailability is defined as the fraction of the AI absorbed (and not metabolised or excreted for pharmaceutical drugs) (Heaney 2001). A low bioavailability, meaning (a) a small fraction of the total AI admission is diffused and absorbed, and (b) the diffusion of the AI into the blood circulation is rather slow and limited, results in a compromised effectiveness of the AI due to the limited concentration in the circulation. For example, epigallocatechin-3-gallate (EGCG, one of polyphenols from green tea extract) with potent antioxidant and anti-cancer activity is reported to have a low bioavailability of only 1.6 % in animal tests (Henning, Niu et al. 2004; Lambert, Hong et al. 2004; Lambert, Sang et al. 2006). For those AIs with a low bioavailability, to gain a specific concentration high enough to be beneficial in the circulation, an increased dose would be required, which could also raise issues of toxicity and costs. Thus, the absorption of an AI is a critical factor if it is to be delivered orally.

In order to examine the bioavailability of an AI, the absorption rate is very often investigated by *in vivo* or *in vitro* approaches and techniques (Veber, Johnson et al. 2002). Such techniques include a permeability assay of a drug candidate, which is critical at a very early development stage to obtain an accurate prediction of the human GI absorption for eliminating those that are poorly absorbed. Permeability assays are usually required to be low cost and high throughput without sacrificing accuracy (Balimane, Chong et al. 2000). This is

particularly the case when being applied to the optimisation of the bioavailability of formulations, which inevitably involves a larger number of assays. It is thus essential to develop a low-cost and highly efficient permeability assay for an accurate prediction of the human absorption of the AI. The application of such assays could be extended to study the impact of diffusion enhancers on the permeability and synergetic effect of two or more compounds in the formulation on their permeability by using the *in vitro* model, which has not been explored extensively.

Those permeability assays that have been well studied in the pharmaceutical industry could be applied to food products, for example, tea polyphenols (TPs) as mentioned above. Improvements in enhancing the diffusion of those highly beneficial antioxidant and anticancer molecules (Yang and Wang 1993) through cell membrane is limited, despite of the awareness of their strong interactions with lipid bilayer (Sirk, Brown et al. 2009). An important factor in the bioavailability oral dosed AIs is their protection from degradation in the stomach and a common approach is to use encapsulation.

1.2 OBJECTIVES

The major objectives of this research are:

- To develop an artificial membrane system for a better prediction of human absorption, which could be extensively employed as a useful procedure to understand and mimic the *in vivo* permeation of various AIs through biological membranes, such that
    - undesirable animal tests could be avoided or reduced,

  - efficiency in drug screening at the very first stage of development could be dramatically increased and
  - it can serve as a low cost, reliable and reproducible artificial system for further investigations of a much more complex biological systems.
- To explore the application of the *in vitro* assay to the physicochemical enhancement of the molecular diffusion and the synergetic effect on the diffusion of various compounds
- To develop a method for encapsulating EGCG and investigate the *in vitro* release profile and long-term leakage of the AI

1.3 THESIS OUTLINE

The organisation of the chapters in this thesis together with brief summaries are given below:

Chapter 2 *Literature review*: the human absorption and *in vitro* assays are introduced, which inspired this work and lead to the development of the liposome membrane system. Recent research on tea polyphenols is summarised.

Chapter 3 *Materials and methods*: the material and methods to make the liposome membrane and the diffusion are introduced, and the applications of the instruments being used to characterise the liposome membrane is described.

Chapter 4 *Molecular diffusion through the liposome membrane*: the diffusion of caffeine is described as well as the absorption in the liposome membrane to establish an improved liposome membrane model.

Chapter 5 *Physicochemical enhancement of the molecular diffusion through the liposome membrane*: the results of the diffusion of five other model diffusants and the characterisation

of the liposome with/without enhancers are presented. In addition, the results are given for an investigation of the possible synergy of caffeine using the improved liposome membrane model.

Chapter 6 *The diffusion of the TPs through the liposome membrane:* this chapter summarises the results obtained using the improved liposome membrane model for the diffusion of the TPs, including the investigation of the absorption of the TPs to understand the interactions with the phosphatidylcholine.

Chapter 7 *Encapsulation of EGCG*: the method and characterisation techniques are introduced for forming beeswax microspheres of EGCG. The results of the release and leakage of the encapsulated EGCG are also described.

Chapter 8 *Discussion*: a discussion of the results in Chapter 4, 5, 6 is presented.

Chapter 9 *Conclusions*: the overall conclusions of the project and future work are presented.

CHAPTER 2: LITERATURE REVIEW

In this chapter, a brief introduction to the human absorption of molecules is made in order to explain the site of the absorption, the absorption process and the factors influencing absorption. Recent research concerning the prediction of human pharmacokinetics are summarised, particularly concerning the widely used *in vitro* assays: the parallel artificial membrane permeation assay (PAMPA) and Caco-2 model. Artificial liposome membranes are introduced as a novel promising model with a physiochemical resemblance to biological membranes and a close correlation with human absorption. In addition, a summary of epigallocatechin gallate (EGCG) and the other tea polyphenols is described including their unique antioxidant properties, their human absorption and work on the current encapsulation techniques for these active ingredients.

2.1 GASTROINTESTINAL ABSORPTION AND PERMEABILITY THROUGH BIOLOGICAL MEMBRANES

The primary absorption site for nutritional compounds and drugs in humans occurs in the gastrointestinal (GI) tract, or more specifically at the inner wall called the mucosa, which is lined with epithelial tissue. As shown in Figure 2.1 (Caceci August 2008), epithelia tissue is composed of a monolayer of columnar epithelium (the top cells) with goblet cells, located at the base membrane that is attached to the connective tissues and blood capillaries for transporting the absorbed nutrition. These epithelia cells thus serve as a major absorption barrier to nutritional compounds, drugs and other active ingredients (Pagliara, Reist et al. 1999).

All cells are enclosed by a cell membrane. Briefly, a biological membrane consists primarily of phospholipids molecules that have a hydrophilic negatively charged phosphate head group, and a hydrophobic tail comprising long fatty acid hydrocarbon chains as shown in Figure 2.2 (a). These amphipathic molecules self-assemble into bilayers in water, with their hydrophobic chains in the interior and the hydrophilic end groups in contact with the water. They enclose living cells as a multi-function boundary (Petty 1993; von Heijne and Rees 2008):

- maintain the territorial integrity of a cell or organelle
- regulate the mass transfer in and out of the cell
- relay trans-membrane signals
- perform some other important functions

[The figures are copyright of other organisations and are not available in this digital version of the thesis.

The original thesis is available for reference use in the University of Birmingham Main Library]

Figure 2.1 Schematic diagram of the columnar epithelium with goblet cells sitting on top of connective tissues: adapted from(Caceci August 2008).

The current widely accepted fluid mosaic model of a cell membrane structure was proposed by Singer and Nicholson in 1972 (see Figure 2.2 (b)) (Singer and Nicolson 1972): a sheet of phospholipids is organised as a discontinuous fluid bilayer in which globular protein

molecules (and cholesterols) are embedded. Such membranes are semi-permeable to small non-polar molecules with rapid rates of diffusion while charged molecules cannot cross the membrane barrier irrespective of their size (Rastogi 2007).

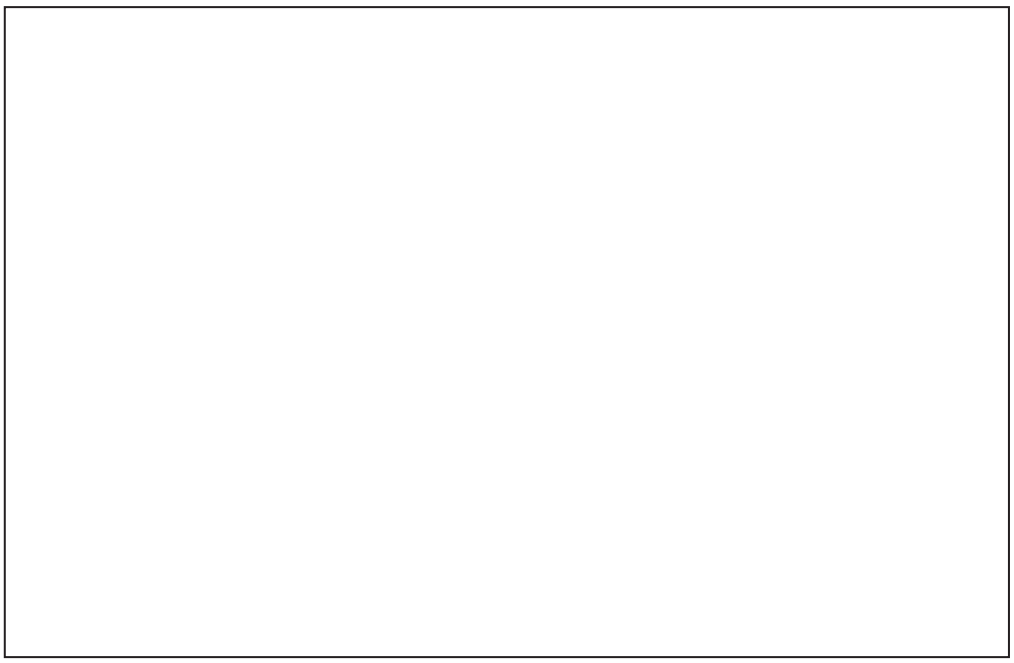

Figure 2.2 Schematic diagram of a phospholipids molecule (a) and the fluid mosaic model of a phospholipid bilayer (b) with proteins (and cholesterols) embedded in the membrane (Singer and Nicolson 1972).

Molecules can be transported across the GI tract barrier either by (a) diffusing across the barrier cells (transcellular transport) or by (b) passing through the intercellular tight junctions between the cells (paracellular transport) (Madara 1998). Most common pharmaceutical drugs traverse cellular barriers by transcellular pathways (Pagliara, Reist et al. 1999). Transcellular transport can be categorised into passive and active transport as shown in Figure 2.3:

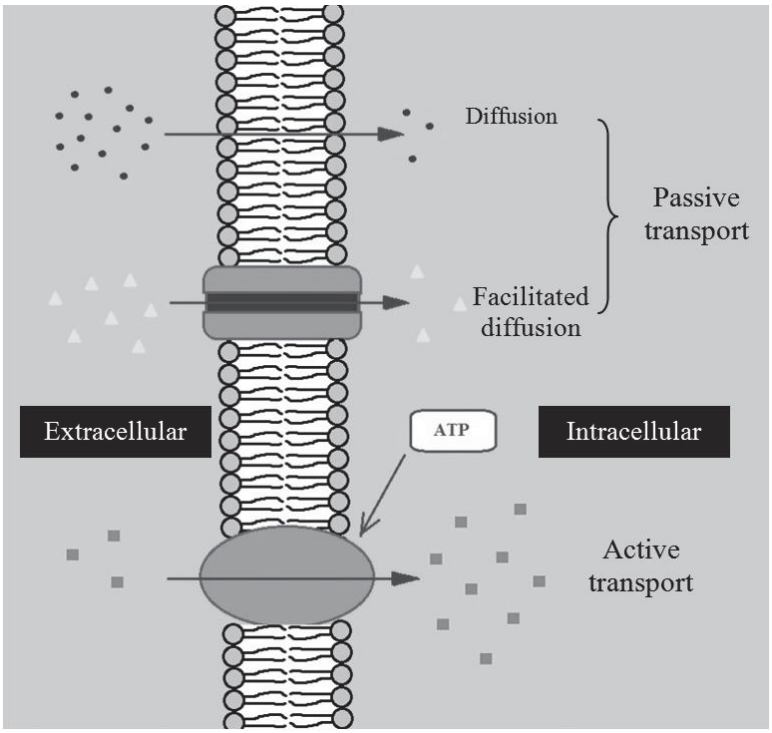

Figure 2.3 Schematic drawing of the mass transport through a biological membrane: passive transport including diffusion and facilitated diffusion, and active transport.

- Passive transport is driven by the concentration gradient of the molecules between extracellular and intracellular fluid
    - Simple diffusion through the lipid bilayer
    - Facilitated diffusion (via membrane transport proteins)
- Active transport occurs without or against a concentration gradient
    - Primary active transport: requires cell energy from the hydrolysis of ATP
    - Secondary active transport: energy that is stored in the electrochemical gradient by pumping other molecules through the membrane

It has been estimated that 80-95 % of orally administered drugs are absorbed by epithelial cells *via* a passive absorption route (Mandagere, Thompson et al. 2002). To evaluate the absorption of such drugs or other active ingredients, the oral drug bioavailability (F) in humans is defined as the rate and extent to which an active ingredient becomes available at the target sites of action. It can be expressed as: $F = F_a F_g F_h$ where F_a is the human absorption fraction, F_g is the fraction that escapes metabolism in the GI tract and F_h the fraction that escapes first pass hepatic metabolism (Cao, Gibbs et al. 2006). It is of great benefit to have a high value of F_a for obvious reasons, and the major determinants are the GI permeability and the solubility of the molecules (Dressman, Amidon et al. 1985).

Permeability is defined as the rate (cm/s) at which a molecule is transported (by passive diffusion and/or active transport) across a membrane, cell, endothelium or epithelium. Solubility here refers to the solubility of the molecule in physiological intestinal fluids (Stegemann, Leveiller et al. 2007). The factors that are important for the permeability in the GI tract will be reviewed in detail in the following sections.

2.2 PHYSIOCHEMICAL DETERMINANTS IN MOLECULAR DIFFUSION

There are two main potential mechanisms for passive diffusion: (1) the molecules are distributed into the apical cell membrane and diffuse within the membrane to the basolateral side; (2) the molecules diffuse across the apical cell membrane and enter the cytoplasm before exiting the cell across the basolateral membrane (Potts and Guy 1993; Pagliara, Reist et al. 1999). In either case, the interactions between the membrane and the diffusants are

based on their properties, which govern the diffusion process. The controlling factors for the permeability through a membrane are listed in Figure 2.4.

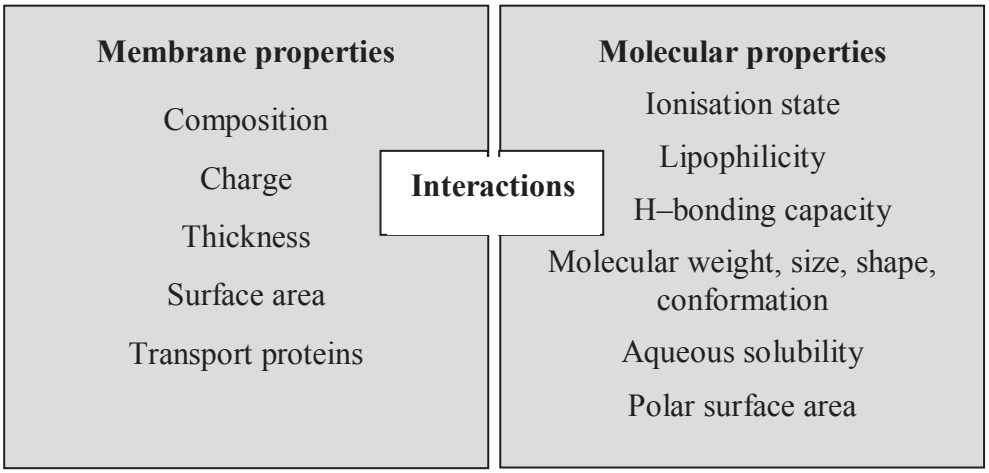

Figure 2.4 Physiochemical properties of membrane and diffusants and their interactions that determine the diffusion.

2.2.1. Physiochemical properties of the membrane

Despite the analogies of n-octanol with lipids (both have long alkyl chain and the polar hydroxyl group), the development of different solvent systems to simulate the amphiphilic characteristics of biological membranes has been carried out for lipophilicity determination and understanding the interactions involved (Pagliara, Reist et al. 1999). An increase in the chain length of the lipids causes the permeability of a membrane to protons and ions to decrease sharply (Paula, Volkov et al. 1996), indicating that the composition of the lipids has a huge impact on diffusion. Furthermore, membranes in the GI tract are complex and vary at different sites. For example, basolateral membranes (blood side of intestinal mucosal cells) are usually thinner with less cholesterol and glycolipids, thus these membrane are more fluid and permeable than apical (GI lumen) membranes (Kararli 1995). Transport proteins in the

membranes also differ throughout the GI tract (Fagerholm 2007). The small intestinal mucosa has villi structures that greatly increase the surface area for absorption (Fagerholm, Lindahl et al. 1997).

2.2.2. Physiochemical properties of the diffusants

There are a number of physiochemical properties of molecules that affect their permeability through membranes:

Lipophilicity

A major determinant of permeability by simple diffusion is the lipid solubility of the diffusants (Bonting and Pont 1981). Oral drug absorption was demonstrated to be dependent on the lipophilicity (Balimane, Chong et al. 2000) and the permeability increases with the hydrophobicity (Kamp and Hamilton 2006) as proposed by Overton (Al-Awqati 1999) which is illustrated in Figure 2.5:

C_D and C_A are the bulk concentrations in the donor and acceptor solutions, $C_{x,0}$ and $C_{x,h}$ are the boundary concentrations at $x = 0$ and h, where h is the thickness of the membrane. K is the partition coefficient (an indicator of lipophilicity) for the diffusant, which is defined as:

$$K = C_D / C_{x,0} = C_{x,h} / C_A \quad (2.1)$$

Figure 2.5 Steady-state diffusion through a homogeneous membrane of thickness of *h*: the diffusant has different solubility in the membrane and the solution (G. Giebisch 1978).

The diffusion is driven by the concentration gradient between $C_{x,0}$ and $C_{x,h}$, which are equal to C_D and C_A when K is 1, as shown in the dash line.

For diffusants that have a different solubility in the bulk solution to that in the membrane (G. Giebisch 1978):

$$C(x) = KC_D \text{ at } x = 0 \tag{2.2}$$

$$C(x) = KC_A \text{ at } x = h, \tag{2.3}$$

The driving force for $K = 2$ is then twice that when $K = 1$, while it is a factor two less for $K = ½$, which means that the diffusion flux would be greater for those molecules with a greater value of K. Therefore, a considerable work has been carried out to correlate the permeability with the partition coefficient in different solvent systems such as *n*-octanol-water (Potts and Guy 1992; Lombardo, Shalaeva et al. 2001), propylene glycol dipelargonate (Leahy, Taylor et al. 1989); and liposome systems (Choi and Rogers 1990; Pauletti and Wunderliallenspach 1994). This was established as a convention for predicting human absorption but it is now recognised that the use of only K_{oct} is an over-simplification of a complex process and thus cannot be entirely sufficient (Bonting and Pont 1981; Balimane, Chong et al. 2000).

Ionisation state

While an ionisable molecule may diffuse through a membrane, there are several other forces acting upon it in distinct regions in a biological membrane (Bordi, Cametti et al. 2000):

- the two highly polar interfacial regions influenced by the different aqueous media
- relatively disordered hydrocarbon chain regions in the centre of the bilayer

In general, the transport of ions is considerably slower compared with non-ionised molecules (Hauser, Stubbs et al. 1972; Kobayashi, Komatsu et al. 2004), since the unionised form has a higher lipophilicity than the ionised form (Watkinson, Herkenne et al. 2009).

The pH of the medium influences diffusion (Pagliara, Reist et al. 1999; Wohnsland and Faller 2001) as it determines the ionisation state as well as the solubility of the diffusant. The mean

pH in the human stomach, duodenum, jejunum and ileum is 1.3, 6.5, 6.6 and 7.4 (Horter and Dressman 2001).

H-bonding capacity

The hydrophilic part of lipids having hydrogen-bonding acceptor groups will bind with the hydrogen-bonding donor groups of diffusants, thus retarding the diffusion of such molecules (Pagliara, Reist et al. 1999). It is well established that hydrogen bonding is one of the major factors influencing diffusion through biological membranes (Young, Mitchell et al. 1988; Conradi, Hilgers et al. 1991; Platts 2000). Permeability was calculated and predicted from the number of possible hydrogen-bonds by simply counting:

- the hydrogen-bond acceptor atoms: oxygens and nitrogens
- the hydrogen-bond donor atoms: hydrogens attached to oxygen and nitrogen

or by obtaining the value of log $K_{oct\text{-}alk}$ (n-octanol-water minus alkane-water) as a measure of the hydrogen-bonding capacity (Eltayar, Tsai et al. 1991).

Molecular size, weight, shape and conformation

It has been shown that with increasing molecular size, the 'sieving effect' of a membrane becomes dominant compared with the influence of the electrical field (Adson, Raub et al. 1994). The diffusion coefficients of molecules crossing a membrane have been reported to be highly dependent on their molecular weight (MW) (Walter and Gutknecht 1986; Xiang and Anderson 1994; Bunge and Cleek 1995). Prolate molecules tend to adhere to a membrane rather than diffuse (Fischer, Kansy et al. 2007). Molecular flexibility and the potential

conformational variability will also influence diffusion (Pagliara, Reist et al. 1999) so that a cell membrane will discriminate between straight chains and branched isomers (Finkelstein 1976). Lipinski presented a simple 'rule of five': low absorption is more likely for molecules with log K_{oct} > 5, MW > 500 g/mol, hydrogen-bond acceptors > 10 and donors > 5 (Lipinski, Lombardo et al. 1997).

Polar surface area

Polar surface area (PSA) refers to the surface area of the polar atoms of a diffusant, which is an important predictor of the bioavailability and could be a dominating determinant for oral absorption drugs that are transported by the transcellular route (Kelder, Grootenhuis et al. 1999). For example, a high PSA was reported to have a negative impact on intestinal absorption (Palm, Stenberg et al. 1997; Clark 1999). Since most of the major contributors to the PSA are hydrogen bond donors or acceptors, there is a close correlation between the PSA and the sum of those hydrogen bond donors and acceptors (Veber, Johnson et al. 2002).

2.3 PREDICTION OF GASTROINTESTINAL ABSORPTION

Taking account of (a) preclinical screening including *in vitro*, *in vivo* assays, formulation and stability evaluation and safety assessment, (b) clinical trials, (c) human bioavailability and (d) regulatory approval, the time-to-market for a pharmaceutical formulation containing a potentially viable novel drug molecule usually takes more than 10 years (Kraljevic, Stambrook et al. 2004). Effective preclinical screening techniques would accelerate the drug discovery and development processes by increasing the success rate above the current mean

value by at least 21.5% and, consequently, it would result in major cost savings (DiMasi 2002; Garrett, Walton et al. 2003). Many methods including *in vivo* and *in vitro* have been explored to predict human absorption and a close correlation exists between permeability and the fraction of drug absorbed in the same species (Lennernas 1997; Lennernas 1998; Cao, Gibbs et al. 2006; Fagerholm 2007).

2.3.1. Prediction of gastrointestinal absorption from animal test

Rats have been widely used for *in vivo* assays: a high correlation between F_a values in rats and human has been reported (Chiou and Barve 1998), which supports this approach for predicting human absorption (Fagerholm, Johansson et al. 1996; Zakeri-Milani, Valizadeh et al. 2007). Monkeys and pigs are also commonly used in drug development (Chiou and Buehler 2002; Fagerholm 2007). It should be noted that the difference in the intestinal radius (a factor of ten) is greater than the difference in intestinal permeability (a factor of 3.6) between humans and rats, and gastric emptying is slower in humans, therefore absorption is expected to be less efficient in humans (Fagerholm 2007).

2.3.2. Prediction of gastrointestinal absorption from Caco-2 cell line and 2/4/A1 cell line

The Caco-2 cell model is commonly used for screening/estimation of permeability and prediction of human F_a (Artursson, Palm et al. 2001). These cell lines express several morphological and biochemical characteristics of small intestinal enterocytes with microvilli on the apical side and tight junctions between adjacent cells (Pinto, Robineleon et al. 1983).

Caco-2 cells have been cultivated on a filter membrane (Sambuy, Angelis et al. 2005), and the insert with the cells placed in culture wells to carry out diffusion measurements as shown in Figure 2.6. A high correlation of the permeability of the Caco-2 membranes with human absorption has been obtained (Hilgers, Conradi et al. 1990; Artursson and Karlsson 1991), making it a widely used prediction tool. However the Caco-2 cell line was found to have a very tight monolayer compared with the human small intestine as it originated from the colonic carcinoma cell line (Grasset, Pinto et al. 1984). Consequently, the results from Caco-2 are not useful for molecules with low permeability. It was also reported that Caco-2 has a poor correlation with human absorption for molecules that involve active transport (Irvine, Takahashi et al. 1999; Parrott and Lave 2002; Fagerholm 2007). However, 2/4/A1 cells have been shown to be a more effective mimic of the epithelial barrier to passive drug transport *in vivo* (Matsson, Bergstrom et al. 2005). Nevertheless, the cells are sensitive to changes in the culture temperature that may introduce variability in terms of the formation and integrity of the cell monolayer, and they lack the proteins for active transport (Tavelin, Taipalensuu et al. 2003).

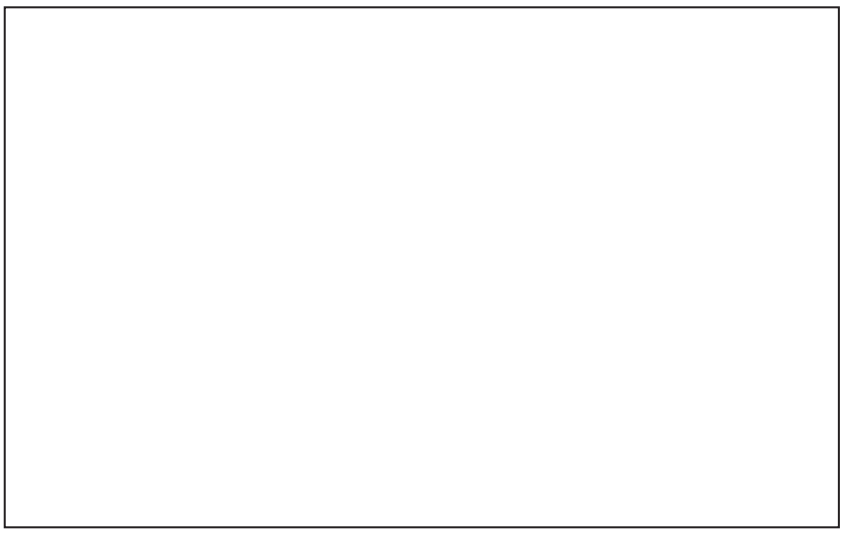

Figure 2.6 Diffusion through Caco-2 in culture wells: the diffusant are dissolved in the donor chamber of the insert with Caco-2 cell. It was then placed in culture wells as an acceptor chamber to carry out diffusion (Cyprotex 2012).

2.3.3. Prediction of gastrointestinal absorption from artificial membrane assay

Artificial membranes are *in vitro* assays that are not based on animals or cells. They have been widely used for permeability involving passive diffusion as they lack transporter proteins. The first parallel artificial membrane assay (PAMPA) was proposed by Kansy *et al* (Kansy, Senner et al. 1998), which is a rapid and simple test of the diffusion through a filter membrane coated with lecithin dissolved in organic solvent as shown in Figure 2.7. The permeability results showed a close correlation with human absorption and it is a high throughput technique that enables drug screening to be much more effective and economical. Developments include the use of a hydrophilic filter membrane (Zhu, Jiang et al. 2002), the selection of alternative phospholipids and solvents (Sugano, Nabuchi et al. 2003; Corti, Maestrelli et al. 2006) and the construction of a lipid/oil/lipid tri-layer in the filter membrane (Chen, Murawski et al. 2008) to obtain a better correlation of the permeability from PAMPA and human absorption.

Figure 2.7 PAMPA diffusion through a filter membrane coated with phospholipids. The diffusant is dissolved in the donor chamber and transported through the membrane into the culture wells. (Cyprotex 2012).

Generally PAMPA is a much better predictor for oral absorption than log K_{oct}, and is similar to Caco-2 for passive diffusion. However, it is not suitable for active transport prediction and the success of using PAMPA in drug discovery depends on careful data interpretation and use of optimal assay condition (Avdeef, Bendels et al. 2007).

2.3.4. Alternative methods for prediction of gastrointestinal absorption

There are a number of alternatives to *in vivo* assays using artificial membranes for predicting human absorption, for example, the measurement of the permeability either through isolated intestinal tissues from animals/human, or by organ perfusion (Stewart, Chan et al. 1997). In addition, *in-silico* methods have been used to model the relationships between the molecular properties (their interactions with the membrane) and permeability or human absorption. (Lee, Ayyarnpalayarn et al. 2007). This approach has a good predictability but it is highly dependent on the quality of the parameters used in the modelling (Fagerholm 2007).

2.4 INTRODUCTION OF THE LIPOSOME MEMBRANE AS AN ARTIFICIAL MEMBRANE ASSAY

Bangham and co-workers (Bangham, Hill et al. 1974) introduced the use of a liposome to more realistically mimic the lipid bilayer structure of biological membranes for passive diffusion (Stein 1986). A liposome is a vesicle with an outer bilayer of amphiphilic phospholipids molecules with bulk water in the core as shown in Figure 2.8, thus it has a morphological and physiochemical structure of biological membrane.

Figure 2.8 Schematic drawing of a liposome, a phospholipid molecule and cell membrane (Dhatfield 2008; UK 2011).

While the octanol-water partition constant is still widely used, it is increasingly being replaced by liposomes as a surrogate for biological systems as a more effective molecular descriptor (Escher, Schwarzenbach et al. 2000). Liposomes have been immobilised by entrapment in the pores of gel beads as a chromatographic model system to correlate the capacity of the drug retention with human absorption (Lundahl and Beigi 1997). However, liposome may be deposited onto a substrate membrane to form a tight barrier for molecular permeation with the permeability being obtained by a similar procedure to that adopted for PAMPA (Flaten, Bunjes et al. 2006; Flaten, Dhanikula et al. 2006; Flaten, Skar et al. 2007; Flaten, Luthman et al. 2008). The results of the permeability were claimed to be better than the conventional PAMPA and comparable to Caco-2 with a strong correlation between permeability values and human absorption involving oral administration. Nevertheless, the permeability of those moderately and poorly absorbed molecules were not distinguished clearly and a few of the molecules were incorrectly predicted to have poor bioavailability in the human GI tract.

2.5 TEA POLYPHENOLS AND THE ENCAPSULATION TECHNIQUES

2.5.1. Tea polyphenols

Tea is widely consumed globally and is considered to be beneficial to human health due to the biologically active tea polyphenols (TPs), also called green tea catechins (GTC) (Yang, Chung et al. 2000). TPs constitute about 30-42% of the dry weight of the solids in brewed tea (Balentine, Wiseman et al. 1997), including (-)-epigallocatechin-3-gallate (EGCG), (-)-epigallocatechin (EGC), (-)-epicatechin-3-gallate (ECG), and (-)-epicatechin (EC) as shown in Figure 2.9. ECGC is the major catechins in tea, which accounts for more than 10 % of the total TPS. (Balentine, Wiseman et al. 1997).

The scavenging activity of the TPs is related to the number of o-dihydroxy and o-hydroxyketo groups, C_2-C_3 double bonds and their concentration, solubility and the stability (Dufresne and Farnworth 2001). Thus ECG and EGCG have the highest radical scavenging activity (Henning, Fajardo-Lira et al. 2003), such as antioxidant and antitumor activities (Higdon and Frei 2003; Kuzuhara, Suganuma et al. 2008). Other benefits of EGCG have also been studied including the protection of the skin from UV radiation-induced damage (Katiyar, Elmets et al. 2007) and in the treatment of HIV infection (Yamaguchi, Honda et al. 2002; Nance and Shearer 2003; Hamza and Zhan 2006; Williamson, McCormick et al. 2006; Ma, Xia et al. 2007). Due to these health benefits of the TPs, their human absorption has been investigated which showed low bioavailabilities of 0.2 to 2.0 % (dose-dependent) for EGCG, EGC and EC (Nakagawa, Okuda et al. 1997; Pietta, Simonetti et al. 1998).

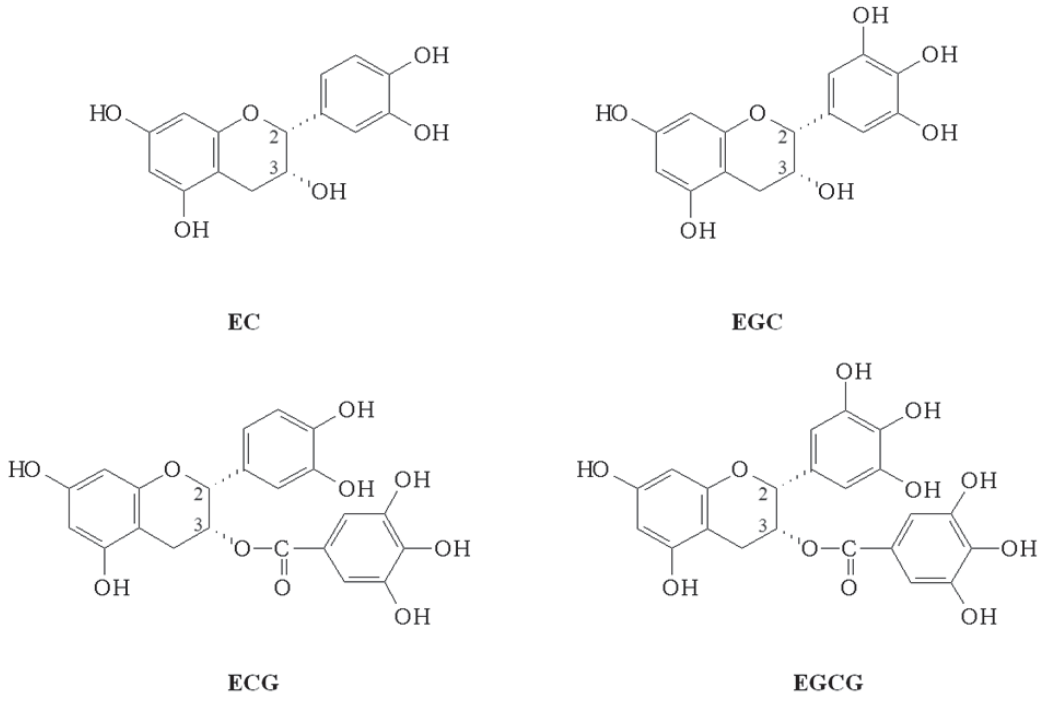

Figure 2.9 Chemical structure of the tea polyphenols.

2.5.2. Stability of the TPS

Due to the presence of the phenolic hydroxyl group, when TPs are exposed to light, heat and oxidants, they can be rapidly oxidized (Friedman, Levin et al. 2009). The stability of tea theaflavins and catechins have been carefully examined in various solutions and drinks by Chen's group (Chen, Zhu et al. 2001; Su, Leung et al. 2003). Over 96% of GTC remained in water at 24 ^{o}C while 29% was destroyed at 70 ^{o}C after being heated for 3 h. The stability of GTC is considerably dependent on pH and is much more unstable when the pH is > 6. According to research carried out by Henning *et al.* (Henning, Niu et al. 2004), TPs are more bioavailable when delivered as encapsulated green tea extract than when taken as a traditional

beverage. Therefore it is beneficial to encapsulate TPs in order to stabilise them during storage as well as to enhance the human absorption.

2.5.3. Encapsulation of the TP

Encapsulation is a technique by which one material or a mixture of materials is coated with or entrapped within another material system (Madene, Jacquot et al. 2006). The purpose of encapsulation is summarised as follows: (1) to protect the core material from the environment (*e.g.* heat, light, moisture) while allowing small molecules to diffuse through the coating (this has been widely applied to the pharmaceutical and food industries as a way to improve the stability of some sensitive products such as vitamins and enzymes) (Dziezak 1988)); (2) to acquire a controlled release of the core material or to release the core at specific locations and times, such as some baking additives, and (3) to achieve a uniform dispersion of the core material into a host material when only very small amounts are required (Desai and Park 2005).

There are two basic forms of capsules as shown in Figure 2.10: microcapsules, which are have core/shell structures, and microspheres, which are also referred to as 'matrix' encapsulation. For different applications, both forms can be employed and more complicated forms can be designed. For food and pharmaceutical applications, the coating materials are required to not only provide protection to the ingredients or drugs from the environment and a controlled release in the gastrointestinal (GI) track, but also to be food grade so as not to have adverse side-effects to the human body.

The encapsulation of TPs has received considerable attention recently because of their excellent scavenging activity in spite of a low oral bioavailability and a short half-life due to the strong systemic clearance (Cai, Anavy et al. 2002). The incorporation of TPs into certain carriers can overcome their instability and provide a better delivery to the human intestine. Hu *et al.* (Hu, Pan et al. 2008) investigated the polyanion-initiated gelation process in fabricating chitosan-tripolyphosphate (CS-TPP) nanoparticles as carriers for delivering TPs, with a mean diameter of 129 nm. They identified some governing parameters including the contact time, CS molecular mass, CS concentration, CS-TPP mass ratio, initial pH value of the CS solution, and the concentration of tea catechins, which have a range of effects on encapsulation efficiency and their release profile.

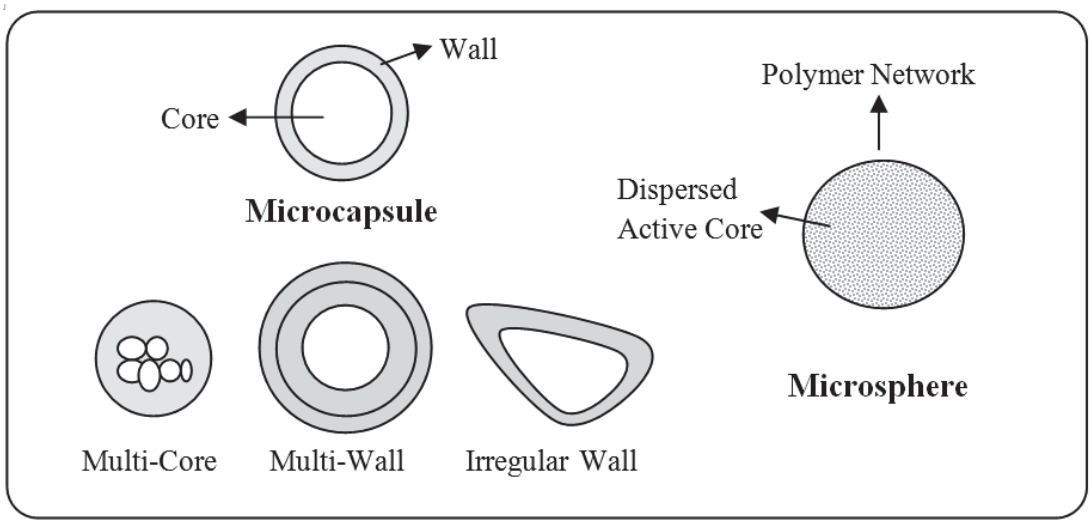

Figure 2.10 Various structures of microcapsules produced by different process.

Fang et al. (Fang, Lee et al. 2006) used a liposome to encapsulate EGCG in order to increase accumulation of the EGCG in basal cell carcinomas; the sizes of the particles varied from 104 to 378 nm with the process involving different surfactants or extrusion.

Recently beeswax was used to prepare drug loaded microspheres due to its good stability at varying pH and moisture levels, well established safe application in humans, minimal effect on food in the GI tract and no dose dumping (Ranjha, Khan et al. 2010). Beeswax is a natural product used in the pharmaceutical, cosmetics, food and other industries. However, among the reported conventional methods, the manufacturing process involves the use of a toxic solvent, which is undesirable in terms of environmental factors and human safety. Thus a more promising and simple technique was introduced to prepare wax microspheres using a meltable dispersed emulsified cooling induced solidification method (Gowda, Ravi et al. 2009) as shown schematically in Figure 2.11.

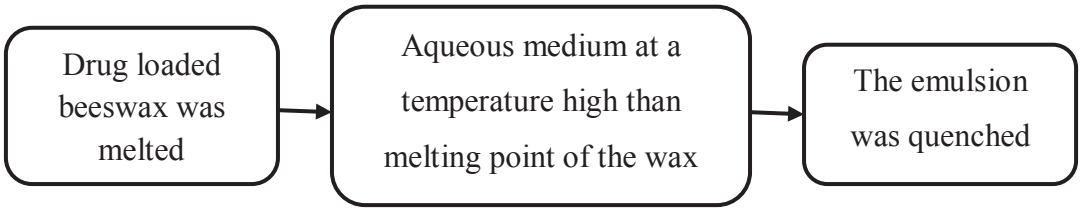

Figure 2.11 The preparation method of wax microspheres.

2.6 DISCUSSION

Permeability assays are usually required to be low cost and high throughput without sacrificing accuracy. This aim is particularly the case when being applied to the optimisation of the bioavailability of formulations, which inevitably involves a larger number of assays. As reviewed in this chapter, permeability assays vary in their nature and thus lead to different prediction results. Table 2.1 summarises the advantages and limitations of the major three widely used assays.

Table 2.1 Advantages and limitations of different permeability assays for prediction of human absorption.

Permeability Assay	Advantages	Limitations
Animal testing	Direct *in vivo* methods Good correlation with human absorption	Cruel, inhuman High cost and material consuming Labour intensive
Cell line assays	Predict both passive and active diffusion Good correlation for moderate and highly absorptive molecules	Variation of the results from different cell line origins (Sambuy, Angelis et al. 2005) Poor correlation for molecules with low absorption (Irvine, Takahashi et al. 1999)
PAMPA	Rapid, simple and high throughput A complementary method to predict human GI absorption (Chen, Murawski et al. 2008)	Limited ability to predict human absorption A poorly characterised system for a simple classification of molecules (Pagliara, Reist et al. 1999)

Due to its rapid and simple procedure, artificial membrane assays are particularly useful and successful in drug discovery and development to prioritise compounds for *in vivo* studies and pre-drug screening. In order to improve the performance of predicting human absorption, the use of a liposome deposited on a membrane was introduced with its morphological resemblance to biological membrane (Flaten, Dhanikula et al. 2006). However, there were

important factors that might result in errors in the determination of the permeability. Firstly, there was an initial time lag before steady state diffusion occurred that probably arose from the time involved in the partitioning of the diffusant into the liposome membrane. The complication of identifying the lag time was ignored and the permeability was only calculated from the last four time points of the diffusion. It is particularly a problem for compounds having a high partition coefficient since it can result in a false 'zero' permeability due to a large proportion of the compound being absorbed by the membrane. Secondly, the permeation procedure was incremental (Flaten, Dhanikula et al. 2006), which involved transferring the donor solution of the diffusant at a given time to a fresh acceptor chamber that it was considered as a steady state under sink conditions. However the influence of the decrease in the concentration in the donor chamber and the increase in the acceptor chamber with time was not considered.

Despite the issues mentioned above, the use of a liposome membrane is a promising *in vitro* technique for predicting human GI absorption since a reasonable correlation has been found by Flaten *et al* (2006). The first part of the current work was to improve the experimental and data analysis procedures based on a more rigorous theoretical treatment of the system. The mass absorption was investigated and the permeability measurements were carried continuously rather than incrementally. A mathematic model was used to calculate accurate values of the permeability and the results were compared with those published from *in vivo* human GI absorption studies.

The second part of the current work was then carried out to use the established method for permeability measurements and physiochemical enhancement of the molecular diffusion of the model diffusants (including acyclovir, amphotericin B, caffeine, nadolol, paracetamol and theophylline) by ethanol and DMSO, the most potent permeation enhancers in the literature (Williams and Barry 2004; Rebecca Notman 2006). These molecules were selected since it had been established that they diffuse passively through cell membranes (Pagliara, Reist et al. 1999; Zhu, Jiang et al. 2002).

EGCG and the other TPs were investigated using the improved liposome membrane model, since their permeability through artificial membrane or improving their human absorption has not been studied previously. Attempts were made to enhance the permeability of EGCG by changing the ionisation state as it could influence both aqueous solubility and permeability (Lee, Ayyarnpalayarn et al. 2007),

Finally, a major challenge of encapsulation of EGCG is that it has active phenolic hydroxyl groups and they can only be stabilised in solution at pH values of <5. It turns out that the particular property of this core material greatly limits the selection of an edible wall material to meet the special requirements here. Beeswax is used in the current work as a protection material to prepare microspheres of EGCG as it is inert and a natural food grade product.

2.7 SUMMARY

The morphology of biological membranes and different transport routes of molecules through such membranes were introduced in this chapter. To predict the human absorption in the GI tract, a variety of *in vivo* and *in vitro* assays were reviewed and an artificial liposome membrane was selected as a high-throughput screening tool due to its morphological properties and good prediction of human absorption. Moreover, factors that influence the permeability were summarised including the physiochemical enhancement of diffusion that can be made by considering these determinants.

It is concluded that the challenges based on the existing literature are to improve the experimental and data analysis procedures for a better prediction of the diffusants including TPs, and to obtain an enhanced diffusion for improved human absorption. More work is required to enhance the stability of TPs such as EGCG, for example, to provide protection from the environment or the delivery formulation.

CHAPTER 3: MATERIALS AND METHODS

In this chapter, the detailed description of materials and methods will be described in three sections: firstly liposome membrane was made and caffeine was chosen as a model molecule for evaluating the liposome membrane in order to obtain an improved *in vitro* assay. The following section involves further work on the investigation of the molecular diffusion through the liposome membrane with five model diffusants. This section also includes the physicochemical enhancement of diffusion using the liposome protocol. The third section considers the use of the liposome membrane to measure the diffusion of four tea polyphenols, and the attempts made to increase the extent of diffusion of EGCG.

3.1 MOLECULAR DIFFUSION THROUGH THE LIPOSOME MEMBRANE

3.1.1. Materials

3.1.1.1. The egg phosphatidylcholine, the model molecules and the reaction chemicals

Egg phosphatidylcholine (Lipid E-80), a kind gift from Lipoid, Germany, was chosen due to its appropriate phase transition temperature (~ -8 ^{o}C) that enables the experiment to be carried out under ambient conditions. The chemical structure of the egg phosphatidylcholine is shown in Figure 3.1. Caffeine (ReagentPlus®, powder) was purchased from Sigma, U.K.

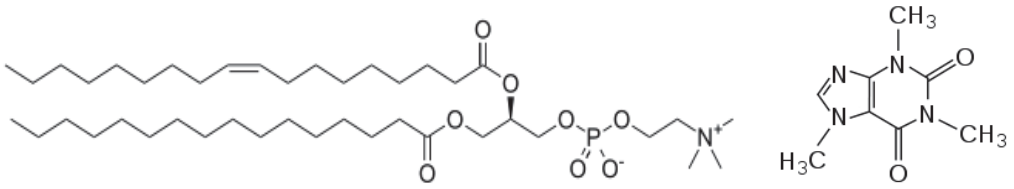

(a) **(b)**

Figure 3.1 Chemical structure of (a) egg phosphatidylcholine, with a hydrophilic phosphate head and the hydrophobic tail constituted by long fatty acid hydrocarbon chains and (b) caffeine.

Well culture plates (PIMWS2450), swinnex filter holder (25 mm in diameter), 0.4 and 0.8 μm polycarbonate membrane filters, and 0.65 μm cellulose ester membrane filters were purchased from Millipore (U.K) Ltd as shown in Figure 3.2 and Figure 3.3. The 0.4 and 0.8 μm polycarbonate membrane filters were used to obtain specific target sizes of the liposome. The cellulose ester membrane filter, which is hydrophilic, was used as a supporting membrane since a hydrophobic supporting membrane has a tendency to resist the permeation of hydrophilic or ionised compounds (Zhu, Jiang et al. 2002).

Figure 3.2 The 24 well culture plate from Millipore.

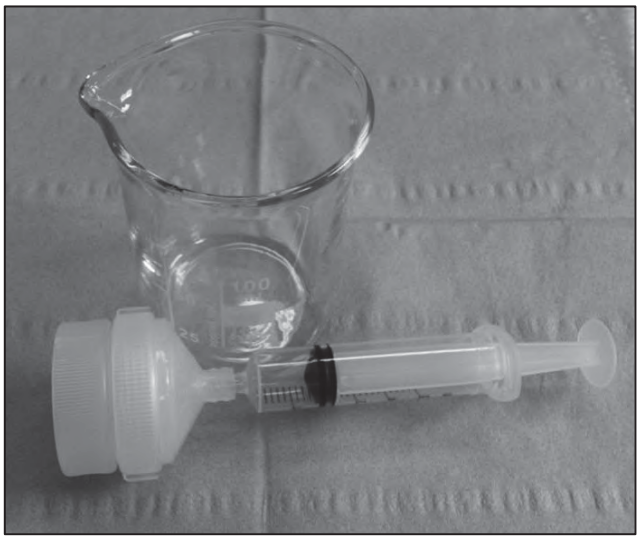

Figure 3.3 The Swinnex filter holder fitted with disposable syringe.

3.1.1.2. Donor chamber

The donor chamber was designed and made by Longshore Systems Engineering, UK. It includes a punch tool, sets of inserts, and an insert locking tool. The punch tool was designed for cutting the cellulose ester membrane with a diameter of 9.5 mm to be used as the substrate membrane as shown in Figure 3.4 (a) and (b). The inserts are 316L stainless comprising two parts: the outer part has three supporting 'feet' for stability while immersed in the culture plate with sufficient space for mass transfer in solution; the inner sleeve is used for clamping the 0.65 μm filter membrane between the outer and the inner parts as shown in Figure 3.4 (c) and (d). The exposed area at the lower end of the insert has a diameter of 8.0 mm. The locking tool shown in Figure 3.4 (e) locks the two parts of the inserts tightly with the membrane between them (Figure 3.4 (f)). The insert/membrane assemblies were located in centrifuge tubes for further preparation.

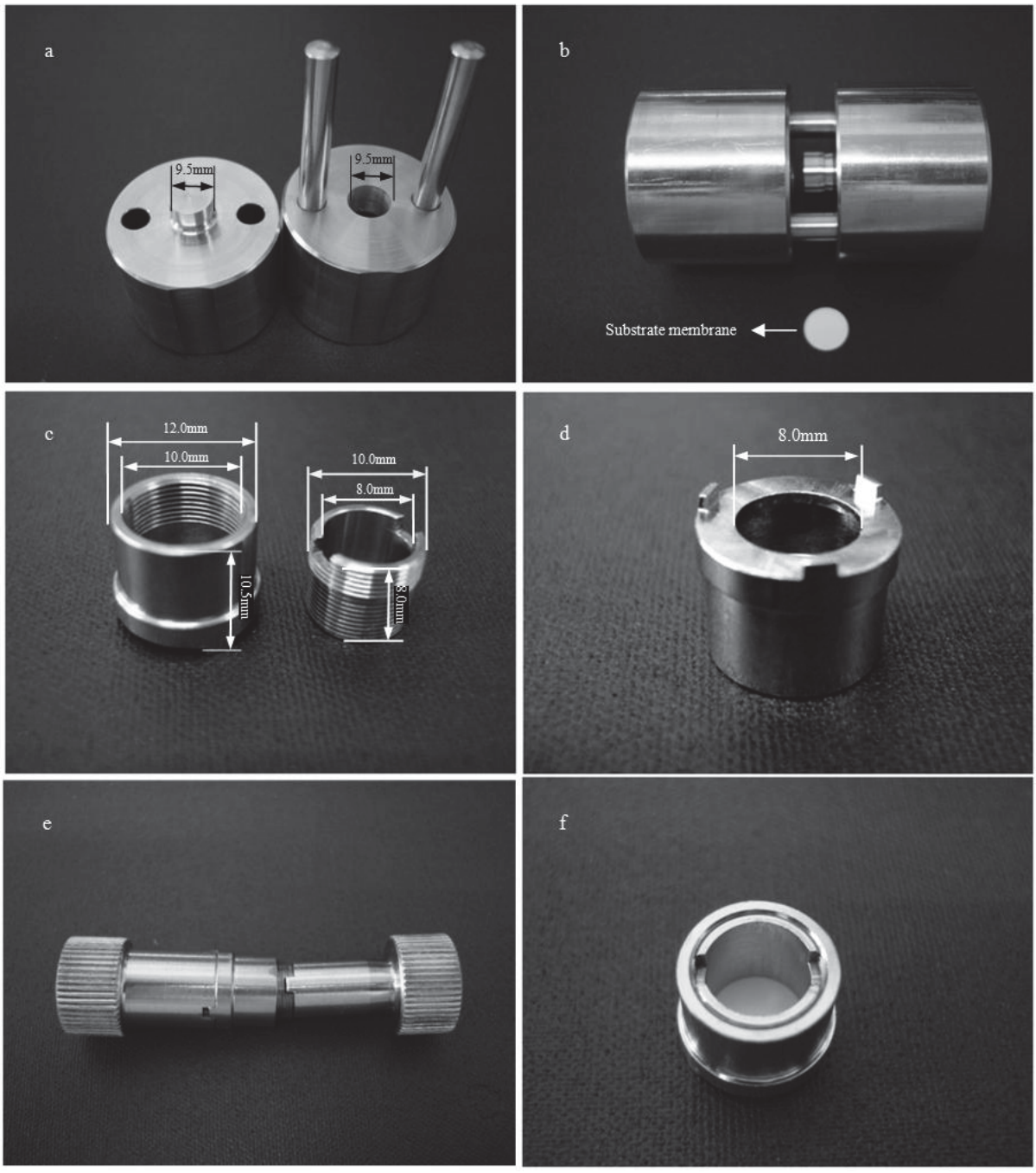

Figure 3.4 The donor chamber kit consists of a punch tool (a) and (b), an insert made of the outer and the inner part (c) and (d), a locking tool (e). The donor chamber with the membrane locked between the two parts is shown in (f).

3.1.2. Manufacture technique of the liposome membrane

3.1.2.1. Formation of the liposome suspension

Egg phosphatidylcholine was dissolved in chloroform and methanol (2:1 v/v) in a round-bottom flask followed by evaporation at about 50 ^{o}C to obtain a thin film of the lipid. A 6% (w/v) liposome suspension was formed using a vortex mixer (Fisherbrand Vortex Mixer ZX Classic) by hydration of the film with a phosphate buffer solution at pH 7.4, as illustrated in Figure 3.5. The suspension was then extruded through 0.8 μm polycarbonate membrane filters to obtain the desirable size of liposome, and some of those liposome was further extruded through 0.4 μm polycarbonate membrane filters for even smaller liposome.

3.1.2.2. Manufacture of the liposome membrane

A 0.1 mL aliquot of the liposome suspension that had been extruded through a 0.4 μm filter was added to the insert/membrane assembly followed by a centrifugation (Sigma swing centrifuge) at 2000 rpm for 4 min in order to impregnate the liposome into the pores of the substrate membrane as illustrated in Figure 3.6. This was repeated with a fresh aliquot of the liposome but centrifuged for 10 min instead. The inserts were then transferred into an incubator at 50 ^{o}C for 45 min. A 0.1 mL aliquot of the liposome suspension that had been extruded through a 0.8 μm filter was then added to the insert following the incubation and centrifuged at 2000 rpm for duration of 90 min. Most of the liposome suspension did not penetrate the membrane and the supernatant liquid was removed by inverting the inserts followed by centrifugation for 5 min at 300 rpm. The inserts with the liposome membranes were then freeze-thawed and stored in a refrigerator at 3°C for at least 12 h.

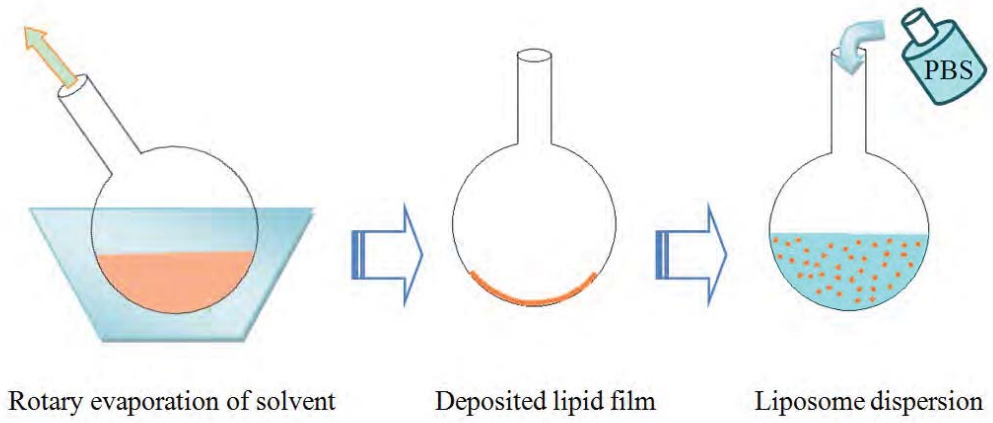

Figure 3.5 Formation of the liposome suspension.

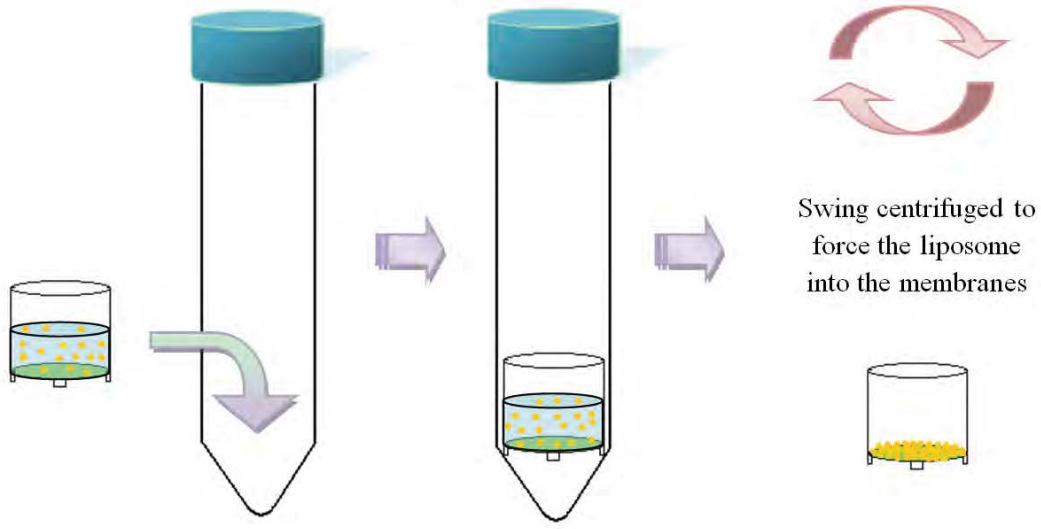

Figure 3.6 Illustration of depositing the liposome onto the substrate membrane clamped in the insert by centrifugal force.

3.1.3. Size measurement of the liposome

A Malvern ZetaSizer High Performance Particle Sizer (HPP5001, Malvern instruments Ltd, UK) was used for the measurement of the particle size distribution (PSD) of the liposome after extruding through the 0.8 and 0.4 μm polycarbonate filters (Figure 3.7). The measurement technique is based on dynamic light scattering (DLS) such that the intensity of the scattered light fluctuates at a rate that is dependent on the size of the particles as smaller particles are 'kicked' further by the solvent molecules and move more rapidly (Malvern 2012). The particle size could then be analysed by the intensity fluctuations induced by the Brownian motion of the particles in the suspension, according to the Stokes-Einstein relationship. The Malvern HPPS with a Non-Invasive Back-Scatter technology, is capable of a wide size range from 0.6 to 6000 nm and a high sensitivity for both low and high concentrations, and can perform measurements in the temperature range 10-55^{o}C. Thus it is suitable for an immediate measurement of the size distribution of the liposome suspension after the extrusion.

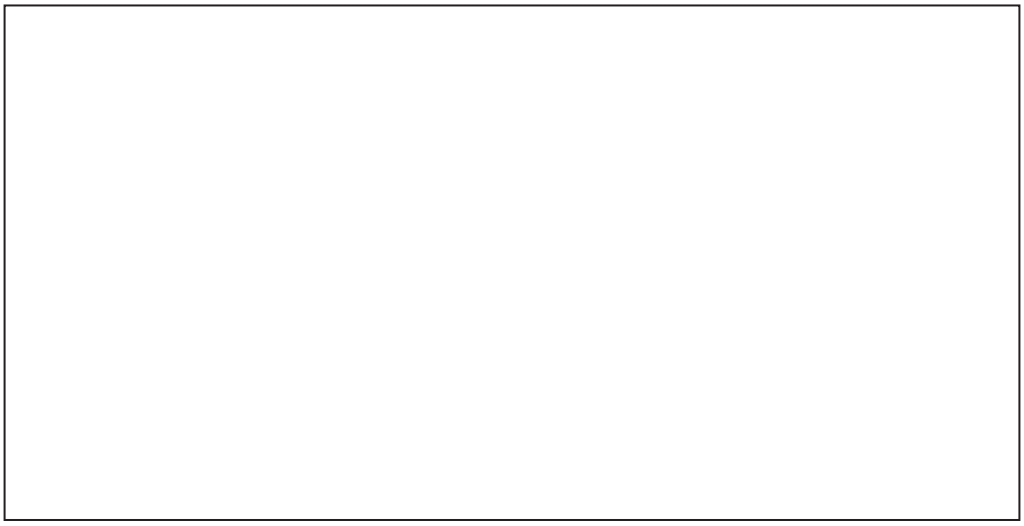

Figure 3.7 Malvern ZetaSizer HPPS (HPP5001, Malvern instruments Ltd, UK) and its optical system (Malvern 2012).

To investigate the influence of the extrusion on the size: liposome samples were extruded through the 0.8 μm polycarbonate filter for 5, 10, 15 and 20 times. Those subject to 10 repeated extrusions were further extruded through the 0.4 μm polycarbonate filter for 5, 10, 15, 20 times. Aliquots of the samples were then taken into disposable cuvettes for the measurement in the HPPS (viscosity 1.0383 cP, refractive index 1.345 (Tester, Brock et al. 2011)). The measurements were repeated for all the samples after intervals of 2 and 24 h to examine the stability of the liposome. All of the measurements were performed in triplicates and the size distribution was represented by a plot of the relative intensity of light scattered by particles in various size classes.

3.1.4. Characterisation of the liposome membrane

3.1.4.1. Morphology characterisation of the liposome membrane by cryo-SEM

Since a conventional scanning electron microscope (Semenov) may cause a wet and fragile sample shrink, distort or even be damaged, an ESEM (Philips XL-30 FEG Environmental SEM with Oxford Inca EDS) with Cryo stage (PolarPrep 2000 cryo-stage system) was used to observe the morphological characteristics of the liposome membrane (Quorum 2001). The cryo-method enables vulnerable biological structures to be well preserved and a clean cryo-fractured cross-section without malformation may be obtained.

The hydrated liposome membrane was firstly mounted on a flat disc holder, which is itself mounted on to a freezing/vacuum transfer rod. It was then plunge frozen in liquid nitrogen to -140 °C and transferred under vacuum onto the cool stage of the cryo-SEM preparation chamber of the PolarPrep 2000. The liposome membrane was then fractured and coated with

metal by sputtering. Finally the specimen was transferred under vacuum into the ESEM chamber where it was maintained at -140 °C, and the cross-section of the liposome membrane was examined at 3.00 kV.

3.1.4.2. Lipid assay of the liposome membrane

The quantitative determination of the phospholipid in the liposome membrane could be achieved by lipid assay (LabAssay Phospholipid, Wako Chemicals, GmbH, Germany). It is based on the following chemical reactions: the phospholipid is hydrolysed to choline by phospholipase D and then the so formed choline is oxidised by choline oxidase in a reaction that produces hydrogen peroxide, which causes DAOS and 4-Aminoantipyrine to undergo a quantitative oxidative condensation catalysed by peroxidise (POD), producing a blue pigment as shown in Figure 3.8. The amount of phospholipids in the sample could thus be determined by measuring the absorbance of the blue colour in a UV spectrophotometer.

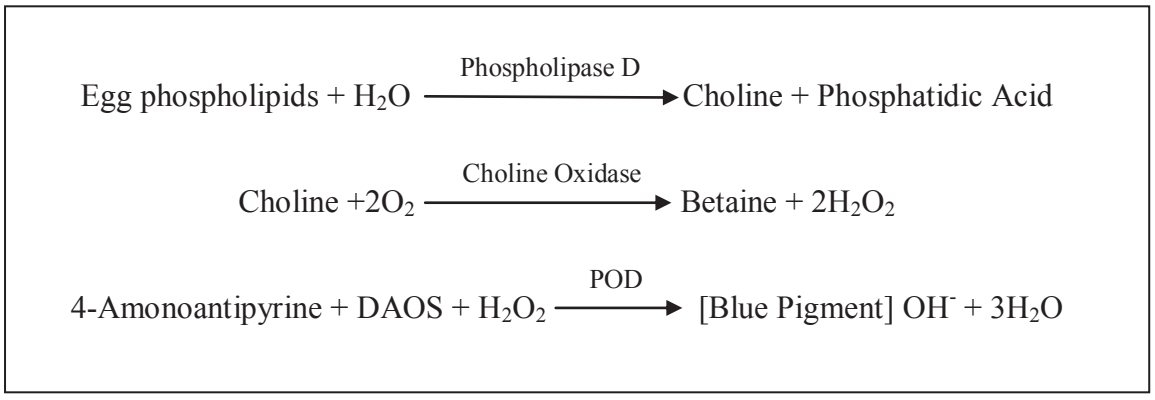

Figure 3.8 The chemical reaction of the colour reagent with egg phospholipids for UV measurement.

A calibration was first carried out of the liposome: the egg phospholipid liposome suspension was prepared in the phosphate buffer solution (pH 7.4) at 1.5, 3.0 and 6.0 mg/mL in a culture plate (PIMWS2450, Millipore Ltd, UK) and well mixed with the colour reagent, which was prepared by dissolving 1 vial of Chromogen substrate to 50 mL of buffer (50 mmol/L Good's buffer, pH 7.5, provided by Wako LabAssay kit). They were then placed in an oven (MINO/50, Genlab Ltd, UK) at 37 ^{o}C for 5 min. The solution was then measured by the UV spectrophotometer (CE 2021 Spectrophotometer, Cecil instrument, England) at a wavelength of 600 nm. All the measurements were performed in triplicates and an average absorbance was plotted as a function of the concentration with standard error bars.

To perform the lipid assay on the liposome membrane, a freshly prepared liposome membrane was incubated in 5 mL of 2 mg/mL cholate solution (BioReagent, Sigma-Aldrich, UK) under bath sonication (Ultrasonic bath, Fisherbrand, Fisher Scientific, UK) for 45 min to solubilise the phospholipids in the substrate membrane. The solution was then well mixed with the colour reagent and incubated at 37 ^{o}C as described previously, followed by measurement in the UV spectrophotometer. The measurements were performed in triplicates to obtain the amount of phospholipid molecules in each liposome membrane.

3.1.4.3. UV spectra of the model diffusant

A UV spectrophotometer (CE 2021 Spectrophotometer, Cecil instrument, England) was used in this work to obtain the concentration of the sample solutions. UV spectrophotometers are widely used for measuring the concentration of a liquid sample: they are based on the principle that when a molecule is exposed to UV with an energy that matches the electronic

transition within the molecule, the energy will be absorbed to cause the electron to jump to a higher energy orbit, which typically occurs in the region of ultraviolet spectrum (200-380 nm) (Mehta 2011; Straube, Aicher et al. 2011).

Basically a UV spectrophotometer consists of an energy source, a sample cell, a dispersing device (prism or grating) and a detector, arranged as shown in Figure 3.9. The detector records the wavelengths at which absorption occurs and the degree of absorption at each wavelength as shown in Figure 3.10.

The absorbance of a sample is proportional to the concentration and path length given by:

$$A = log\ (I_0/I) = \varepsilon\ c\ L \tag{3.1}$$

where A is the measured absorbance, I_0 is the intensity of the incident light at a given wavelength, I is the transmitted intensity, L is the pathlength through the sample, c is the concentration of the absorbing species and ε is a constant for a species defined as the molar absorptivity or extinction coefficient (Mehta 2011). A calibration of the standard solution of the model diffusant was then carried out and the absorbance at λ_{max} was plotted as function of the concentration to obtain the absorptivity ε.

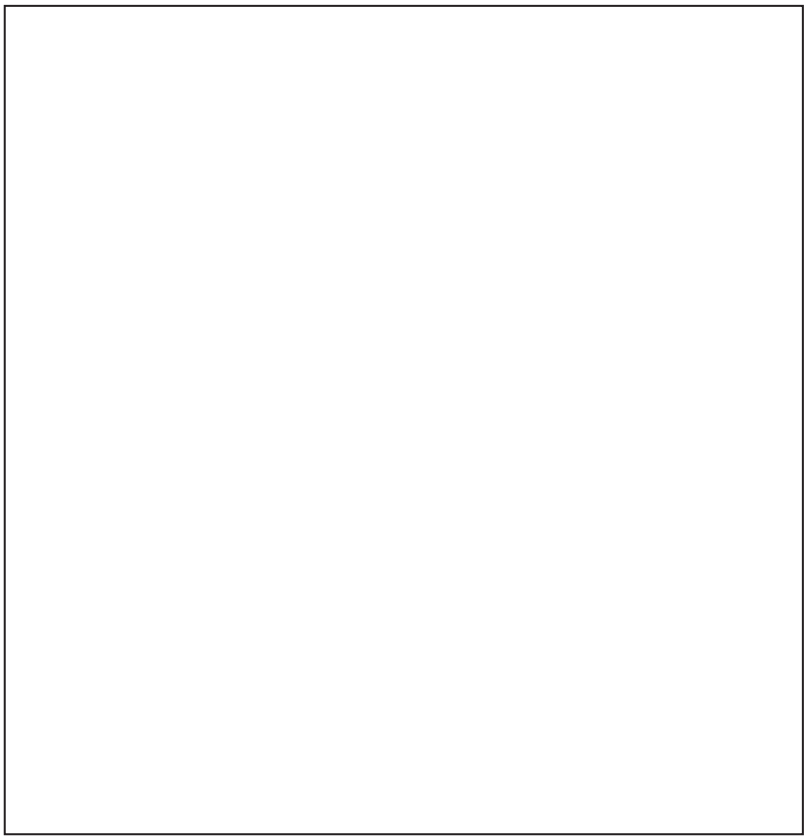

Figure 3.9 A CE 2021 UV Spectrophotometer and its optical system (Field, Sternhell et al. 2008).

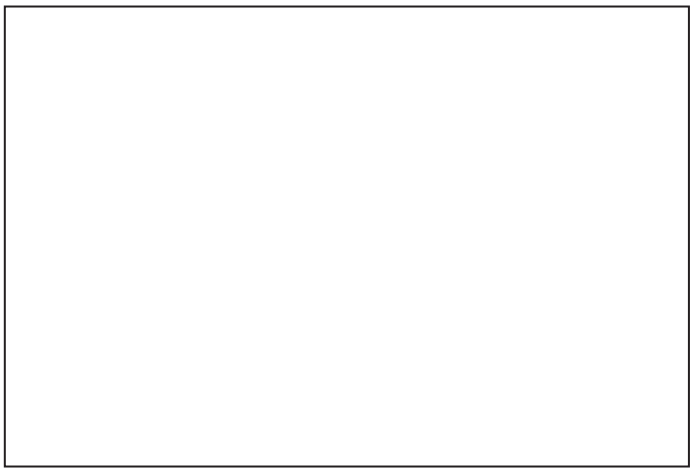

Figure 3.10 Absorbance curve of UV spectrophotometer (Field, Sternhell et al. 2008).

3.1.5. Permeability measurements

For the *incremental diffusion* method, each diffusant of a given quantity was dissolved in a phosphate buffer solution (PBS) at pH 7.4 and 0.1 mL of the solution was added into an insert as the donor chamber. In addition, 0.6 mL of the PBS solution was added into the wells of culture plates that acted as the acceptor chambers. The donor chamber was then placed carefully into a well, to ensure that bubbles were absent (Figure 3.11), and inserted into fresh acceptor chambers at a 0.5 h or 1 h intervals. This method was modified in the current work to avoid a small UV absorption (see below) for some diffusant as well as to establish a continuous diffusion profile within 5 h. The *continuous diffusion* method involved five donor chambers (pre-treated or untreated) that were placed at the same time in five acceptor chambers. One donor chamber was removed at hourly intervals over a period of 5 h. For both methods, the concentrations in the acceptor chambers were measured using a UV spectrophotometer (CE 2021 Spectrophotometer, Cecil instrument, UK). All experiments were performed in triplicates and the mean concentration was plotted as a function of time with standard errors.

3.1.5.1. Influence of pre-treatment and agitation on the permeability of caffeine

The inserts with the liposome membrane were immersed in 0.7 mL of the donor solution for 1 h, then removed from the solution and carefully dried with a tissue to extract the any trace of visible liquid. Both the incremental and continuous diffusion of a 1.51 mg/mL caffeine solution in the donor chamber were measured with these pre-treated membranes and the results were compared with those that were untreated.

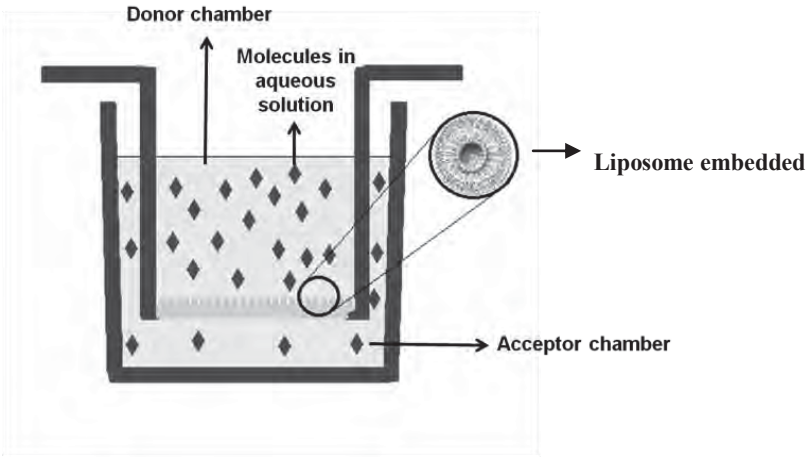

Figure 3.11 Schematic diagram of the liposome membrane permeability assay: model molecules were dissolved in the PBS in the insert as the donor chamber. The molecules diffused through the liposome membrane into the wells of the culture plate as the acceptor chamber that contained PBS solution.

The effect of agitation was examined using two such pre-treated membranes for a 10.00 mg/mL caffeine solution in the donor chamber. The results for an unagitated condition were compared with those that were agitated using a shaking incubator (L12425 New Brunswick G25 cooled orbital incubator) set at 100 rpm.

3.1.5.2. Influence of pre-treatment time and donor concentration on the permeability of caffeine

The liposome membranes were pre-treated with a 10.00 mg/mL donor solution of caffeine for 1, 5, 16 and 24 h respectively. The membranes were also pre-treated for 1 h with donor solutions of caffeine with concentrations of 0.50, 1.51, 10.00 and 20.00 mg/mL. The diffusion was then carried out in a continuous way and repeated for three times.

3.1.6. Mass absorption measurements

It was not possible to measure accurately the mass absorption of the caffeine using only a single membrane due to the very small amount of absorption. Therefore, three liposome membranes were immersed in 2 mL of 1.51 mg/mL aqueous caffeine solution. Aliquots of 10 µL were taken for UV absorption measurements at intervals of 10, 20, 30, 60 min; these aliquots were negligibly small (0.5 %) compared with the total volume and, consequently, would not significantly affect the results.

A desorption study was also carried out after the saturation of the three liposome membranes in the caffeine solution by immersing each in 0.6 mL of PBS solution. Aliquots of 10 µL were sampled at 10, 20, 30, 60, 120, 180, 240 and 300 min for measuring the concentration of caffeine desorbed.

3.1.7. Mathematic modelling of the diffusion through the liposome membrane

A mathematic model of the diffusion through a membrane has been derived from Fick's diffusion law (Crank 1979), for which the rate of diffusion depends on the concentration gradient between the donor and the acceptor chamber:

$$\frac{\mathrm{d}n}{\mathrm{d}t} = \frac{K\,D}{h} A (C_D - C_A) \tag{3.2}$$

where n is the number of moles, t is the time, D is the coefficient of diffusion, C_D and C_A are the bulk concentrations in the donor chamber and acceptor chambers, h is the thickness of the membrane, A is the cross-sectional area of the membrane and K is the partition coefficient for the diffusant, which is given by C_H / C_D where C_H is the concentration of the diffusant in the hydrophobic regions of the liposome.

For cell membranes or artificial membrane systems, the thickness h of the membrane is usually difficult to obtain, just as in many cases the partition coefficient K cannot be determined directly. Therefore Equation 3.2 may be written as:

$$\frac{\mathrm{d}n}{\mathrm{d}t} = PA(C_D - C_A) \tag{3.3}$$

where the parameter $P = K\,D / h$ is called the *permeability coefficient* of the membrane.

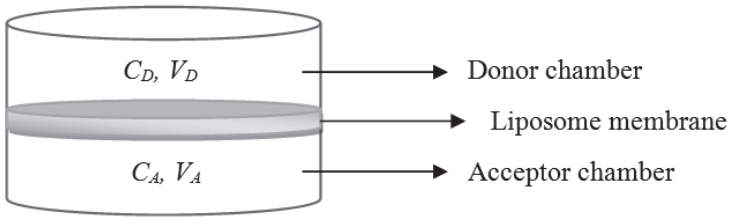

Figure 3.12 Illustration of the diffusion process.

For the continuous process, C_D and C_A are functions of time t, and were considered in the mass balance as illustrated in Figure 3.12:

$$C_0 V_D = C_D V_D + C_A V_A \tag{3.4}$$

where C_0 is the initial concentration in the donor chamber, V_D and V_A are the volumes of the donor chamber and the acceptor chamber. The flow rate of diffusant molecules at time t is the mass decrease in the donor chamber within dt thus:

$$-V_D \frac{dC_D}{dt} = PA(C_D - C_A) \tag{3.5}$$

With the initial boundary conditions, $t = 0$, $C_D = C_0$ and $C_A = 0$, Equation 3.5 has the following solution:

$$C_A = C_0 \frac{V_D}{V_D + V_A}\left\{1 - \exp\left[-P_{app} A\left(\frac{1}{V_D} + \frac{1}{V_A}\right)t\right]\right\} \tag{3.6}$$

The concentration in the acceptor chamber, C_A, as a function of time was then fitted to the above expression to yield the permeability P.

In the model employed by Flaten's (Flaten, Bunjes et al. 2006; Flaten, Dhanikula et al. 2006; Flaten, Skar et al. 2007; Flaten, Luthman et al. 2008), C_D was assumed to be constant and C_A was assumed to be negligibly small. Only the steady state flow rate after 3 h was considered to calculate the apparent permeability:

$$P_{app} = -\left(\frac{1}{AC_D}\right)\frac{\mathrm{d}n_D}{\mathrm{d}t} = \left(\frac{1}{AC_D}\right)\frac{\mathrm{d}n_A}{\mathrm{d}t} \tag{3.7}$$

That is, the permeability was obtained by plotting the accumulative amount in the acceptor chambers as a function of time and the steady state value, which corresponded to those measured in the range 3-5 h, was substituted in Equation 3.7.

3.1.8. The impact of the desorption on the permeability

In the case of the continuous method, when the membrane has been pre-treated by equilibration with the diffusant solution, the concentration in the membrane (C_m) may be greater than its steady state concentration (C_{ms}) as illustrated in Figure 3.13, resulting in a greater concentration in the acceptor chamber $\left(C'_A\right)$compared with C_A. Assuming the amount of the excess diffusant in the membrane is half of the total absorption, as shown in the shaded area of Figure 3.13, a model based on the release data is used, where release is defined as the total amount desorbed from the membrane and that diffused into the acceptor chamber:

$$V_A \frac{dC_A}{dt} = PA(C_D - C_A) + \frac{1}{2}\frac{dM_t}{dt} \tag{3.8}$$

where M_t is the mass release at time t, which may be obtained from the modelling the desorption according to the following empirical expression (Aminabhavi and Harlapur 1997):

$$\frac{M_t}{M_\infty} = At^B \tag{3.9}$$

where M_∞ is the mass release at time $t = \infty$, A and B are constants that can be determined from the desorption data.

Equation 3.8 was integrated with the initial condition, C_D=C_0 and C_A= 0 at t = 0, using MATLAB (see Appendix A) to determine the permeability on the basis of the best fit to $C_A(t)$.

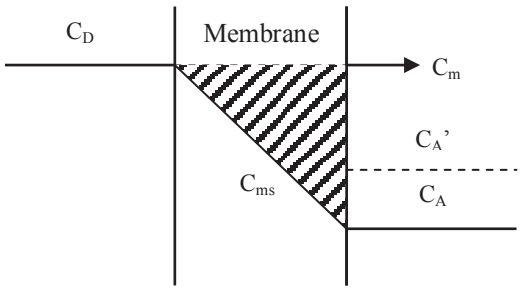

Figure 3.13 The assumption of a linear concentration gradient in the membrane after pre-treatment.

3.2 PHYSICOCHEMICAL ENHANCEMENT OF THE MOLECULAR DIFFUSION THROUGH THE LIPOSOME MEMBRANE

3.2.1. Materials

Paracetamol (acetaminophen, BioXtra, ≥99%), theophylline (anhydrous, ≥99%, powder), nadolol (analytical standard), acyclovir (≥99%, HPLC, powder), amphotericin B (powder, BioXtra), ethanol (200 proof) and dimethyl sulfoxide (DMSO, BioReagent, ≥99.7%) as shown in Figure 3.14, were all purchased from Sigma, UK. The concentrations of the molecules in the work were nearly the saturation concentration so that they could be detected by UV, as listed in Table 3.1. The liposome membranes and culture plates were from the preparation as described before. MeCN, phosphoric acid and H_2O used for HPLC analysis were all of analytical reagent grade and were kindly provided by the School of Chemistry, University of Birmingham, UK.

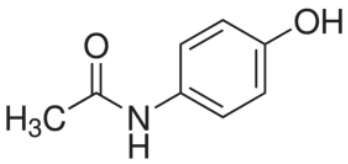

Paracetamol (151.17)

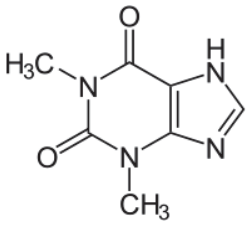

Theophylline (180.16)

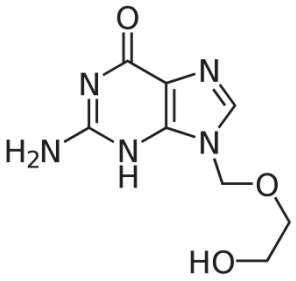

Acyclovir (225.50)

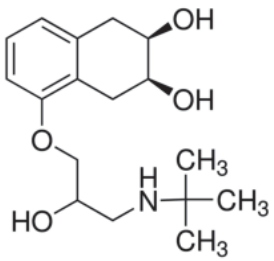

Nadolol (309.40)

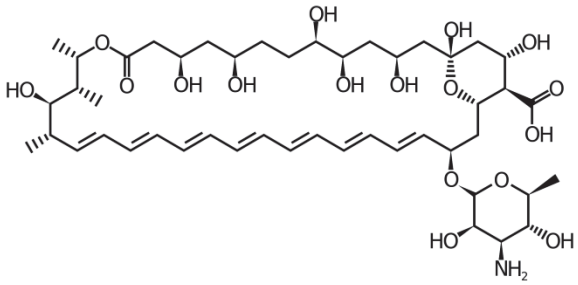

Amphotericin B (924.08)

Ethanol (46.07)

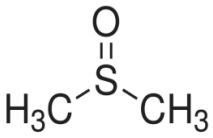

DMSO (78.13)

Figure 3.14 Chemical structures of the molecules in this work with the molecule weight in parentheses.

Table 3.1 The concentrations of the model diffusants in the donor chamber.

Paracetamol	Theophylline	Caffeine	Acyclovir	Nadolol	Amphotericin B
1.00 mg/mL	6.00 mg/mL	10.00 mg/mL	0.10 mg/mL	1.00 mg/mL	0.1 mg/mL

3.2.2. UV calibration of the model molecules

A calibration of the standard solution of the five model molecules was carried out and the absorbance at λ_{max} was plotted against the concentration to obtain the absorptivity ε. All measurements were performed in triplicates and the average UV absorbance was shown in the figures with standard errors.

3.2.3. HPLC analysis

Since the two λ_{max} of the UV spectra of paracetamol and caffeine are close (242 nm for paracetamol and 273 nm for caffeine), they would interfere with each other. Consequently, a high-performance chromatography (HPLC) was used. HPLC is a technique that separates a mixture of compounds due to their different affinity to a stationary and a mobile phase. As shown in Figure 3.15, the solvent as the mobile phase is pumped under a high pressure into the stationary phase: a HPLC column. When solutions of the compounds are injected into the system, the component with a stronger interaction with the stationary phase would thus lead to a longer retention time. The compounds could thus be separated and analysed by a UV spectrophotometer.

The analysis of a mixture of paracetamol and caffeine was performed by HPLC (Shimadzu LC20 system) with a UV detector (SPDM20A) in the School of Chemistry, University of Birmingham, UK. A Supelco Ascentis Express C18 150 × 4.6 mm column was used and the mobile phase consisted of 10% MeCN and 90% of H_2O and was adjusted to pH 2.36 using phosphoric acid at a flow rate of 1.0 mL/min for an optimised separation. A calibration of the paracetamol with caffeine was carried out before the HPLC analysis of the diffusant in the donor chamber.

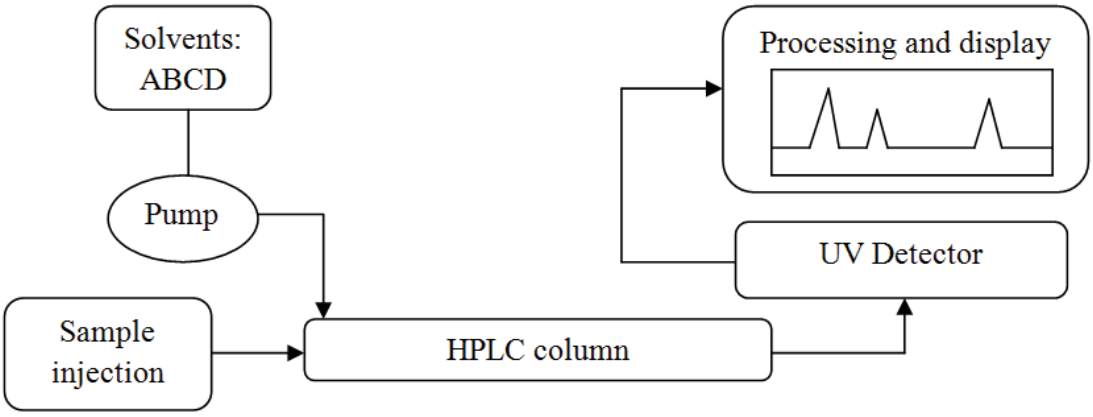

Figure 3.15 A schematic drawing of a HPLC system.

3.2.4. Diffusion of the model diffusants through the liposome membrane

3.2.4.1. Diffusion of the model diffusants

The permeabilities of the five model diffusants were measured using the optimised procedure developed for caffeine based on a continuous diffusion method with a pre-treatment of the liposome membrane using the same concentration as that for the donor solution. The diffusion experiment was performed in triplicates and the average concentrations in the acceptor chambers were plotted against time with standard errors. The data were then fitted with the continuous diffusion model with 95 % confidence intervals.

3.2.4.2. Physiochemical enhancement of the molecular diffusion

Diluted ethanol and DMSO were chosen as a diffusion enhancer. The diffusion of caffeine (10 mg/mL) with 1, 10 and 40 % ethanol, and with 10, 30 and 50 % DMSO was firstly

carried out after the membranes were pre-treated with the same solution as that for donor chamber. The diffusion of the five model diffusants with those proved to be most potent formulations were then carried out. All the experiments were performed in triplicates and the average concentration of the diffusant in the acceptor chamber was plotted against time with standard errors, and was then fitted with the continuous model with 95% confidence intervals.

3.2.4.3. Elastic properties of the liposome membrane with ethanol /DMSO by AFM

Automatic force microscopy (AFM) is a unique technique where the cantilever of AFM can move up and down over a move up and down over a point on the sample surface to probe the elastic and adhesive properties of material or properties of material or force mapping (Liang, Mao et al. 2004). As shown in

Figure 3.16, a cantilever attached to a Piezoelectric scanner can move away or towards a sample at a controlled rate. The adhesive or repulsive force between the sample and the cantilever tip will make it bend downwards or upwards. The top surface of the cantilever reflects the laser beam from a laser diode so that any spatial change of the reflected beam due to deflection of cantilever is collected by a position sensitive photodiode (Liu 2010).

In this work, the Young's modulus and hardness of the liposome in the membrane were measured using an atomic force microscope (D3100 AFM with a NanoScope III controller, Digital Instruments, Santa Barbara, CA). This involved the indentation of a colloid probe with a tip radius of 8.2 μm and a cantilever with a spring constant of 27 N/m; the approach velocity was 10 μm/s. The liposome membrane and the liposome membrane pre-treated with 40% ethanol/30% DMSO were freshly prepared, and they were mounted onto glass slides

fixed by super glue. The force measurement was performed at 25 spots on one membrane at room temperature (18^{o}C-19^{o}C) and a humidity of 30-40%. The approaching force distance data was then fitted to the Hertzian model to calculate the Young's modulus and hardness of the liposome membranes.

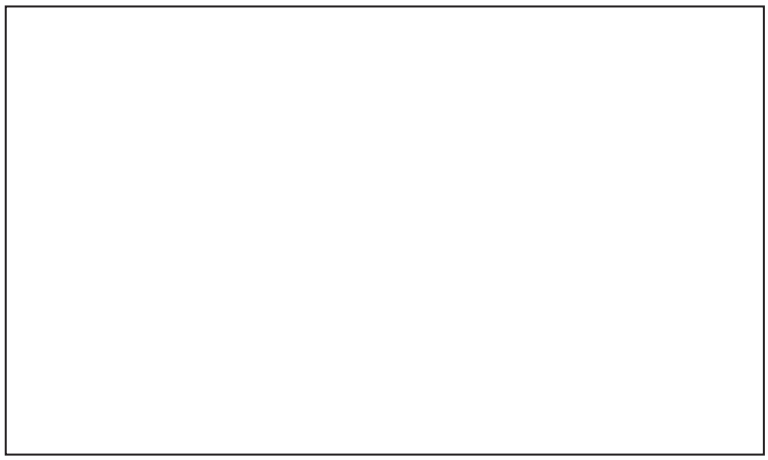

Figure 3.16 Schematic diagram of an AFM system (Liu 2010).

3.2.4.4. The impact of ethanol on the size of the liposome

The size and size distribution of the liposome with ethanol was compared with those without ethanol to examine if the liposome remained intact. The liposome extruded through the 800 nm and the 400 nm polycarbonate membrane filters were measured by HPPS and those in 10 % and 40% ethanol solution were also measured. All the measurements were performed in triplicates.

3.2.4.5. The synergetic effect of paracetamol and caffeine on their diffusion

The diffusion of paracetamol (1 mg/mL) was carried out with caffeine (1 mg/mL, 10 mg/mL and 20 mg/mL) after the membranes were pre-treated with the same solution as that for donor chamber. The diffusion experiment was performed in triplicates and the average concentrations in the acceptor chambers for each molecule were plotted against time with standard errors. The data was then fitted with the continuous diffusion model.

3.3 THE DIFFUSION OF THE TPS THROUGH THE LIPOSOME MEMBRANE

3.3.1. Materials

EGCG was kindly provided by Unilever, UK. ECG (≥98%, HPLC, from green tea), EGC (≥95%, HPLC, from green tea), EC (≥98%, HPLC, from green tea), ethanol (200 proof) DMSO (BioReagent, ≥99.7%) NaOH and HCl (analytical grade) were all purchased from Sigma, UK.

3.3.2. UV calibration of the TPs

A calibration of the standard solution of the TPs was carried out and the absorbance at λ_{max} was plotted against the concentration obtain the absorptivity ε. All measurements were performed in triplicate and the average UV absorbance was plotted against concentration with standard errors.

3.3.3. Absorption of the TPs by the liposome membrane

Absorption of the TPs was performed to obtain the mass absorption by the liposome membrane. 10 liposome membranes were carefully removed from the inserts and immersed in 2 mL of the TPs solution so that a small decrease in the concentration due to absorption could be detected by UV, with the following concentrations: 1.0 mg/mL for EGCG, 1.0 mg/mL for ECG, 1.0 mg/mL for EC and 0.5 mg/mL for EGC. Aliquots of 10 µL of the TPs solution were sampled at 300, 600, 1200, 1800, 3600, 5400, 7200, 10800, 14000 and 18000 s. The concentration was measured by the UV spectrophotometer; the volume removed was sufficiently small that it did not significantly affect the concentration of the solution in the chamber. All the absorption experiments were performed in triplicates and an average concentration was plotted against time with standard errors.

The absorption of the TPs by the liposome membrane could be modelled by the first order kinetics as:

$$\frac{1}{V}\frac{dm}{dt} = \frac{k}{V'}\left(m' - m'_{\infty}\right) \tag{3.10}$$

where m is the mass absorbed in the membrane and V is the volume of the membrane at $t = t$, m' and m'_{∞} are the masses in the donor solution at $t = t$ and $t = \infty$, and V' is volume of the donor solution.

And $m + m' = m'_0$ (3.11)

where m'_0 is the mass in the donor solution at $t = t$.

By solving Equation 3.10 with initial condition that at $t = 0$, $m = 0$

$$\frac{(m'_0 - m'_\infty) - m}{m'_0 - m'_\infty} = \exp(-t/\lambda) \quad (3.12)$$

where $\lambda = V'/kV$

The absorption data of the TPs were thus fitted by Equation 3.12 and the absorption constant *k* could be obtained.

3.3.4. The diffusion of the TPs through the liposome membrane

3.3.4.1. The diffusion of the TPs

The permeabilities of the TPs were measured on the basis of the results obtained with caffeine; a continuous diffusion method was used with a pre-treatment of the liposome

membrane overnight using the same concentration as that for the donor solution. The diffusion experiment was performed in triplicates and the average concentrations in the acceptor chambers were plotted against time with standard errors. The data was then fitted with the continuous diffusion model with 95% confidence intervals.

3.3.4.2. Washing off test of the TPs from the pre-treated membrane

The washing off test was carried out to investigate whether the TPs in the acceptor chamber were those released from the liposome membrane. To wash off the TPs, the liposome membranes were placed in the acceptor chamber with 0.6 mL PBS without a donor solution after pre-treatment. The washed off concentrations of the TPs in the acceptor chamber were measured by the UV. The tests were performed in triplicates and an average concentration was plotted against time with standard errors.

3.3.5. The physicochemical enhancement of the diffusion of EGCG through the liposome membrane

3.3.5.1. Diffusion of EGCG through the liposome membrane with ethanol and DMSO

40% Ethanol and 30 %/50 % DMSO were used as an enhancer for the diffusion of EGCG to improve its poor permeability through the liposome membrane. The permeation enhancer was added into both the donor and pre-treatment solution and the continuous diffusion was thus carried out in triplicates as described before. The average concentration in the acceptor chamber was plotted against time with standard errors.

3.3.5.2. Diffusion of EGCG through the liposome membrane at pH 2, 5 and 8

As the ionisation state of a molecule influences its permeability as introduced in Chapter 2, the pH in both the donor and acceptor chamber were adjust to 2, 5 and 8 by HCl/NaOH for the diffusion of EGCG. The continuous diffusion was thus carried out in triplicates as described before. The average concentration in the acceptor chamber was plotted against time with standard errors.

3.3.5.3. Raman spectra of liposome and EGCG

Raman spectroscopy (Yvon) is a light scattering technique where a laser photon is scattered by a sample molecule and loses/gains energy (wavelength) during the process which can be detected. This energy change is characteristic for a particular bond in the molecule, and a Raman spectrum is similar to FTIR that it can produce a precise spectral fingerprint. The distinct advantage of a Raman spectrophotometer is that it can be used to analyse aqueous solutions since it does not suffer from the large water absorption effects found with IR techniques. A confocal Raman microscope (WiTec, laser length 785 *nm*, Germany) was used in this work to analyse the solution of liposome (6 % w/v) and EGCG (10 mg/mL).

3.3.5.4. Elastic properties of the liposome membrane with EGCG at pH 2, 5 and 8 by AFM

The Young's modulus and hardness of the liposome in the membrane with EGCG at pH 2, 5 and 8 were measured using AFM (D3100 AFM with a NanoScope III controller, Digital Instruments, Santa Barbara, CA). As described in section 3.2.4.3: a colloid probe with a tip radius of 8.2 μm and a cantilever with a spring constant of 27 N/m were used; the approach

velocity was 10 μm/s. The liposome membranes were immersed in EGCG solution at pH 2, 5 and 8 and control membranes were also prepared by immersed in PBS solution adjusted to pH 2, 5 and 8. The membranes were then mounted onto glass slides fixed by super glue. The force measurement was performed at 25 spots on one membrane at room temperature (18^{o}C-19 ^{o}C) and a humidity of 30-40 %. The approaching force distance data was then fitted to the Hertzian model to calculate the Young's modulus and hardness of the liposome membranes.

CHAPTER 4: MOLECULAR DIFFUSION THROUGH THE LIPOSOME MEMBRANE

4.1 INTRODUCTION

A liposome membrane method (Flaten, Bunjes et al. 2006; Flaten, Dhanikula et al. 2006; Flaten, Skar et al. 2007; Flaten, Luthman et al. 2008) has been developed with improved prediction of GI absorption. For this method, the amount of the diffusant from a donor chamber into a number of fresh acceptor chambers are measured in sequence to calculate the permeability, assuming that the concentration in the donor chamber remains constant (it will be referred to as the *incremental method* in this work). However, there was an initial time lag for the diffusion that could not be described by the theory used to interpret the data; in the current work it is shown that it is due to the absorption of the diffusant in the liposome membrane. This could lead to an underestimation of the permeability, for example, the permeability of nadolol with a high partition coefficient was reported to be 'zero' although this is known not to be the case (Sugano, Hamada et al. 2001; Wohnsland and Faller 2001; Zhu, Jiang et al. 2002; Avdeef and Tsinman 2006; Flaten, Bunjes et al. 2006; Flaten, Dhanikula et al. 2006; Flaten, Skar et al. 2007; Chen, Murawski et al. 2008; Flaten, Luthman et al. 2008). Another possible contributory factor to errors is the assumption that the concentration of diffusant in the donor chamber is constant since the reduction may not be negligible.

In the current work, the experimental procedure and data analysis for the incremental method was modified to improve the accuracy; it will be termed the *continuous method.* It involved a pre-treatment of the membrane with the diffusant to avoid the underestimation of the permeability. A continuous rather than incremental method was employed together with a model that accounts for the time-dependant concentration in the donor chamber. To analyse the data, in this way the absorption and desorption isotherms of the diffusant in the liposome membrane were measured. The impact of the desorption on the diffusion was examined by MATLAB programming.

4.2 RESULTS

4.2.1. Size distribution of the liposome after extrusion

Since the size control of the liposome by extrusion is important in making the liposome membrane, the size distribution was obtained from HPPS as shown in Figure 4.1: the liposome before extrusion showed a wide distribution with a mean size of 2930±52 nm, where there was a small peak of light intensity at around 150±16 nm. After being extruded through an 800 *nm* filter membrane 10 times, the size was reduced to approximately 535±20 nm with a moderate distribution and a further reduction to 320±14 nm by another 10 times of extrusion through 400 nm filters.

In Figure 4.2, the mean size of the liposome decreased considerably down to 585±28 nm after being extruded through an 800 nm filter membrane 5 times, and down to 535±20 nm with a further extrusion by another 5 times. There was no significant decrease in the sizes with

extrusion passes up to 20 times. When extruded through a 400 nm filter membrane 5 times, the size reduced to 320±14 nm and a further extrusion of 10 passes resulted in 289±9 nm vesicles. There were no significant reductions in the sizes when extruded up to 20 times. As shown in Figure 4.3 and Figure 4.4, the liposome extruded through 800 and 400 nm filter membranes were both stable for 24 hours.

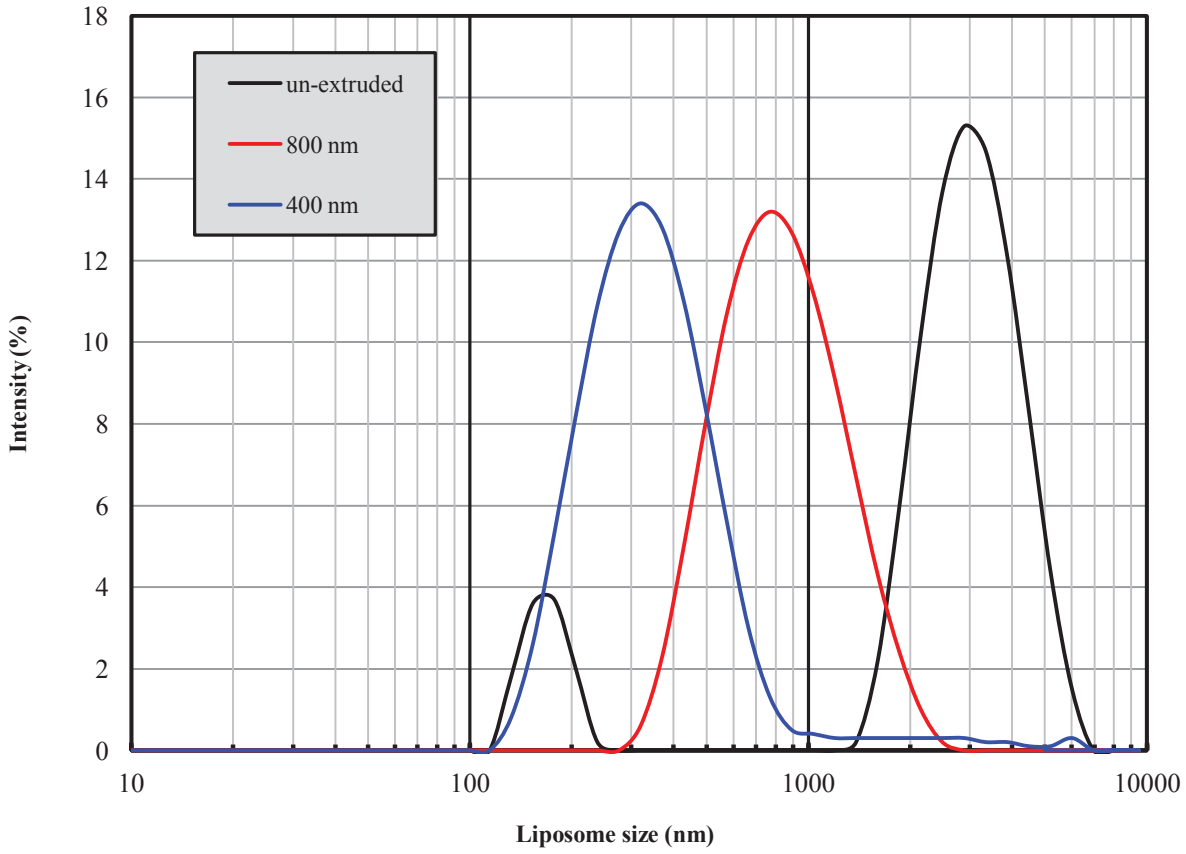

Figure 4.1 The size distribution of the liposome before extrusion (black line), after extrusion through 800 nm filter membrane (red line) and after successive extrusion through 800 nm and 400 nm filters (blue line).

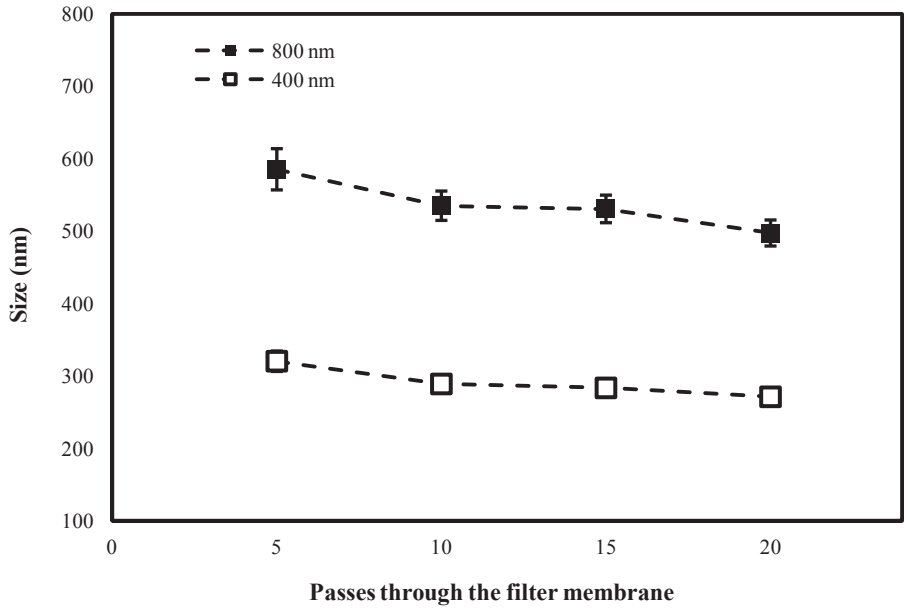

Figure 4.2 The sizes of the liposome extruded through 800 nm filter (filled squares) and 400 nm filter (open squares) membrane after 5, 10, 15 and 20 passes. The measurements were performed in three triplicates and an average size was plotted against passages through the filter membrane with standard errors.

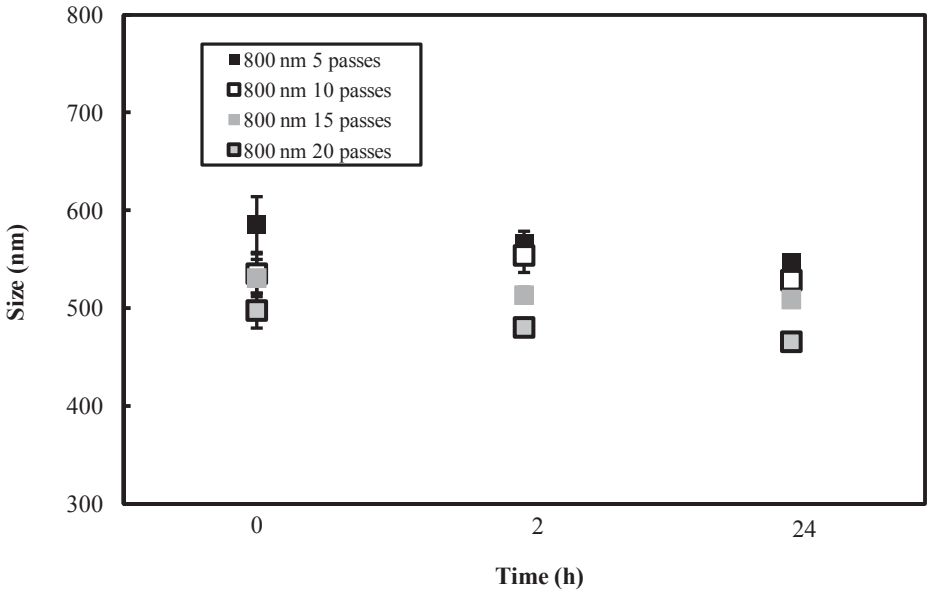

Figure 4.3 The sizes of the liposome extruded through 800 nm filter membrane after 5 (filled black squares), 10 (open black squares), 15 (filled grey squares) and 20 (open grey squares) passes within 24 hours. The measurements were performed in three triplicates and an average size was plotted against time with standard errors.

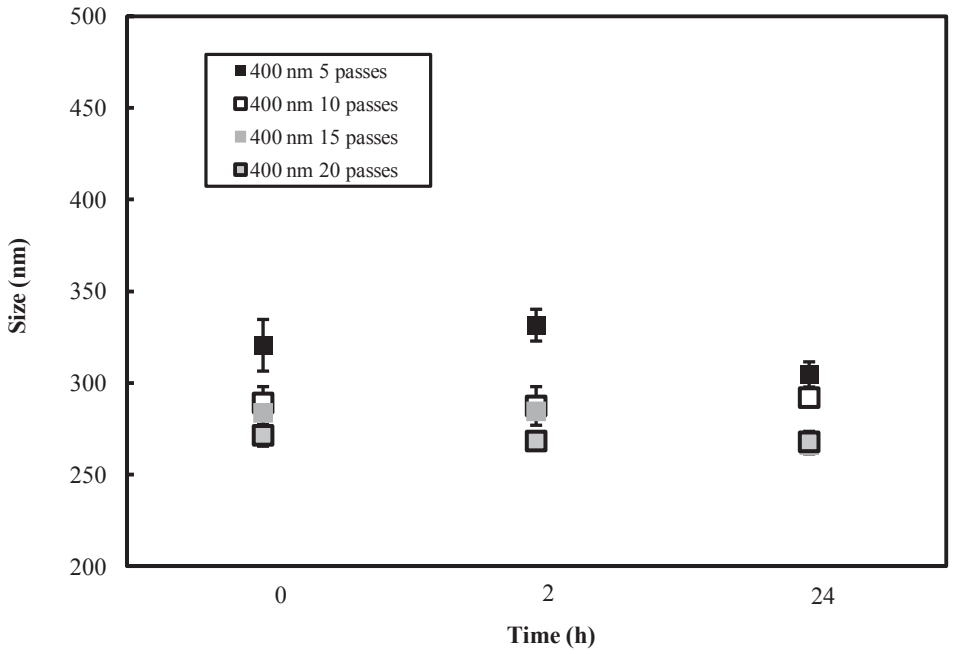

Figure 4.4 The sizes of the liposome extruded through 400 nm filter membrane after 5 (filled black squares), 10 (open black squares), 15 (filled grey squares) and 20 (open grey squares) passes within 24 hours. The measurements were performed in three triplicates and an average size was plotted against time with standard errors.

4.2.2. Cryo-SEM examination of the liposome membrane

Cryo-electron micrographs of cross-sections of the liposome and substrate membranes are shown in Figure 4.5. The porous substrate membrane has a thickness of 143±2 μm (Figure 4.5 (a)). The smaller liposomes are clearly embedded in the pores of the substrate membrane during the first step of centrifugation, occupying a thickness of 90±3 μm as shown in Figure 4.5 (b), while the larger liposomes are retained on the surface of the smaller liposome layer, forming a tight permeation barrier for mass diffusion with a thickness of 95±2 μm. Figure 4.5 (c) and (d) show the interior morphology of the smaller liposome layer in the membrane, in which pores are visible and the fractured liposome resulting from cutting the frozen membrane can be seen.

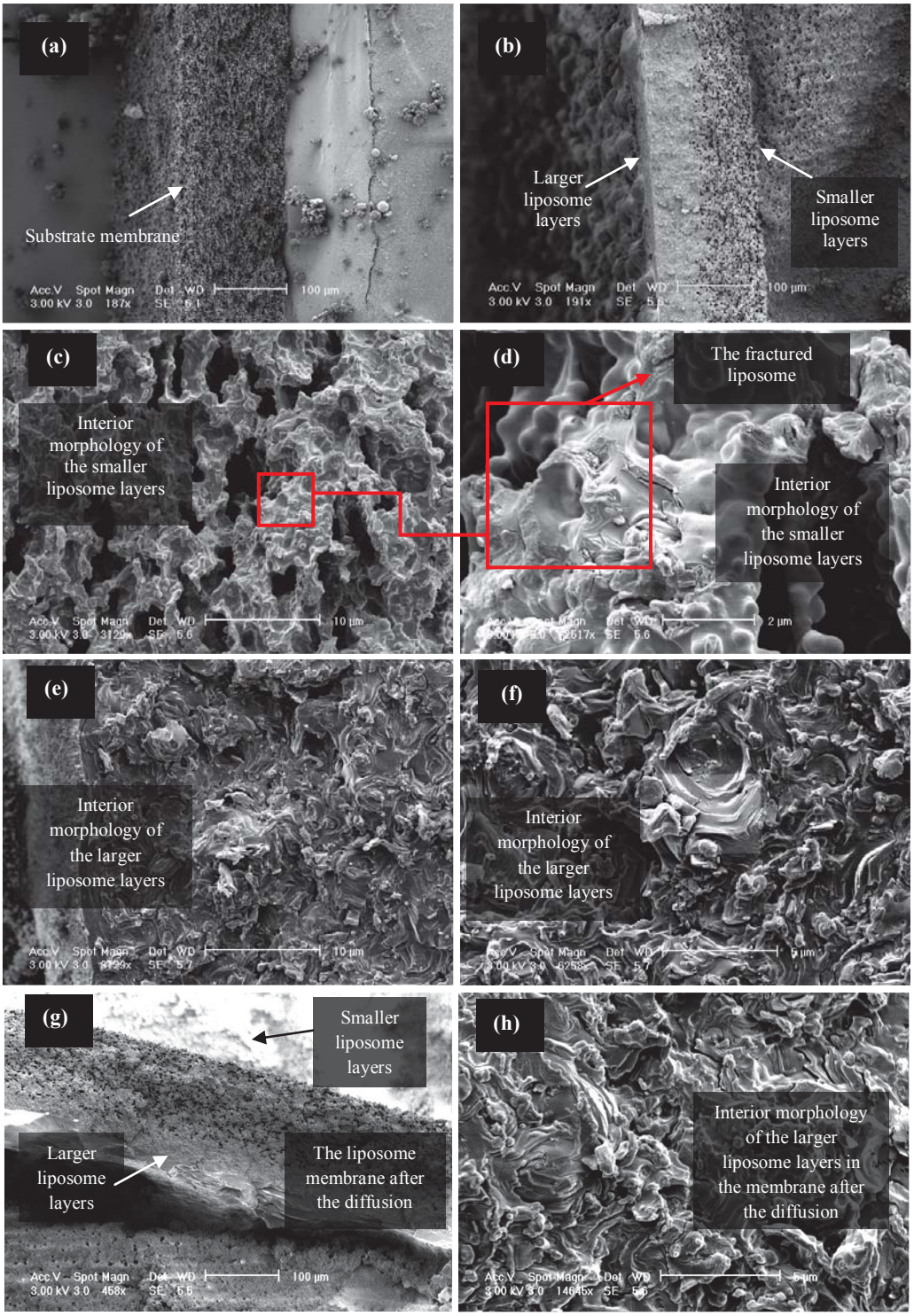

Figure 4.5 Cryo-SEM images of the (a) substrate membrane, (b) liposome membrane, (c) interior morphology of the smaller liposome layer, (d) typical fractured liposome in the smaller liposome layer, (e) interior morphology of the larger liposome layer, (f) compact liposome in the larger liposome layer, (g) liposome membrane after the diffusion and (h) interior morphology of the larger liposome layer in the membrane after the diffusion.

Figure 4.5 (e) and (f) show the interior morphology of the larger liposome layer on the membrane, which is considerably more compact with few visible pores. The liposomes were not necessarily regular in shape or size but rather squeezed or stretched globular vesicles with multilayer structures (Knight 1981). The liposome membrane was also examined after being saturated with caffeine as shown in Figure 4.5 (g) and (h). There are no visible changes suggesting that the absorbed caffeine did not cause significant swelling or other morphological changes.

4.2.3. Phospholipid assay of the liposome membrane

The calibration of egg phospholipid solution is shown in Figure 4.6, the obtained absorptivity ε from the linear fitting of the UV absorbance at λ_{max} (600 nm) against the concentration was 0.12 mL/mg with $R^2 > 0.99$. As an example, the mean absorbance of the phospholipid in one liposome membrane was 0.090±0.003, which means there was 3.87±0.14 mg, which was 21.5±0.7 % of the total lipid input was embedded in each membrane.

4.2.4. Pre-treatment of the liposome membrane

The caffeine was calibrated by the UV spectrophotometer before the diffusion was carried out. As shown in Figure 4.7, the obtained absorptivity ε from the linear fitting of the UV absorbance at λ_{max} (273 nm) against the concentration was 52.2 mL/mg with an $R^2 > 0.99$.

The influence of the pre-treatment of the liposome membrane with the diffusant is illustrated by comparing the diffusion results of the original method with/without pre-treatment as follows: the permeability of caffeine, as the selected molecule for validating the method, was initially measured according to the reported method (Flaten, Dhanikula et al. 2006) where one donor chamber with caffeine solution (1.51 mg/mL) was placed into a fresh PBS solution at pH 7.4 in an acceptor chamber. The inserts were sequentially repositioned in different acceptor wells with the same quantity of the PBS solution at various time intervals up to a period of 5 h and the concentrations were measured using the UV spectrophotometer.

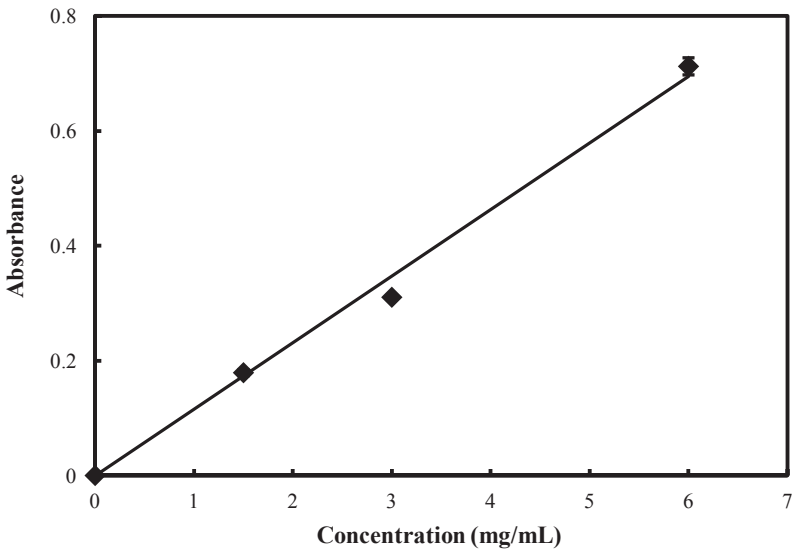

Figure 4.6 The calibration of the phospholipid assay: the experiments were performed in triplicates and an average UV absorbance was plotted against concentration with standard errors.

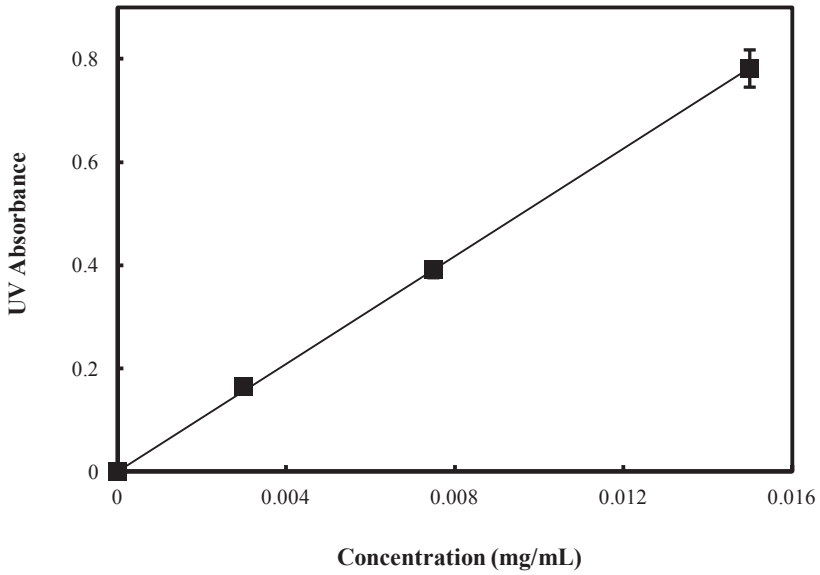

Figure 4.7 The calibration of caffeine at 273 *nm*: the measurements were performed in triplicates and the average UV absorbance was plotted against concentration with standard errors.

The influence of the pre-treatment of the liposome membrane with the diffusant was examined by comparing the results of the incremental method with and without pre-treatment. The results for caffeine are plotted in Figure 4.8 and there is an initial time lag before a steady state diffusion rate is achieved as reported previously (Flaten, Dhanikula et al. 2006). The measurements were repeated using the same liposome membrane with fresh caffeine donor solution. The data in Figure 4.8 show that the time lag was reduced and that the amount diffused increased. When the liposome membrane was pre-treated with caffeine only on the donor side, the time lag decreased further with steady state being achieved in < 2 h. When the membrane was pre-treated by complete immersion in the caffeine solution, there was no evidence of a time lag and the amount of diffused caffeine increased by $2.2\pm0.7 \times 10^{-7}$ mol (a factor of 6) at 1 h compared with the first diffusion. The values of the permeability were calculated by fitting Equation 3.7 to the linear regions of the data (10,800 - 18,000 s)

and are given in Table 4.1. The value for a pre-treatment by complete immersion was about 25% greater than that for the incremental method. However, it is clearly necessary to account for the absorption of the diffusant in the membrane, which will be considered in the next section.

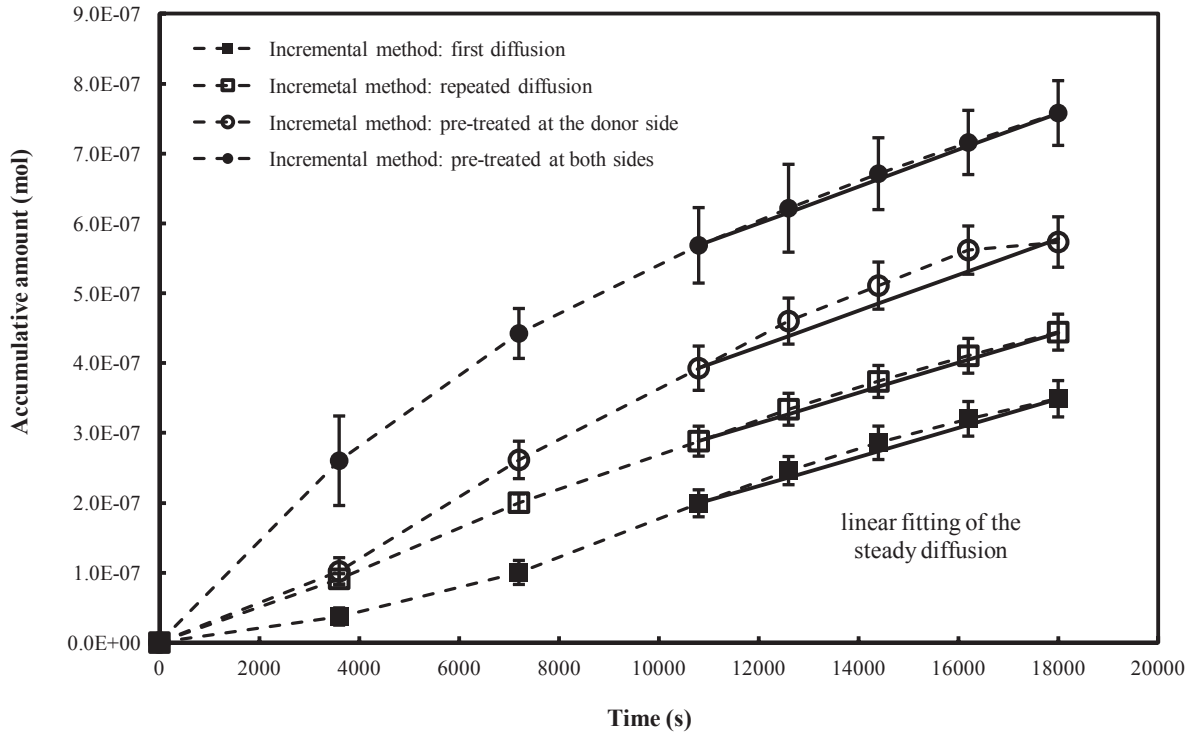

Figure 4.8 The incremental diffusion of caffeine (1.51 mg/mL) through a liposome membrane: the first diffusion (filled squares), the repeated diffusion (open squares), the diffusion after the donor side of the membrane was pre-treated with caffeine (open circles) and the diffusion after the both sides of the membrane were pre-treated with caffeine (filled circles). The error bars represent the standard error of three repeats. The lines are the best fit to Equation 3.7.

Table 4.1 Permeability values from the incremental method fitted to Equation 3.7

	first diffusion	**repeated diffusion**	**pre-treated at the donor side**	**pre-treated at both sides**
Permeability ($\times 10^{-6}$ cm/s)	5.32±0.23	5.54±0.26	6.60±0.15	6.74±0.46

4.2.5. Mass absorption of caffeine in the liposome membrane

As shown in the previous section, the pre-treatment of the liposome membrane with the diffusant eliminates the time lag which was probably due to the absorption of the diffusant in the membrane. The mass of absorbed caffeine as a function of time is shown in Figure 4.9. It increased rapidly until a saturated value of $7.62\pm0.03 \times10^{-3}$ mg/mg was achieved after 20 min, which corresponds to $29.5\pm1.1 \times10^{-3}$ mg caffeine absorbed in a single liposome membrane. This is equivalent to $1.52\pm0.05 \times10^{-7}$ mol of caffeine and is thus consistent with the increase of the diffused caffeine at 1 h ($2.2\pm0.7 \times10^{-7}$ mol) in Figure 4.8.

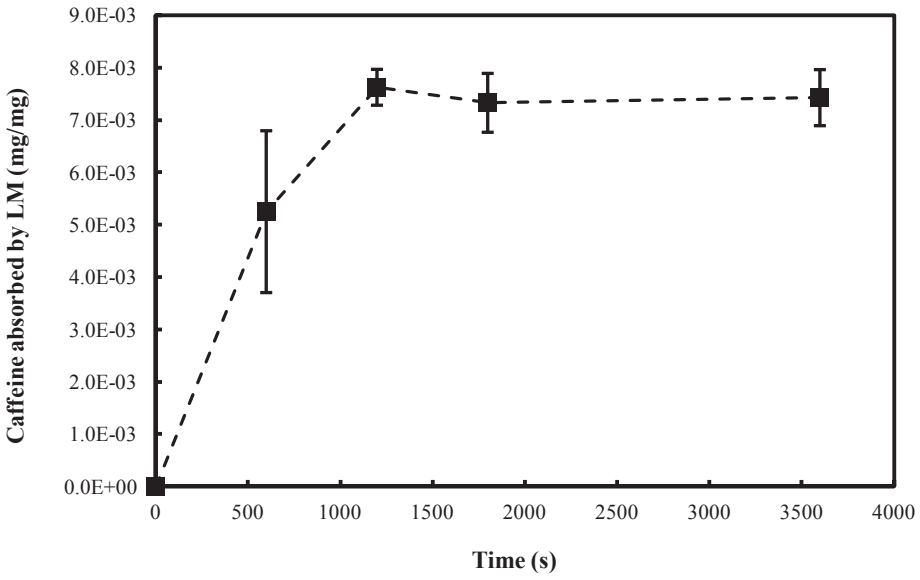

Figure 4.9 The absorption of caffeine by a liposome membrane (LM): 3 liposome membranes were immersed in a 2 ml of 1.51 mg/mL caffeine solution and 10 µL aliquots of the solution was sampled for UV measurement at intervals of 10, 20, 30, 60 min. The error bars represent the standard errors of three repeats.

In Figure 4.8, the concentration of caffeine in the donor chamber reduced by nearly 45 % after 5 h for the incremental method (first diffusion), indicating that the assumption of a constant value of C_D in Equation 3.7 is not justified. The permeability at each time interval was calculated from Equation 3.6 as shown in Figure 4.10. The value for the incremental method (first diffusion) at 1 h was only 30±7 % of that at the steady state due to the absorption by the liposome membrane. The permeability then increased gradually until it reached an approximately steady state value. In contrast, the permeability was constant within experimental error when the liposome membrane was pre-treated with the diffusant, which was more than a factor of two greater than that measured without the pre-treatment.

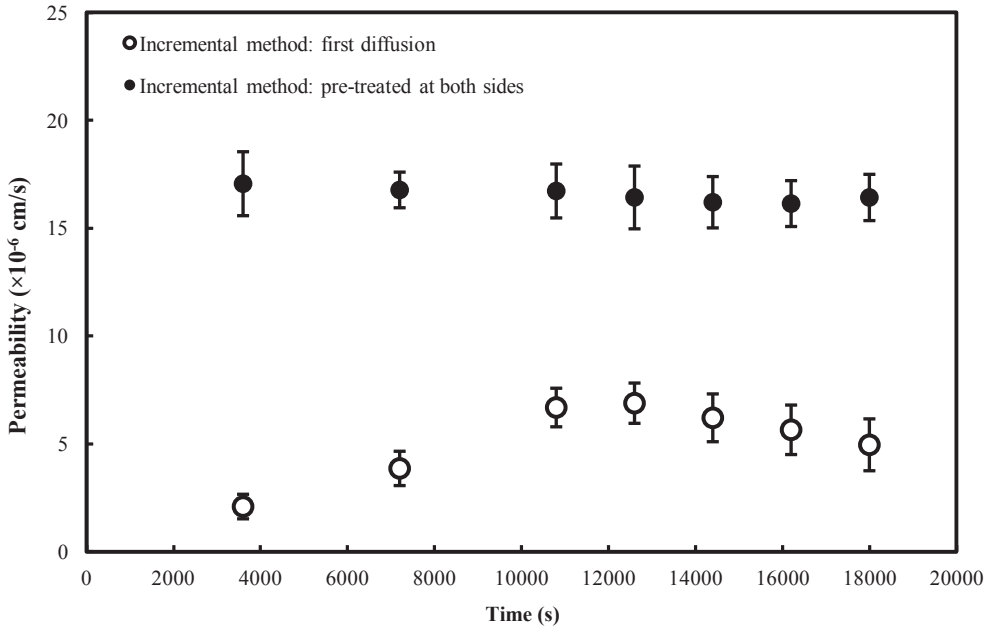

Figure 4.10 The permeability obtained from the incremental method for caffeine: the first diffusion (open squares) and the diffusion after the membrane was pre-treated on both sides (filled squares). The error bars represent the 95% confidence intervals of three repeats.

The desorption of the caffeine was carried out to investigate its impact on the permeability. As shown in Figure 4.11, initially the rate of desorption was rapid until it reduced after approximately 1 h. Over a 5 h period, a total of 5.8±0.5 $\times 10^{-3}$ mg of the caffeine was released per mg of liposome, which was 76±7 % of the total amount originally absorbed.

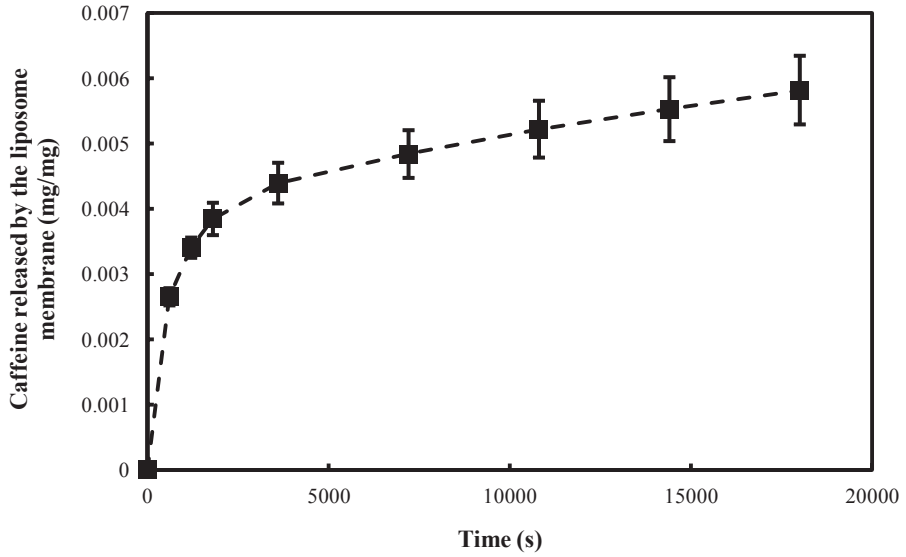

Figure 4.11 The desorption of caffeine from a liposome membrane. Three liposome membranes were first equilibrated in caffeine solution for 1 h. The error bars represent the standard errors of three repeats.

4.2.6. The continuous diffusion of caffeine after pre-treatment and the influence of agitation

For diffusants with a small permeability or small UV absorbance, the concentration in the acceptor chamber after several hours is too small to be detected using the incremental method. The continuous method overcomes this disadvantage. Figure 4.12 shows the diffusion data for caffeine (1.51 mg/mL) using this method without pre-treatment of the liposome membrane and with pre-treatment involving immersion of the membrane in the donor

solution for 1 h. The concentration of the diffused caffeine in the acceptor chamber as a function of time was fitted to Eq. (6) with $R^2 \geqslant 0.98$. After 5 h, the amount of diffused caffeine was 1.6±0.5 $\times 10^{-7}$ mol greater for the pre-treated membrane compared with the untreated membrane. This value is comparable to the amount (1.52±0.05 $\times 10^{-7}$ mol) that was absorbed in the pre-treatment on the basis of that measured by the procedure described in the previous section. The permeabilities for the untreated and pre-treated membranes correspond to 5.68±0.05 $\times 10^{-6}$ and 11.5±1.3 $\times 10^{-6}$ cm/s, and thus the pre-treatment increased the value by about a factor of two. It will be shown in Chapter 8 that the value corresponding to that obtained by pre-treatment is correct. In addition, this value is nearly a factor of two greater than that from the incremental method with pre-treatment assuming there is no absorption of the diffusant by the membrane, which is 6.7±0.5 $\times 10^{-6}$ cm/s (see Figure 4.8) from a linear fitting to Equation 3.7.

The effect of agitation on the permeability was also investigated by using a shaking incubator at 100 rpm. Figure 4.13 shows diffusion data for caffeine (initial donor concentration of 10.00 mg/mL) using the continuous method with a pre-treatment for 1 h with and without agitation. There is no significant difference in the results and thus it may be assumed that the volume in the donor chamber is sufficiently small that it is equivalent to a well-mixed system.

Since the thickness of the liposome membrane was measured, the partition coefficient of caffeine between the liposome and the water phase could be obtained from the absorption data using Eq. (2). The value obtained was 2.2±0.1 and thus the diffusion coefficient of caffeine could thus be calculated from $D = P\,h\,/\,\alpha$ as 9.6±1.2 $\times 10^{-8}$ cm^2/s.

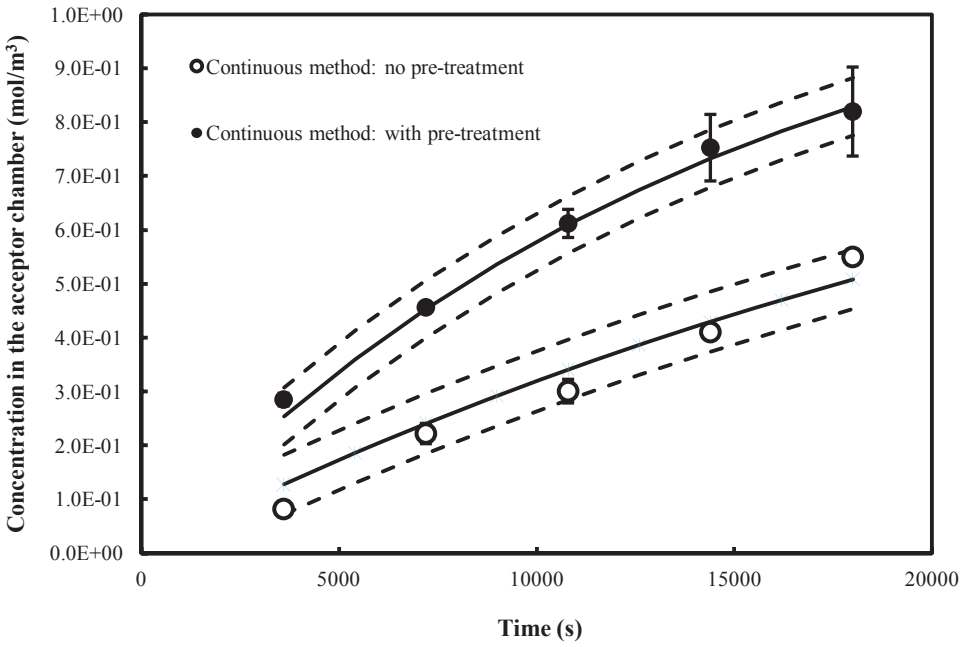

Figure 4.12 The continuous diffusion of caffeine (1.51 mg/mL) through a liposome membrane with pre-treatment (filled circles) and without pre-treatment (circles). The data are fitted to Equation 3.6 (solid lines) with 95% confidence intervals (dashed lines). The errors bars represent the standard errors of three repeats.

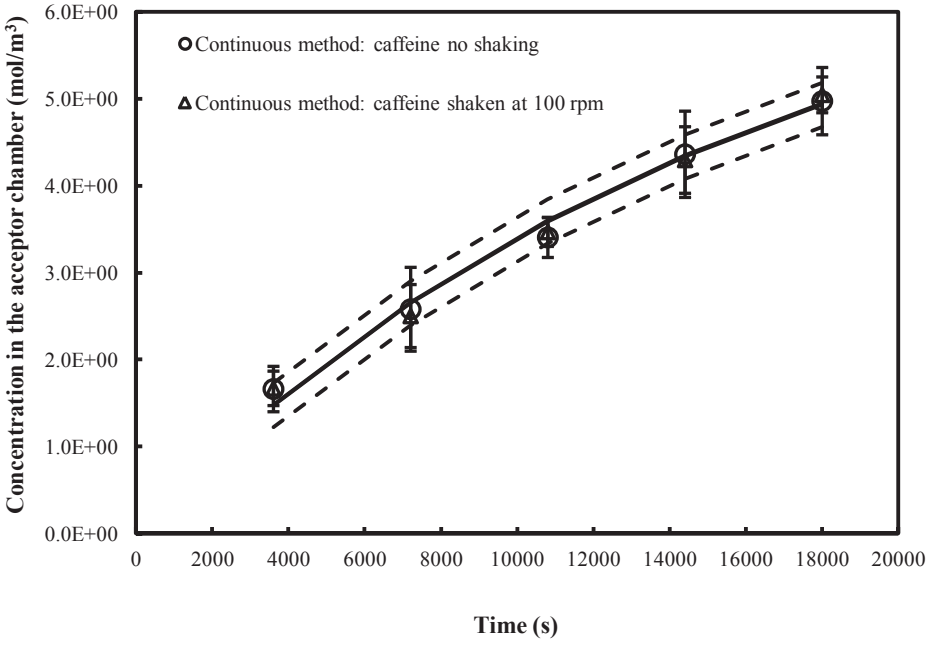

Figure 4.13 The continuous diffusion of caffeine (initial donor concentration of 10.00 mg/mL) without shaking (open squares) and the diffusion in an incubator shaker at 100 rpm kept at 25 ^{o}C (open triangles). The data are fitted to Equation 3.6 (solid line) with 95% confidence intervals (dashed lines). The error bars represent the standard errors of three repeats.

4.2.7. Influence of prolonged pre-treatment time and the concentration gradient on the diffusion of caffeine

Using the continuous method, the influence of the pre-treatment time was studied by immersing the liposome membranes in a caffeine solution for periods of 1, 5, 16 and 24 h with a concentration (10.00 mg/mL) equal to that to be used in the donor chamber. The experimental data are shown in Figure 4.14 and they were fitted to Equation 3.6 with $R^2 \geq 0.987$. The permeabilities are given in Figure 4.15 they are not significantly different and the mean value is $10.6 \pm 0.2 \times 10^{-6}$ cm/s. This also demonstrates that the liposome membrane maintains its integrity and stability over the time period of the pre-treatment solution.

The data in Figure 4.16 were obtained by pre-treating the liposome membrane with the donor solution of caffeine at 0.50, 1.51, 10.00, 20.00 mg/mL for 1 h. The permeabilities obtained by the fitting the data to Equation 3.6 ($R^2 \geq 0.989$) are shown in Figure 4.17; the > 95 % confidence intervals for the concentration at 0.5 and 1.514 mg/mL reflect the greater experimental errors associated with the smaller concentrations. The permeabilities are not significantly different and the mean value is $10.8 \pm 0.7 \times 10^{-6}$ cm/s. This result is consistent with the liposome membrane remaining intact during exposure of high concentrations of the donor solution.

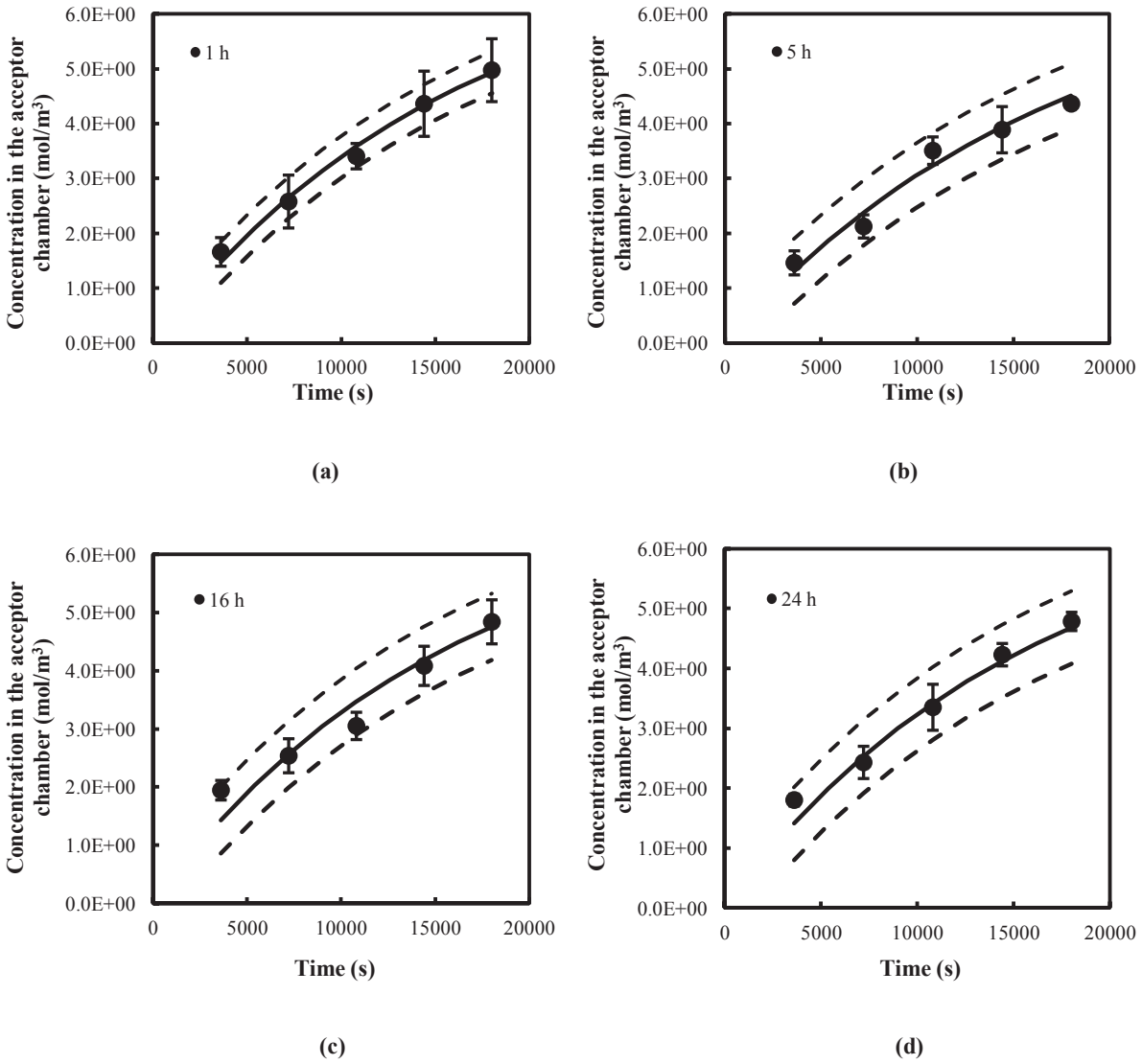

Figure 4.14 The continuous diffusion of caffeine (filled circles) after pre-treatment times of (a) 1, (b) 5, (c) 16 and (d) 24 h. The data are fitted to Equation 3.6 (solid lines) with 95 % confidence intervals (dashed lines). The error bars represent standard errors of three repeats.

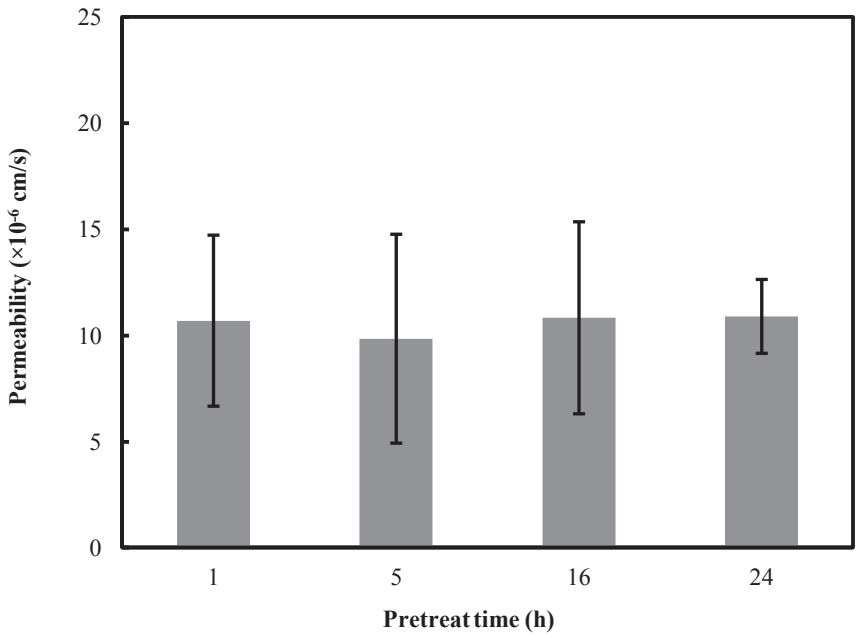

Figure 4.15 Permeability of caffeine from the continuous method after pre-treatment times of 1, 5, 16 and 24 h. The mean values were calculated from three independent repeats and the error bars represent 95% confidence interval of the three repeats.

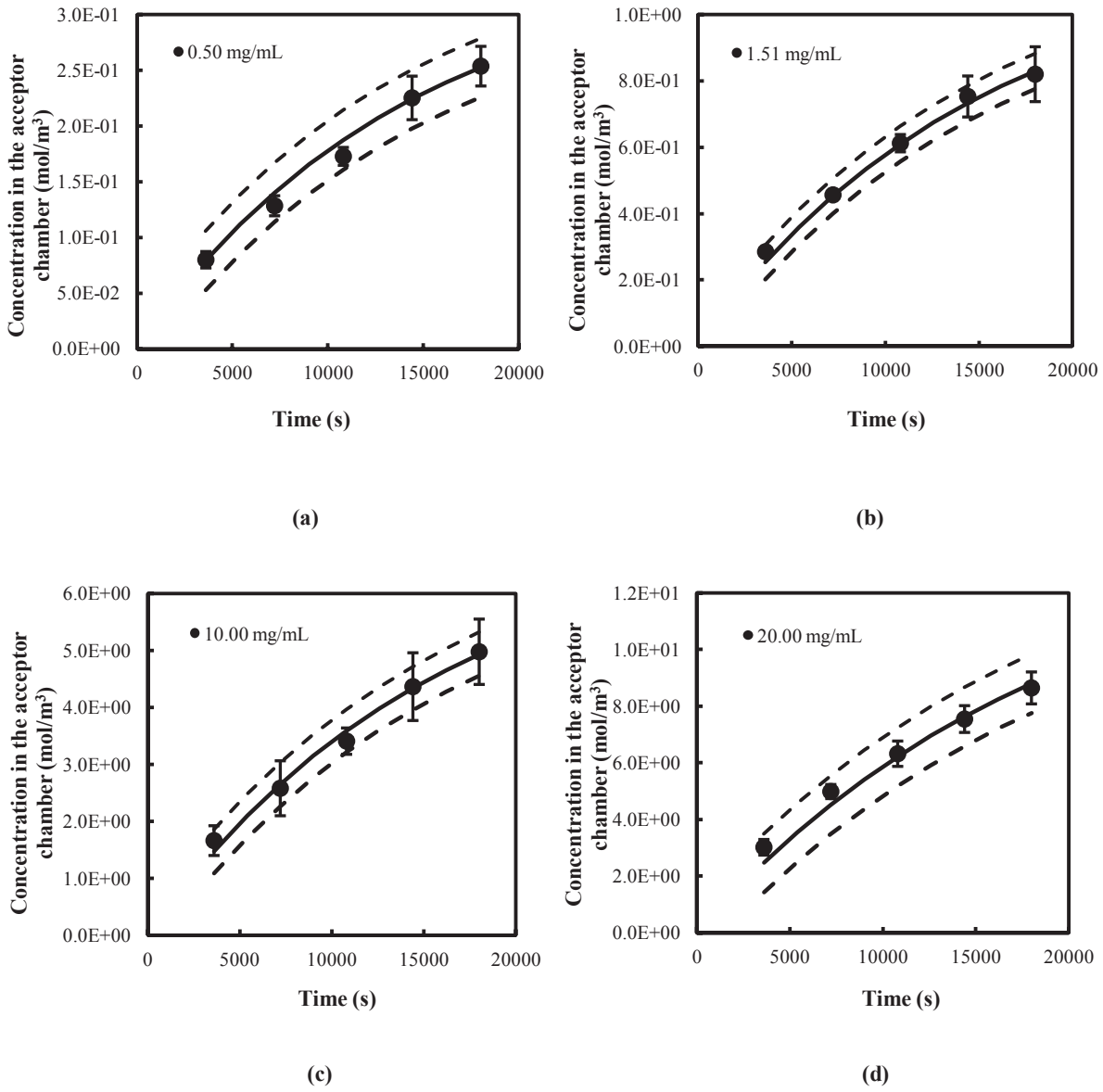

Figure 4.16 The continuous diffusion of caffeine for donor concentrations of (a) 0.50, (b) 1.51, (c) 10.00 and (d) 20.00 mg/mL. The data are fitted to Equation 3.6 (solid lines) with 95 % confidence intervals (dashed lines). The error bars represent standard errors of three repeats.

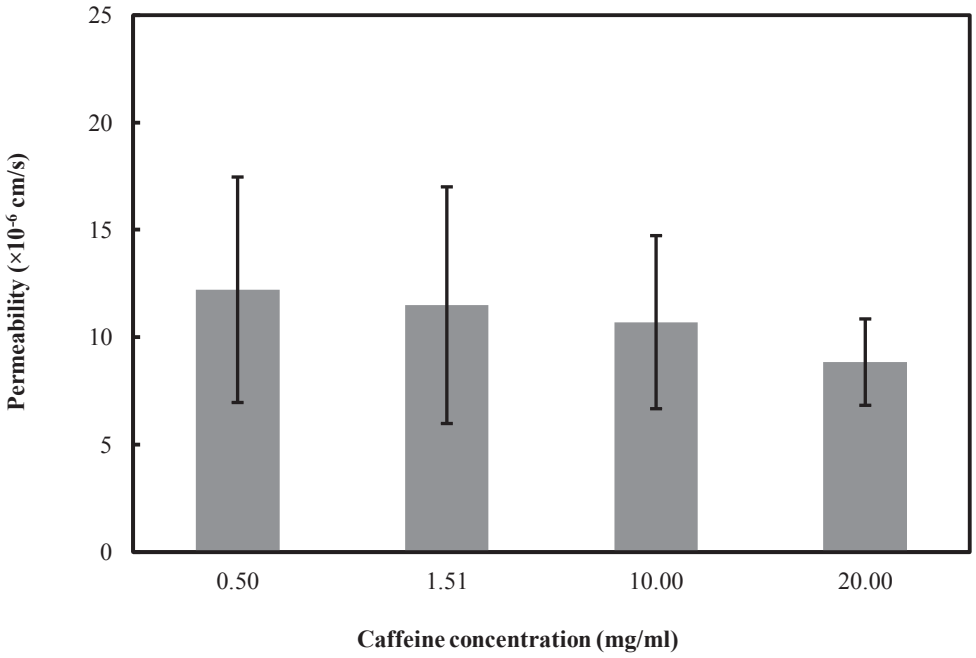

Figure 4.17 Permeability of caffeine for donor concentrations of 0.50, 1.51, 10.00 and 20.00 mg/ml. The mean values were calculated from three independent repeats and the error bars represent 95% confidence intervals of the three repeats.

4.2.8. The impact of the desorption on the permeability

To investigate any over-estimation of the permeability due to the release of caffeine in the acceptor chamber, the values of *A* and *B* were obtained by fitting the desorption data in Figure 4.11 to Equation 3.9, which are 0.097 ($s^{-0.21}$) and 0.21 respectively (see Figure 4.18). In Figure 4.19, the continuous diffusion data of caffeine after pre-treatment in Figure 4.12 is fitted to Equation 3.8 using MATLAB. The best fit value of the permeability is $10.9\pm1.4 \times10^{-6}$ cm/s, which is comparable to the value ($11.5\pm1.3 \times10^{-6}$ cm/s) from the continuous diffusion model.

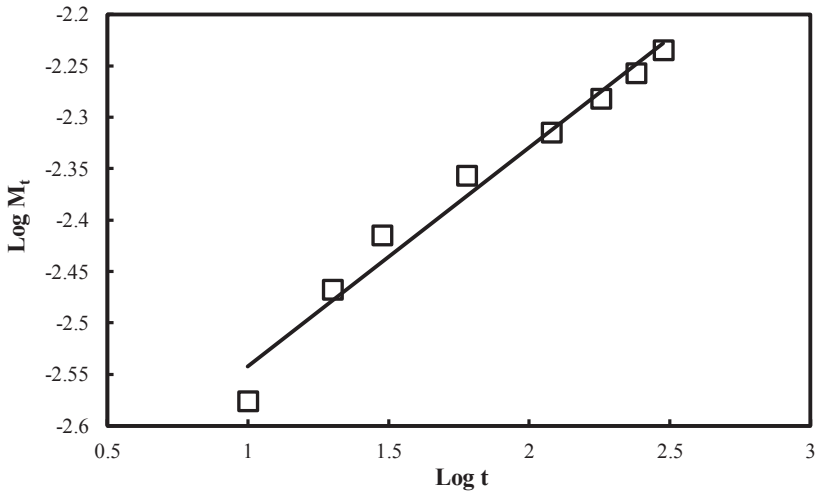

Figure 4.18 Desorption data for caffeine fitted to Equation 3.9 to obtain the values of *A* and *B*, which are 0.097 and 0.21 respectively.

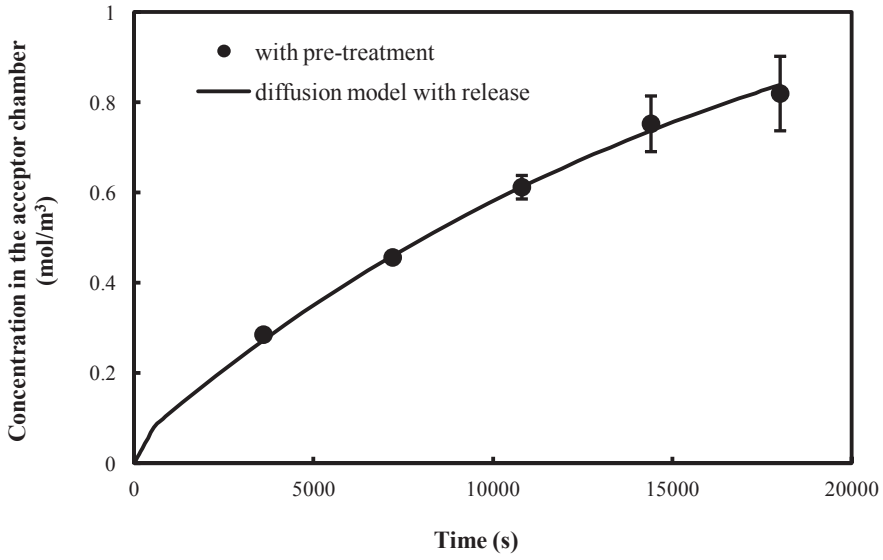

Figure 4.19 The continuous diffusion of caffeine (1.51 mg/mL) after pre-treatment. The data are fitted to Equation 3.8 using MATLAB.

4.3 SUMMARY

In this chapter, the results of the characterisation of the liposome membrane and the molecular diffusion through the liposome membrane can be summarised as:

- The sizes of the liposome could be effectively controlled by extrusion through polycarbonate filter membranes to obtain 535±20 nm with a 800 nm membrane and 320±14 nm with a 400 nm membrane, which were stable for at least 24 h.
- The smaller sized liposome occupied the pores of the substrate membrane by about 90±3 μm in thickness while the larger ones formed a compact layer of about 95±2 μm with few visible pores under the cryo-SEM. The liposome membrane showed no swelling or morphological changes after diffusion.
- The pre-treatment of the membrane with caffeine reduced or eliminated the time lag to the extent that the amount diffused increased after a give time, indicating the importance to account for the absorption of the diffusant in the membrane.
- $1.52\pm0.05 \times10^{-7}$ mol caffeine was absorbed in the liposome membrane, which corresponds to the difference in the amount of the diffused caffeine when the liposome membrane was pre-treated or without pre-treatment.
- The continuous model fits the diffusion closely and the permeability of caffeine through the pre-treated membrane is $11.5\pm1.3\times10^{-6}$ cm/s, which is a factor of two greater than that when untreated. Agitation of the system had no significant impact on the permeability.
- The liposome membrane remains intact during exposure of high concentrations of the donor solution within 24 hours.
- The permeability was not significantly influenced by the desorption of the caffeine.

CHAPTER 5: PHYSICOCHEMICAL ENHANCEMENT OF THE MOLECULAR DIFFUSION THROUGH THE LIPOSOME MEMBRANE

5.1 INTRODUCTION

An improved method of the diffusion through the liposome membrane with a continuous model was established in the previous chapter based on measurements with caffeine. In this chapter, diffusion of the five model diffusants (including acyclovir, amphotericin B, nadolol, paracetamol and theophylline) was carried out to evaluate the improved liposome membrane model by comparing the permeability of the model diffusants obtained from the model in this work with those from the other established *in vitro* models including PAMPA and Caco2, and the human absorption data in the literature.

The application of diffusion enhancers of ethanol and DMSO was explored firstly on caffeine: the diffusion of caffeine was carried out by adding different aqueous solutions of ethanol and DMSO with different concentrations. The diffusion of the other model diffusants was then performed with the most effective formulations. The impact of ethanol and DMSO on the mechanical properties of the liposome was examined; and the sizes of the liposome with ethanol were measured in order to ensure that the enhanced diffusion was not due to damage of the liposome in the membrane.

Finally, the application of the liposome membrane method was explored by considering the synergetic effect of drugs and their formulations. The diffusion of paracetamol with caffeine through a liposome membrane was carried out to examine if they have a positive or negative synergy on each other.

5.2 RESULTS

5.2.1. UV calibration of the model diffusants

Calibration was carried out using UV spectroscopy to obtain the absorptivity, ε, of each molecule and, as shown in Figure 5.1, the data were linear. The values of λ_{max} and the absorptivity, ε, of each molecule are listed in Table 5.1 with $R^2 > 0.99$.

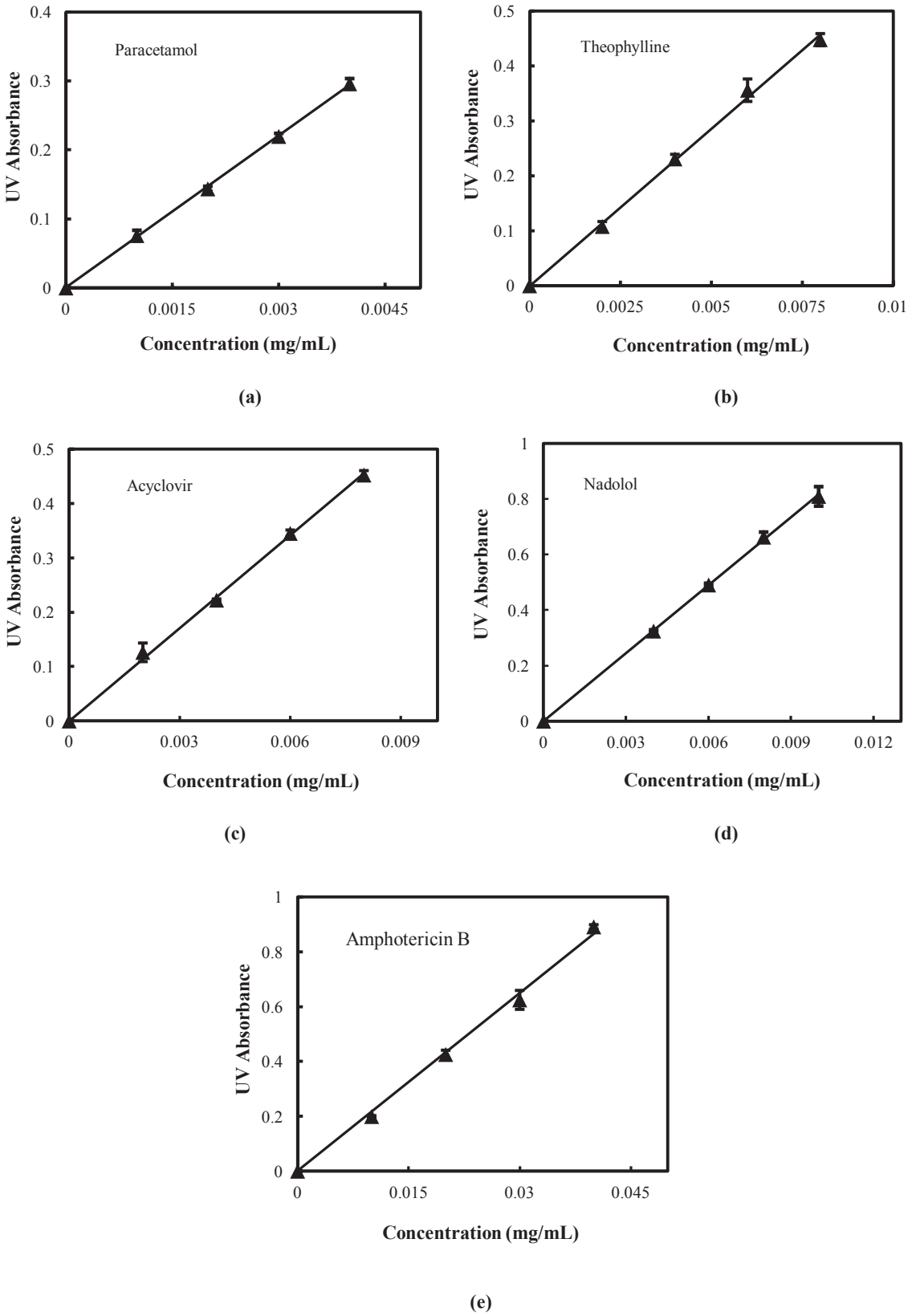

Figure 5.1 The UV calibration of the five diffusants: (a) paracetamol, (b) theophylline, (c) acyclovir, (d) nadolol and (e) amphotericin B. The calibration was performed in triplicates for each diffusant and the average UV absorbance was plotted against concentration with standard errors.

Table 5.1 The λ_{max} and the absorptivity ε of the five diffusants in the UV spectrum.

Diffusant	Paracetamol	Theophylline	Acyclovir	Nadolol	Amphotericin B
λ_{max} (nm)	241.5	272.0	251.0	199.0	332.0
Absorptivity ε	73.5	57.2	56.9	81.7	21.6
R^2 for the linear fitting	0.99	0.99	0.99	0.99	0.99

5.2.2. Continuous diffusion of the model diffusants

On the basis of the results obtained with caffeine, a continuous diffusion method was established with a pre-treatment of the liposome membrane using the same concentration as that for the donor solution. It was indicated in the preliminary experiment that 1 h of pre-treatment is sufficient for all the diffusants in this work to reach equilibrium between the concentrations in the liposome membrane and in the donor solution. The concentrations of the diffusant in the acceptor were plotted as a function of time and fitted to Equation 3.6 as shown in Figure 5.2. The permeability of the diffusant obtained from the fittings are listed in Table 5.2, which were normalised by that of caffeine, together with the previously published date using the original liposome membrane model, PAMPA, Caco-2 methods, and the human absorption data (F_a %, fraction absorbed).

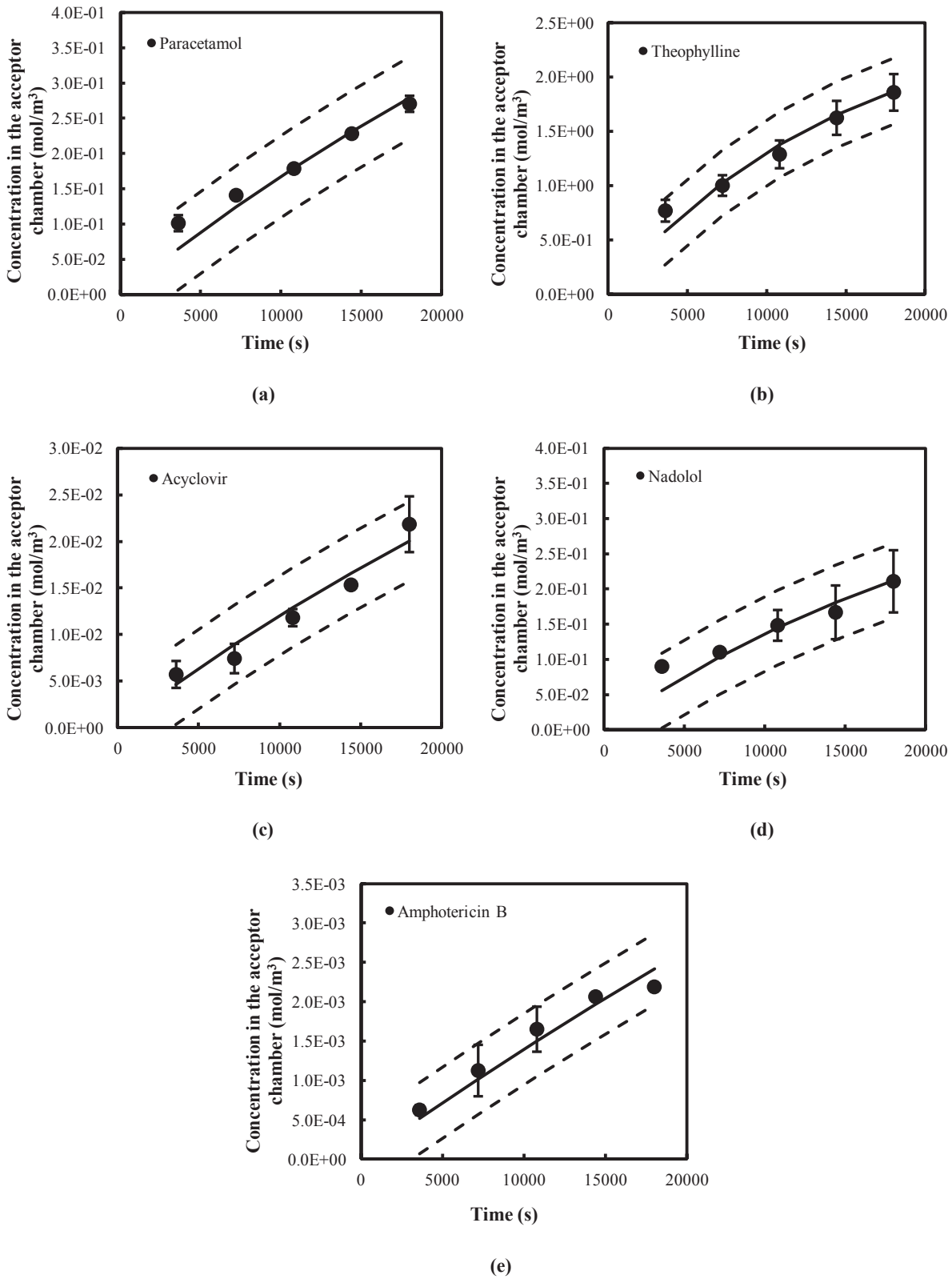

Figure 5.2 The continuous diffusion of the five diffusant through the liposome membrane: (a) paracetamol, (b) theophylline, (c) acyclovir, (d) nadolol and (e) amphotericin B. The experiments were performed in triplicates and an average concentration of the diffusant in the acceptor was plotted as a function of time (filled squares) with standard errors. The diffusion was fitted with the continuous diffusion model (in solid line) with 95 % confidence intervals (in dash lines).

Table 5.2 Permeability values (normalised by caffeine).

	[a]Human Absorption (F_a %)	Normalised permeability				
		[b]Continuous method	[c]Incremental method	[d,e]PAMPA	[f]Tri-layer PAMPA model	[g] Caco-2
Paracetamol	80	0.39±0.00	/	1.29±0.76, 0.32	/	0.97±0.19
Theophylline	97	1.29±0.32	/	0.03±0.00, 0.44	0.36±0.04	0.81±0.04
Caffeine	100	1.00±0.01	1.00±0.08	1.00±0.08, 1.00	1.00±0.15	1.00±0.05
Acyclovir	21	0.40±0.03	/	0.03±0.01, 0.00	0.00±0.00	0.09±0.02
Nadolol	35	0.52±0.15	0.05±0.01	0.23±0.03, 0.00	0.02±0.01	0.12±0.02
Amphotericin B	5	0.19±0.14	/	/, 0.00	/	0.00±0.00

[a] Literature F_a values (Zhu, Jiang et al. 2002).

[b] Data fitted to Equation 3.6.

[c] Literature values (Flaten, Dhanikula et al. 2006).

[d,e] Permeability values using a traditional PAMPA method where a hydrophobic/hydrophilic substrate membrane was coated with EPC solution in solvents (Kansy, Senner et al. 1998; Zhu, Jiang et al. 2002).

[f] Permeability values from a PAMPA model where a PVDF membrane was coated with lipid/oil/lipid tri-layer from reference (Chen, Murawski et al. 2008).

[g] Literature values (Yazdanian, Glynn et al. 1998; Yamashita, Furubayashi et al. 2000; Siissalo, Laine et al. 2010)

The permeability results from the improved liposome model are consistent with human absorption data in that a molecule with a greater F_a had a greater permeability, and *vice versa*. Compared with the other established *in vitro* methods, the improved liposome model achieves an outstanding ranking for the poorly absorbed molecules. For example, amphotericin B was incorrectly predicted to be impermeable in the PAMPA model, while the continuous liposome model gave a permeability of 0.19±0.14, which indicated a low absorption rather than no absorption in the human GI tract. Nadolol had a very low permeability of 0.05±0.01 in the original liposome membrane model; in contrast, it had a permeability of 0.52±0.15 from the improved method that agrees more closely with the 35 % human absorption.

Thus far the continuous diffusion method and associated data analysis has been demonstrated to be a useful *in vitro* tool for an improved prediction of the human absorption, and plots of the human absorption as a function time and the permeability from the *in vitro* methods will be compared in Chapter 8.

5.2.3. Physicochemical enhancement of the molecular diffusion by ethanol and DMSO

5.2.3.1. The diffusion of caffeine with ethanol/DMSO

The potential physicochemical enhancement of ethanol and DMSO on molecular diffusion was firstly investigated using caffeine (10 mg/mL). UV spectra of the ethanol and DMSO used in this work were measured initially and it was observed that they had no UV absorbance across the wavelengths of all the diffusants. Figure 5.3 showed the diffusion of 10 mg/mL caffeine through the liposome membrane with 1, 10 and 40 % (v/v) ethanol and with 30 % DMSO (only the data at 30 % is shown as the data at 10 and the 50% were similar). The diffusion data was fitted to Equation 3.6 with 95% confidence intervals and $R^2 > 0.94$.

The enhancement in diffusion based on the permeability data obtained from the fittings (enhancement is defined as: $\frac{Permeability\ with\ enhancer - Permeability\ without\ enhancer}{Permeability\ without\ enhancer}$) are shown in Figure 5.4. Statistically, there was no significant difference between the enhancement obtained for 1 and 10 % ethanol, which promoted the diffusion of caffeine by an average of 22.8±11.2 %. There was a significant enhancement in the presence of 40 % ethanol for which there was an increase of 58.3±9.0 %. In contrast, DMSO had a very limited effect with a

mean increase of 5.3±2.6 %; there was no significant difference in the three concentrations of DMSO.

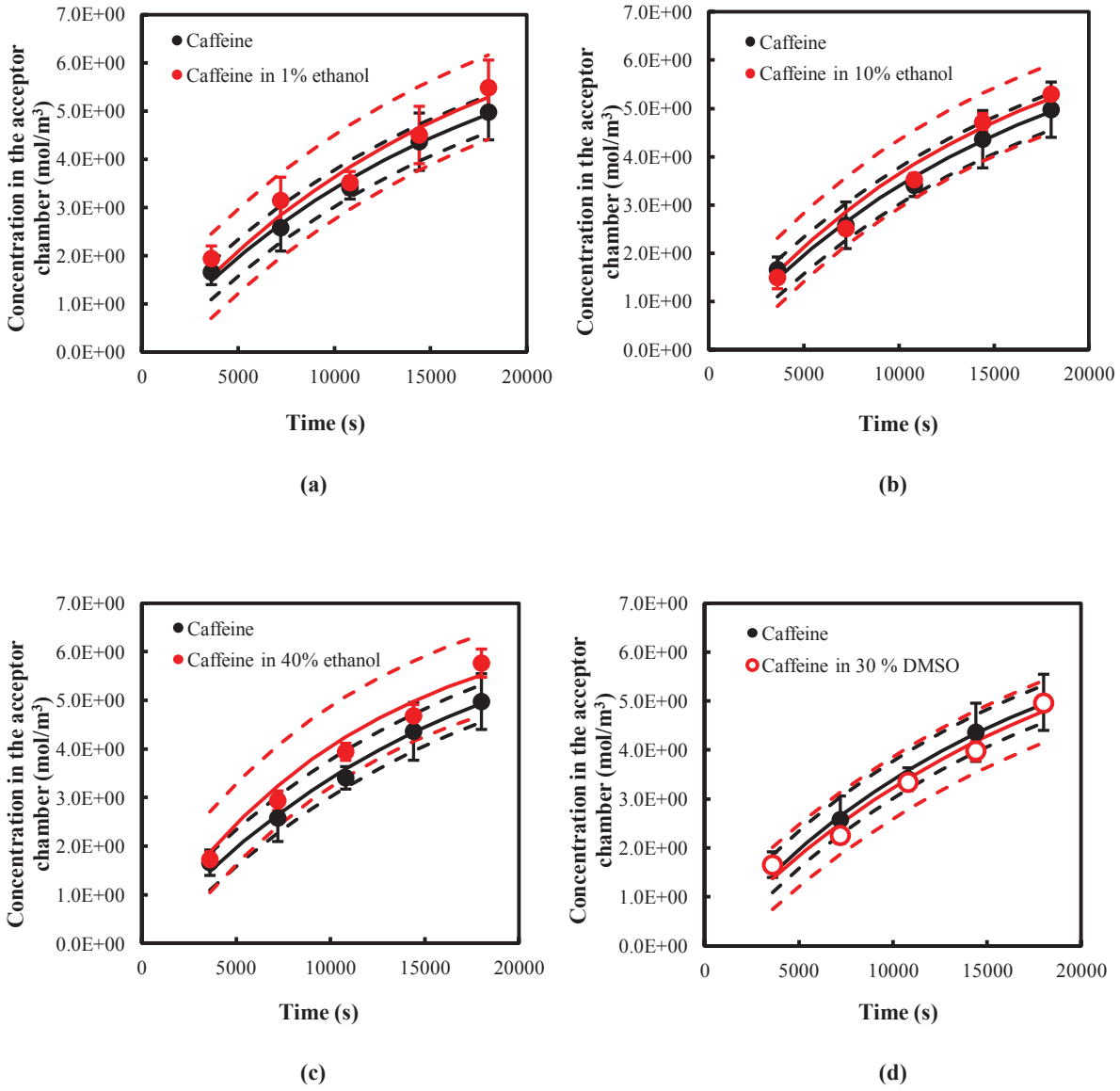

Figure 5.3 The physicochemical enhancement of caffeine diffusion by (a) 1, (b) 10, and (c) 40 % ethanol, and (d) 30 % DMSO: the experiments were performed in triplicates and an average concentration of caffeine with ethanol (filled red squares), DMSO (open red squares) and without (filled black squares) in the acceptor chamber was plotted against time with standard errors. The diffusion was fitted with the continuous diffusion model (in solid line) with 95 % confidence intervals (in dash lines).

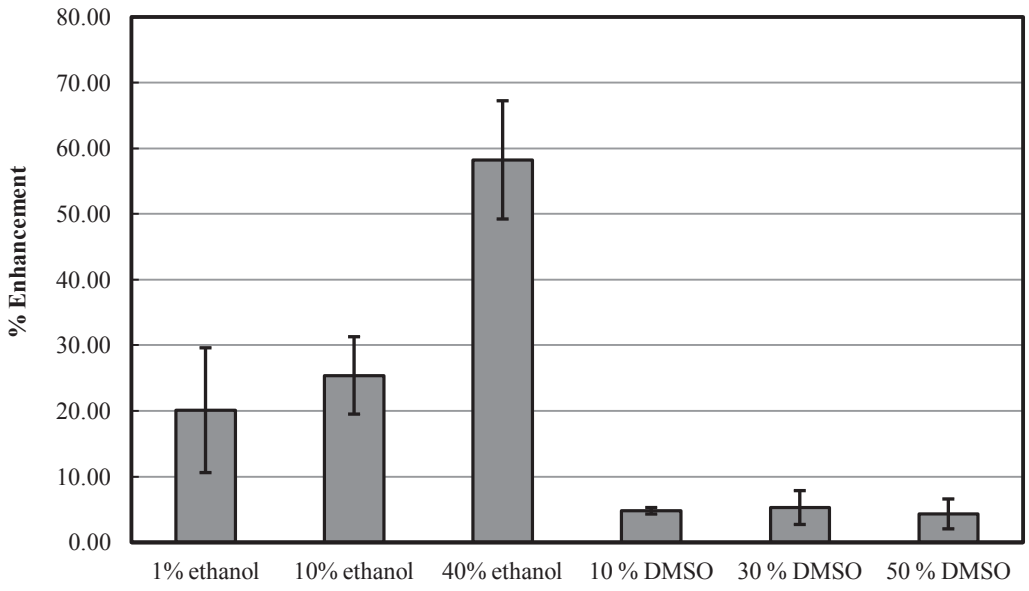

Figure 5.4 The physicochemical enhancement (%) based on the permeability obtained from Figure 5.3 of the 1 %, 10 %, 40 % (v/v) ethanol and 10 %, 30 %, 50 % (v/v) DMSO on the diffusion of 10 mg/mL caffeine. Errors bars are the 95 % confidence intervals of three repeats.

5.2.3.2. The diffusion of the model diffusants with ethanol/DMSO

The permeability measurements of the model diffusants with ethanol/DMSO mixtures were carried out using a similar procedure to that for caffeine. A 40 % aqueous ethanol solution was used as it had proven to be most effective in promoting the diffusion of caffeine, and 30 % DMSO was also used as a comparison. Figure 5.5 showed the diffusion of the five model diffusants and the diffusion data were fitted to the continuous diffusion model with 95% confidence intervals; for all the data fittings, $R^2 > 0.80$.

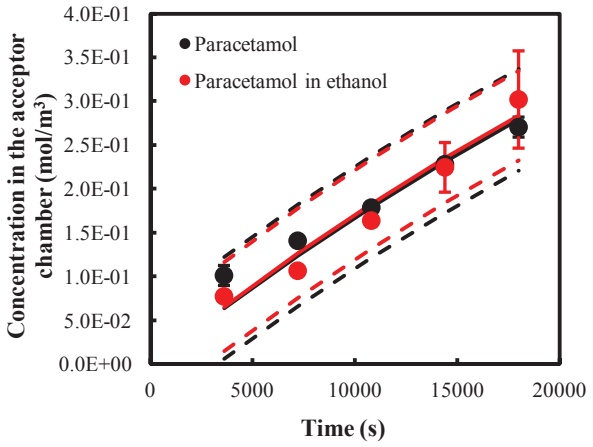
Paracetamol
Paracetamol in ethanol
Concentration in the acceptor chamber (mol/m³)
Time (s)

(a)

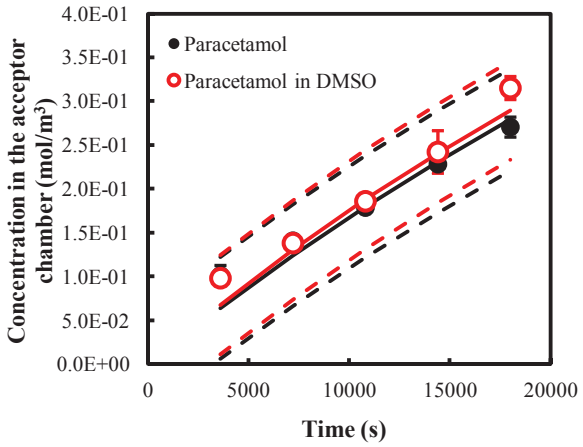
Paracetamol
Paracetamol in DMSO
Concentration in the acceptor chamber (mol/m³)
Time (s)

(b)

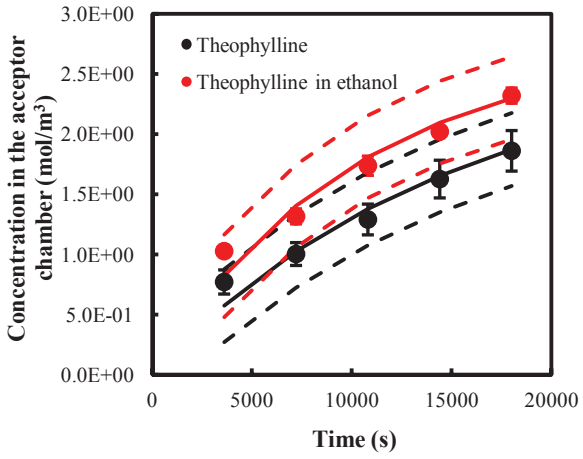
Theophylline
Theophylline in ethanol
Concentration in the acceptor chamber (mol/m³)
Time (s)

(c)

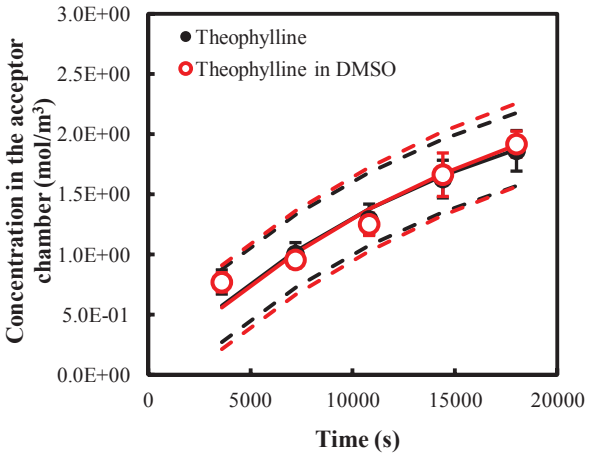
Theophylline
Theophylline in DMSO
Concentration in the acceptor chamber (mol/m³)
Time (s)

(d)

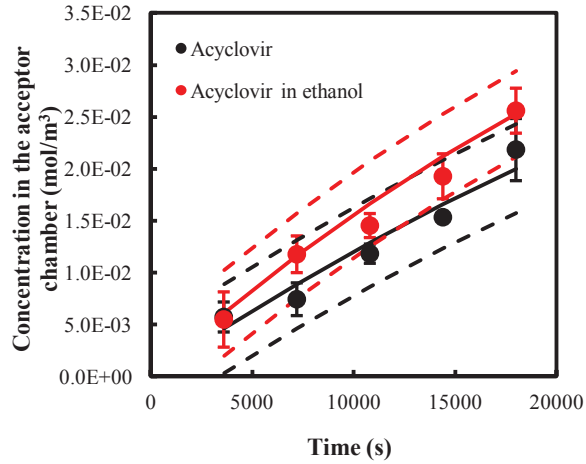
Acyclovir
Acyclovir in ethanol
Concentration in the acceptor chamber (mol/m³)
Time (s)

(e)

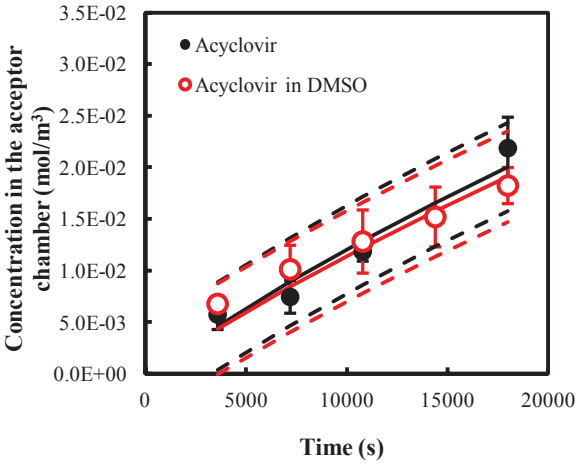
Acyclovir
Acyclovir in DMSO
Concentration in the acceptor chamber (mol/m³)
Time (s)

(f)

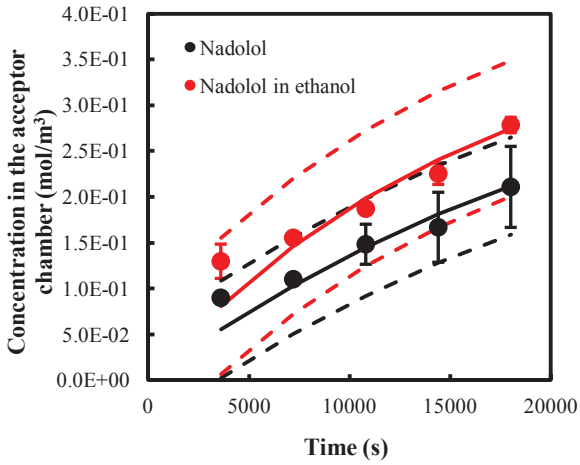

(g)

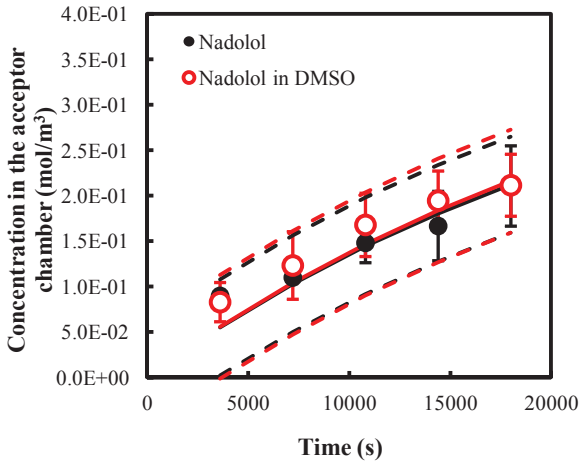

(h)

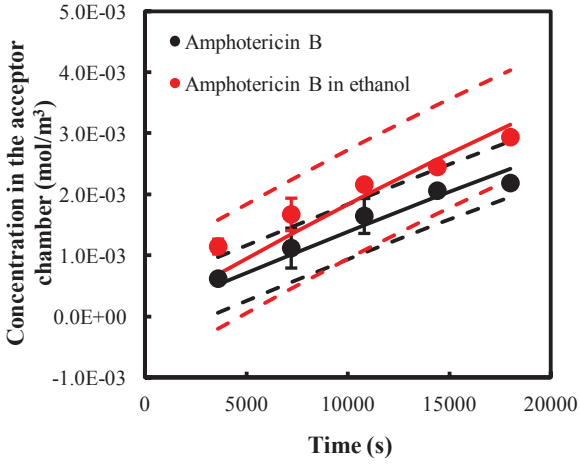

(i)

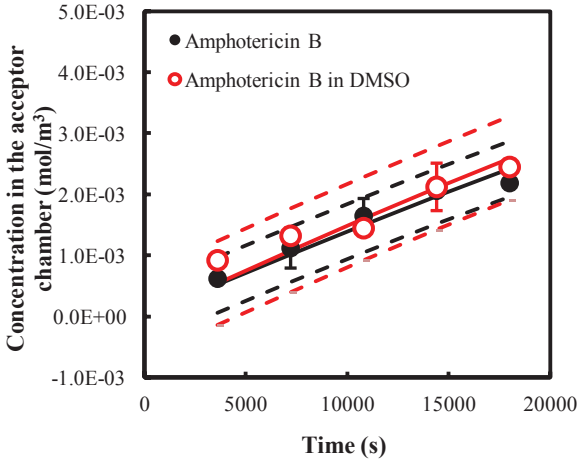

(j)

Figure 5.5 The physicochemical enhancement of molecular diffusion by ethanol/DMSO: (a) paracetamol in 40 % ethanol; (b) paracetamol in 30 % DMSO; (c) theophylline in 40 % ethanol; (d) theophylline in 30 % DMSO; (e) acyclovir in 40 % ethanol; (f) acyclovir in 30 % DMSO; (g) nadolol in 40 % ethanol; (h) nadolol in 30 % DMSO; (i) amphotericin B in 40 % ethanol and (j) amphotericin B in 30 % DMSO. The experiments were performed in triplicates and an average concentration of the diffusant with ethanol (filled red squares), DMSO (open red squares) and without (filled black squares) in the acceptor was plotted against time with standard errors. The diffusion was fitted with the continuous diffusion model (in solid line) with 95 % confidence intervals (in dash lines).

In Figure 5.6, the measured values of the permeability are shown for each diffusant in the order of their molecular weights. Ethanol did not significantly increase the permeability of paracetamol as it did for caffeine; however, it effectively promoted the diffusion of theophylline by 43.8±2.9 %, nadolol by 37.4±2.5 %, acyclovir by 33.8±0.9 % and amphotericin B by 34.3±0.1 %. However, the effect of the DMSO was much less than that of ethanol, with an enhancement of 14.0±0.1 % for the paracetamol and no significant enhancement for the other diffusants. The results indicate that the widely used ethanol and DMSO did not necessarily enhance diffusion through the liposome membranes.

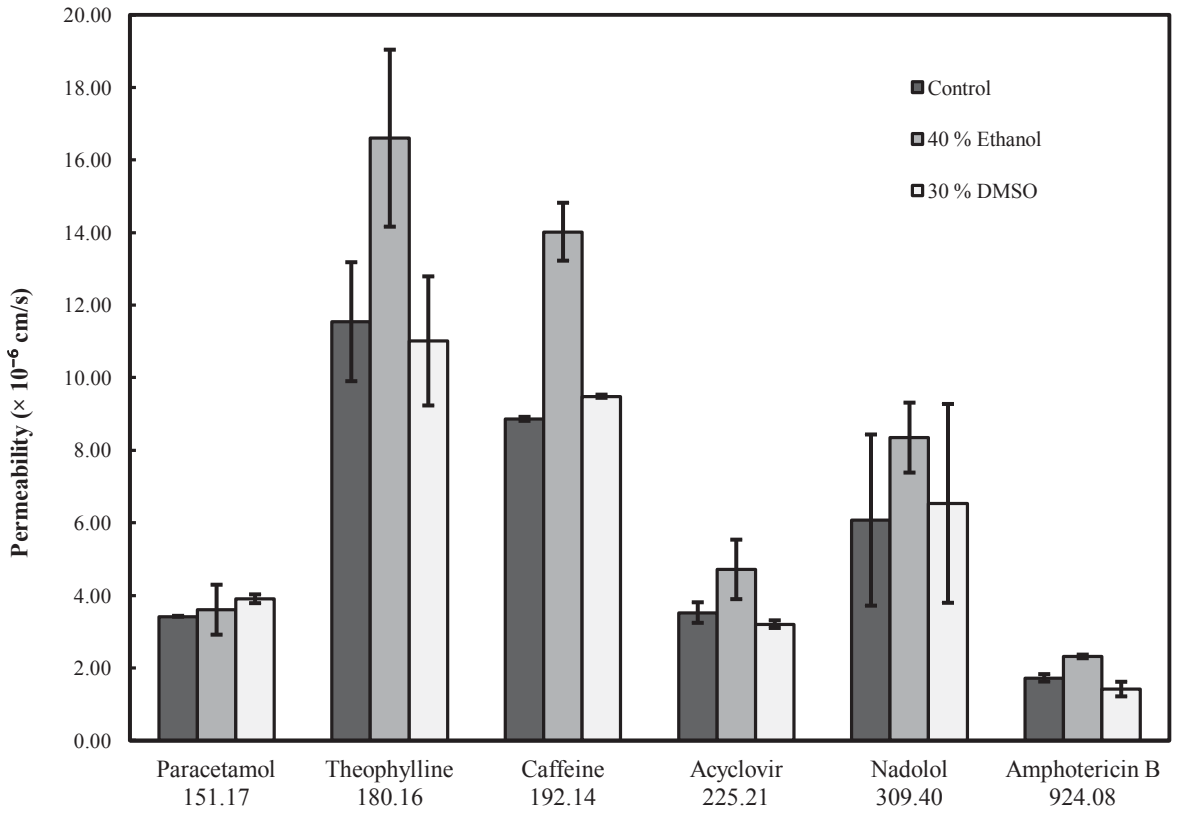

Figure 5.6 The permeability of the model diffusants with/without diffusion enhancers (40 % ethanol/30 % DMSO) obtained from the fittings in Figure 5.5. The error bars are the 95 % confidence intervals of three repeats.

5.2.3.3. The impact of ethanol/DMSO on the mechanical properties of the liposome

The Young's modulus and hardness of liposome membranes after immersion in the PBS solution, and 40% ethanol and 30 % DMSO solutions was obtained by AFM at room temperature (18-19 ^{o}C). These liquids were expected to interrupt the morphology structures and influence the fluidity of the lipid bilayer (Williams and Barry 2004; Rebecca Notman 2006) and thus lead to increased permeability. Ethanol did not reduce the Young's modulus of the liposome significantly while it decreased by 61.7±13.0 % in 30 % DMSO as shown in Figure 5.7. The hardness showed the same trend in that the decrease by the ethanol was not significant while DMSO resulted in a reduction of 33.6±6.1 % (Figure 5.8). Since the mechanical properties should be sensitive to the morphology, the data suggest this is not a significant factor in determining the extent of the permeability enhancement.

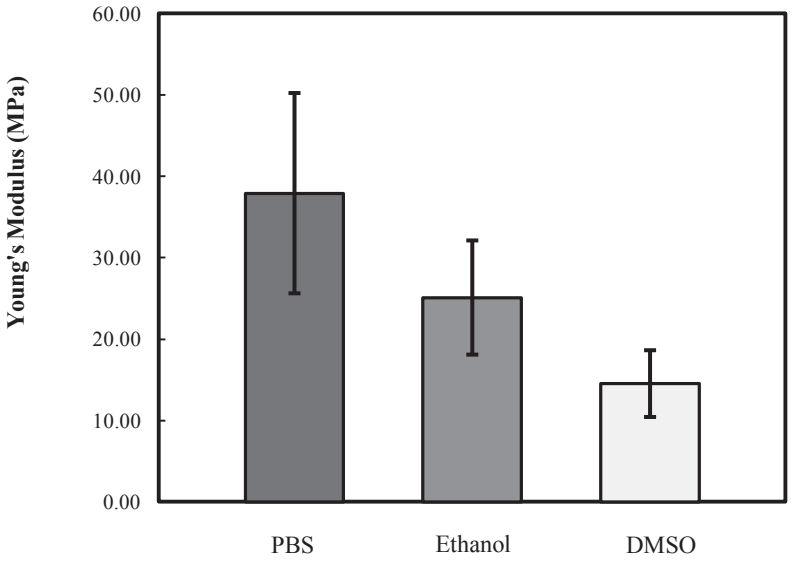

Figure 5.7 The Young's modulus of the liposome membrane after pre-treated with PBS solution, 40% ethanol, and 30 % DMSO solution. The error bars represent the 95 % confidence intervals from 25 measurements.

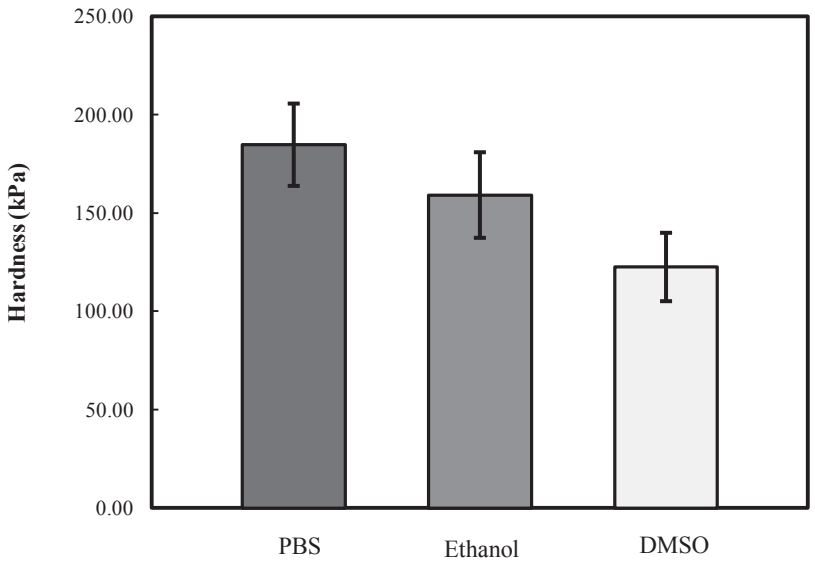

Figure 5.8 The hardness of the liposome membrane after pre-treated with water, 40% ethanol and 30 % DMSO solution. The error bars represent the 95 % confidence intervals from 25 measurements.

5.2.3.4. The impact of ethanol on the size of the liposome

As ethanol appears to induce the most diffusion enhancement, the size distribution of the liposomes extruded through the 800 nm and the 400 nm polycarbonate membrane filter, and those in the 10 % and 40% ethanol solution were measured to examine if the liposome remained intact with ethanol. In Figure 5.9 (a), the liposome in 10 % ethanol after extrusion through an 800 nm filter had a similar size with a slightly narrower distribution and the liposome in 40% ethanol showed a slightly smaller size of 476±52 nm compared without ethanol. Similarly, only small changes were observed after extrusion through the 400 nm membrane filter as shown in Figure 5.9 (b). A statistical analysis indicated that the ethanol did not have a significant impact on the size distribution.

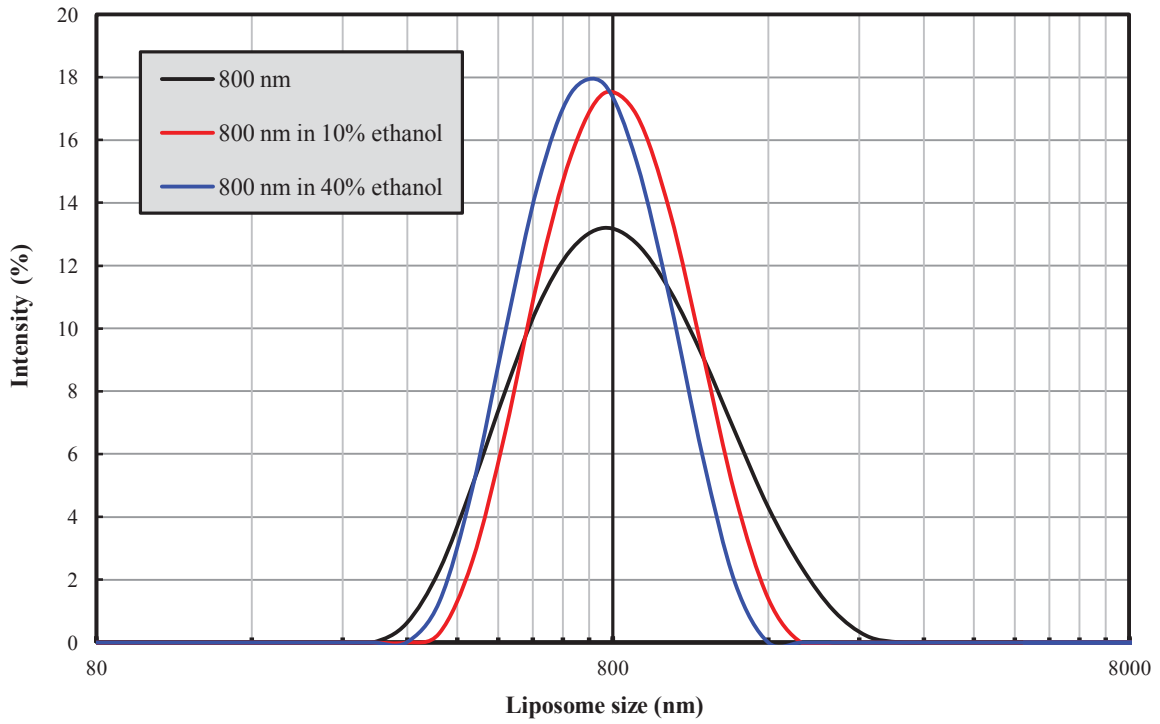

(a)

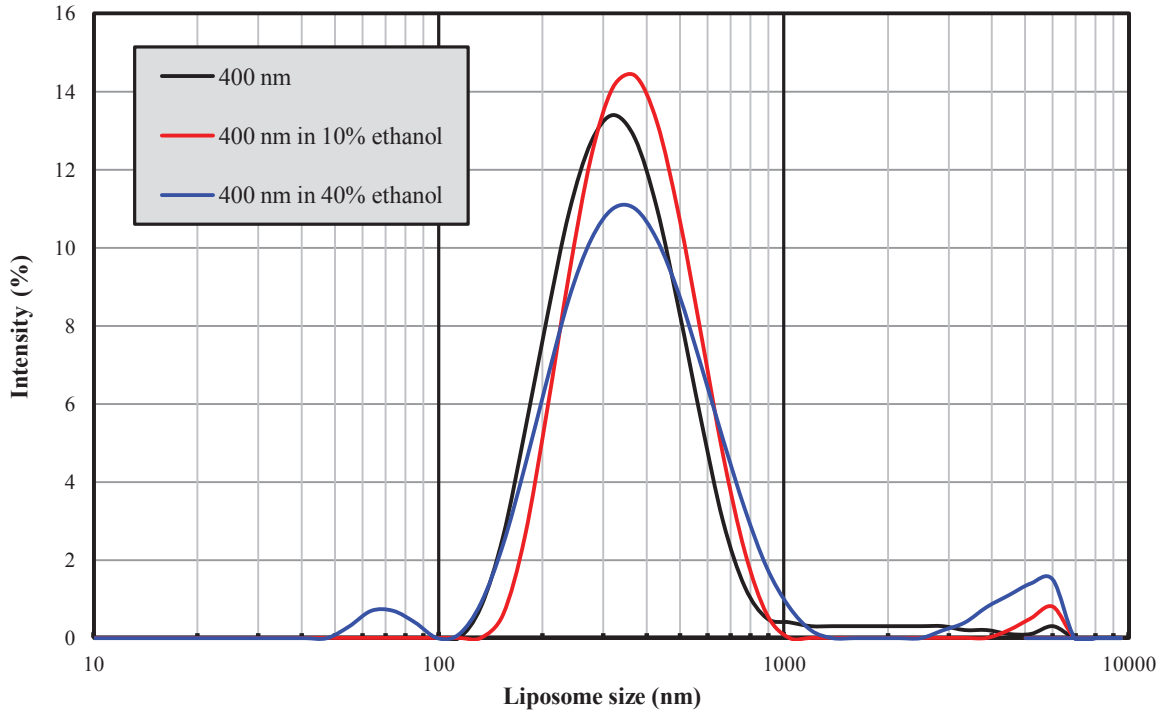

(b)

Figure 5.9 Size and size distribution of the EPC liposome treated with 10 %/40 %ethanol measured by HPPS: (a) liposome extruded through the 800 nm polycarbonate membrane filter and (b) liposome extruded through the 400 nm polycarbonate membrane filter. All the measurements were performed in triplicates and an average light intensity % distribution was plotted.

5.2.4. The diffusion of paracetamol with caffeine through the liposome membrane

5.2.4.1. HPLC calibration of paracetamol with caffeine at the λ_{max} of paracetamol

A typical chromatogram of a standard aqueous solution of 0.06 mg/mL paracetamol with caffeine scanned by HPLC at the λ_{max} of paracetamol is shown in Figure 5.10. The retention times were 2.741 min for paracetamol and 4.789 min for caffeine. The peak area of paracetamol was plotted as a function of concentration in Figure 5.11, the calibration slope was 368.6 mAU*min*mL/mg with an $R^2 > 0.99$.

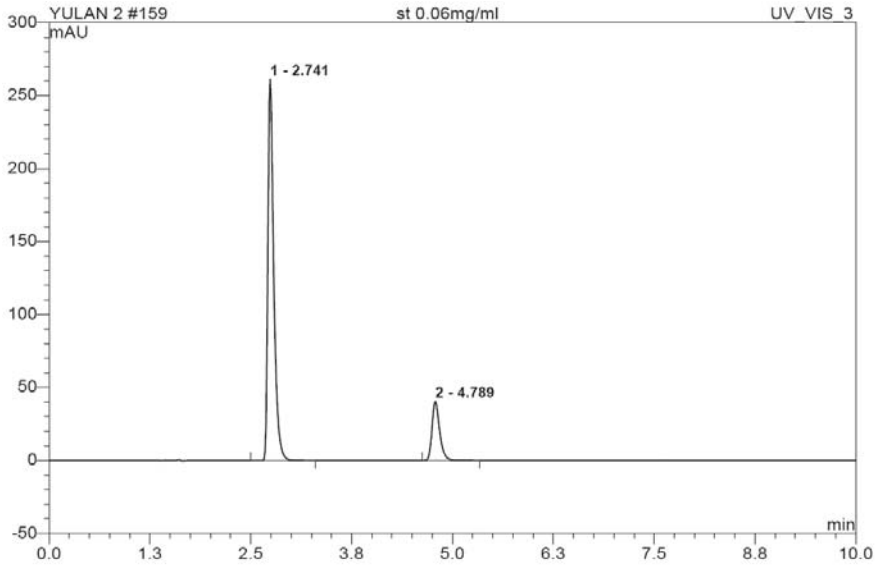

Figure 5.10 An example of the standard solution of 0.06 mg/mL paracetamol in 0.06 mg/mL caffeine scanned in HPLC at 242 *nm*: the peak at 2.741 min is that of paracetamol and 4.789 min is that of caffeine.

5.2.4.2. The diffusion of paracetamol with caffeine

The diffusion of paracetamol (1 mg/mL) with 1, 10 and 20 mg/mL caffeine was carried out after pre-treatment with the same solution as that for donor chambers. The concentration of the paracetamol in the donor chambers was analysed by HPLC and plotted in Figure 5.12, with a control diffusion of paracetamol without caffeine. The diffusion data were then fitted with the continuous diffusion model with $R^2 > 0.87$ to obtain the permeability values.

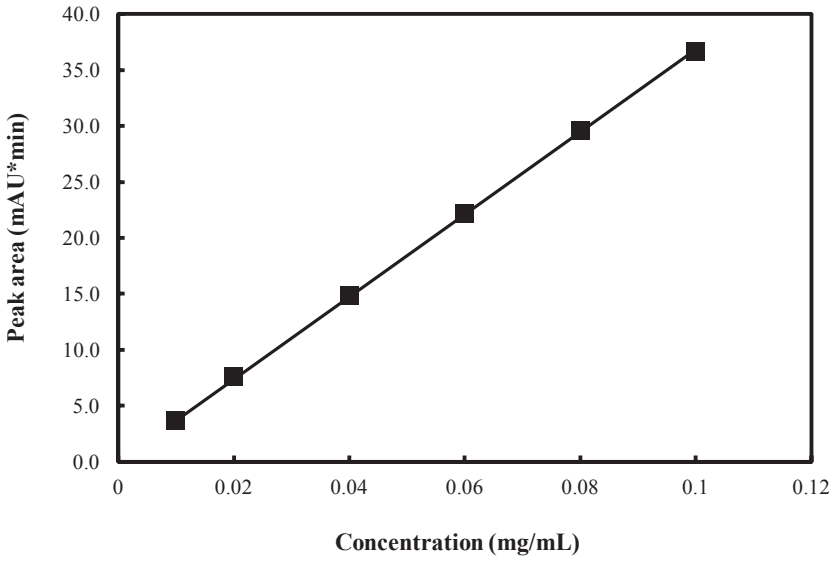

Figure 5.11 The calibration of paracetamol in caffeine by HPLC at 242 nm. The measurements were performed in triplicates and an average peak area was plotted against concentration with standard errors.

In Figure 5.13, the permeability of the paracetamol with and without caffeine obtained from the fittings in Figure 5.12 are shown. There was a significant decrease of 25.0±1.2 % in the permeability of paracetamol with 1 mg/mL caffeine compared without. A greater concentration of 10 mg/mL caffeine resulted in a further decrease in the permeability of

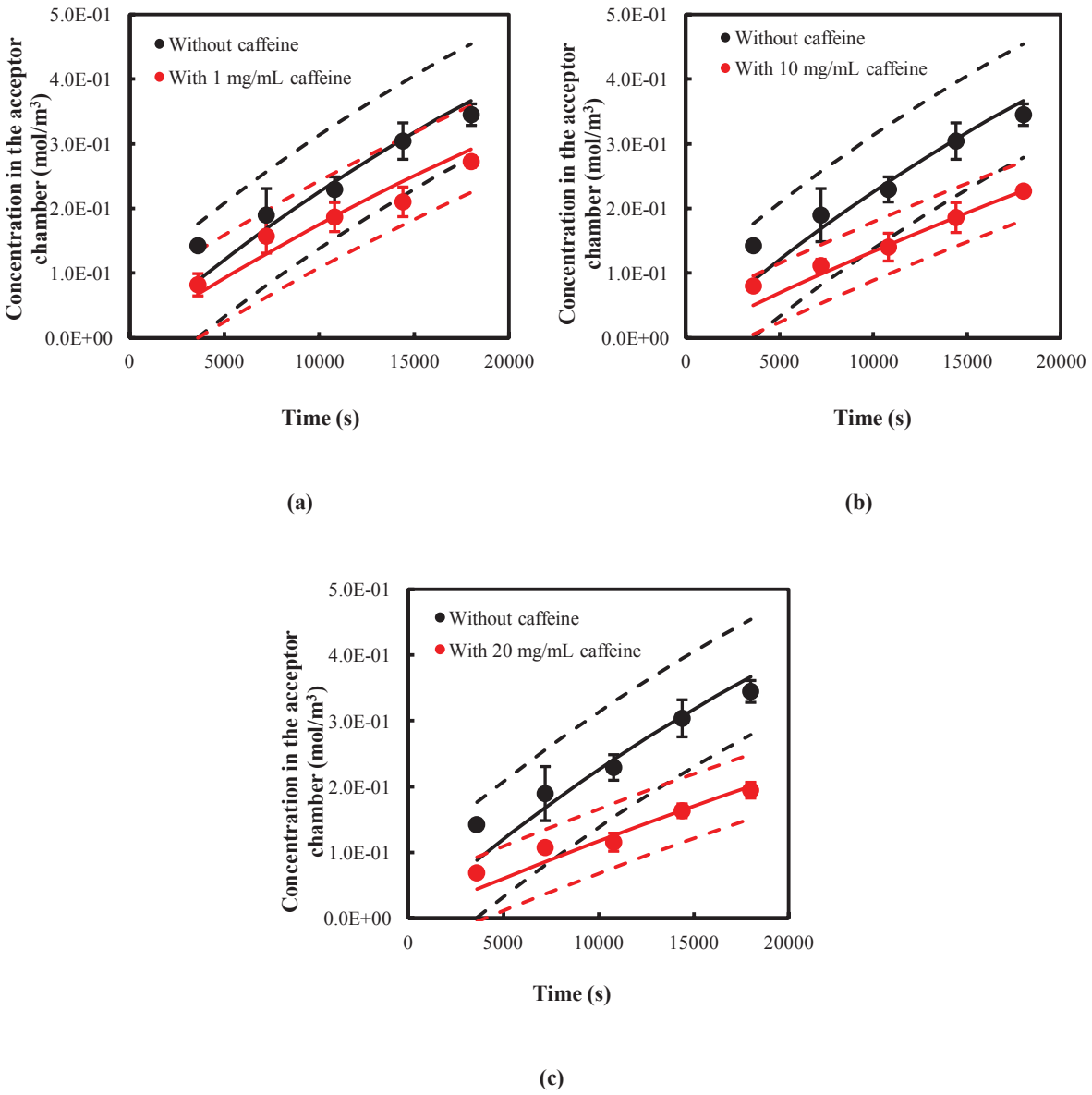

Figure 5.12 The diffusion of 1mg/mL paracetamol without caffeine and with (a) 1 mg/mL caffeine, (b) 10 mg/mL caffeine and (c) 20 mg/mL caffeine: the experiments were performed in triplicates and an average concentration of paracetamol in the acceptor chamber was plotted against time with standard errors. The diffusion data (in filled squares) was fitted with continuous diffusion model (in solid line) with 95 % confidence intervals (in dash lines).

paracetamol by 25.7±1.3 %, which also meant that the permeability of paracetamol was nearly half of that without caffeine. There was no further significant reduction of the permeability when the caffeine concentration increased to 20 mg/mL. This result has

indicated a negative synergetic effect of caffeine on the diffusion of paracetamol through the liposome membrane and the impact was dependent on the concentration of the caffeine for values less than ~ 10 mg/mL.

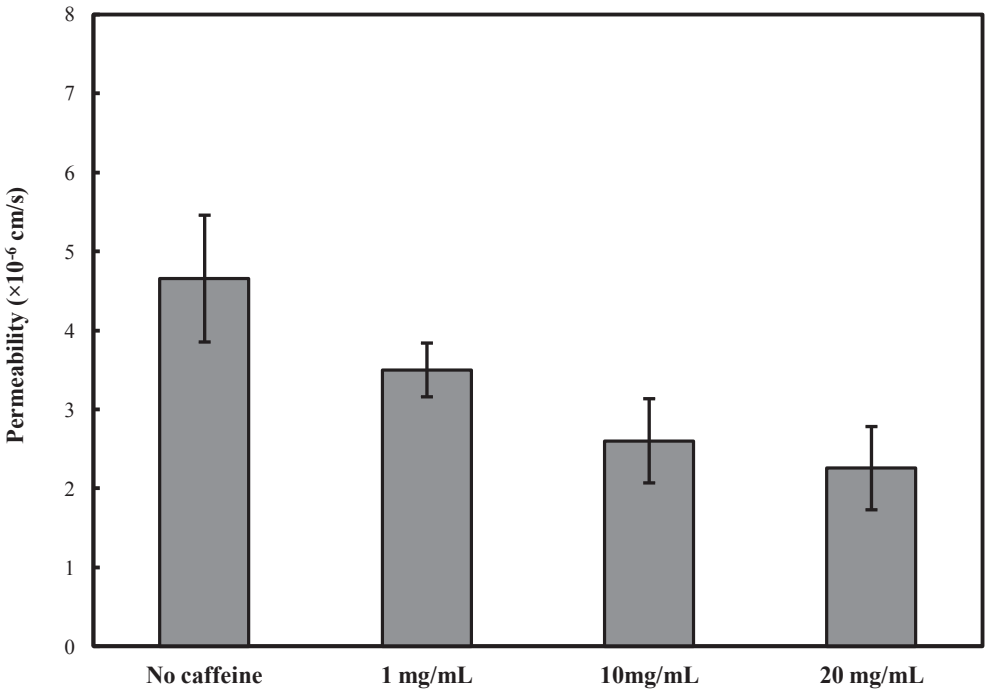

Figure 5.13 The permeability of 1 mg/mL paracetamol in 1, 10 and 20 mg/mL caffeine/without caffeine obtained from the fittings in Figure 5.12. The error bars are the 95 % confidence intervals of three repeats.

5.2.4.3. The diffusion of caffeine with paracetamol

The diffusion of caffeine at 1, 10 and 20 mg/mL with paracetamol (1 mg/mL) could be obtained from analysing the results in section 5.2.4.2 by the HPLC scanning at the λ_{max} of caffeine. A typical chromatogram of caffeine with paracetamol scanned by HPLC at λ_{max} of caffeine is shown in Figure 5.14. The peak area of caffeine was plotted as a function of the

concentration as shown in Figure 5.15. The calibration slope was 246.2 mAU*min*mL/mg with an $R^2 > 0.99$.

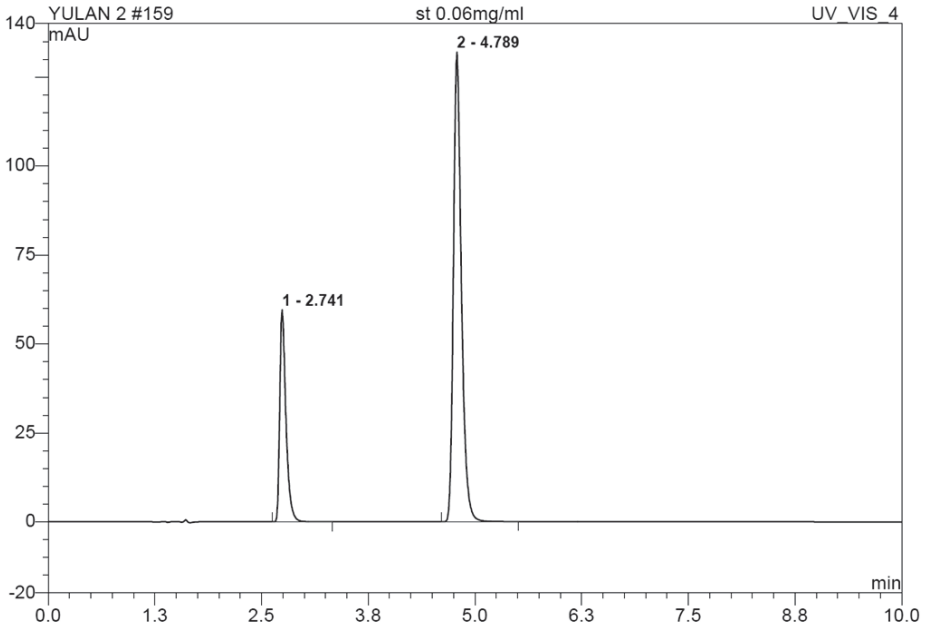

Figure 5.14 An example of the standard solution of 0.06 mg/mL caffeine in 0.06 mg/mL paracetamol scanned in HPLC at 273 *nm*: the peak at 2.741 min is that of paracetamol and 4.789 min is that of caffeine.

The diffusion of caffeine, with the concentration of paracetamol obtained by HPLC at 273 nm, is plotted in Figure 5.16 based on the calibration profile of caffeine. The diffusion data were fitted to the continuous diffusion model with $R^2 > 0.87$ to obtain the permeability values.

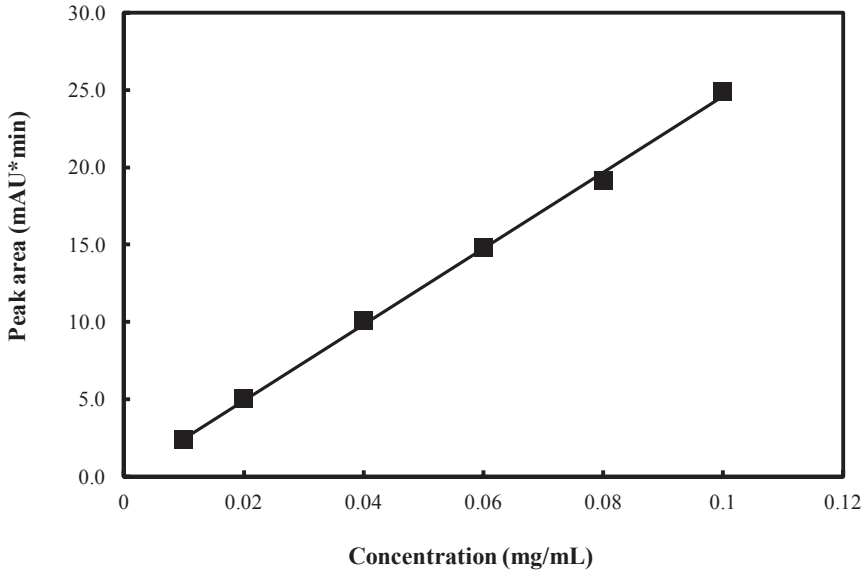

Figure 5.15 The calibration of caffeine with paracetamol by HPLC at 273 nm. The measurements were performed in triplicates and an average peak area was plotted against concentration with standard errors.

In Figure 5.17, the permeability values of the caffeine with paracetamol obtained from the fittings are shown in Figure 5.16. At the 95 % confidence level, there was no significant effect of paracetamol on the diffusion of the three concentrations of caffeine. This result has indicated although caffeine could retard the diffusion of paracetamol, the diffusion of caffeine was not influenced by paracetamol.

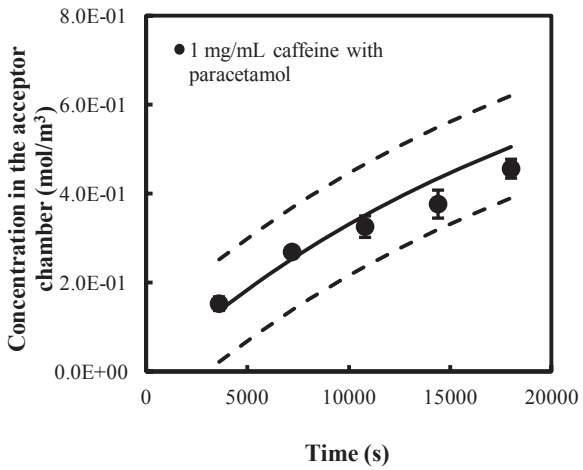

(a)

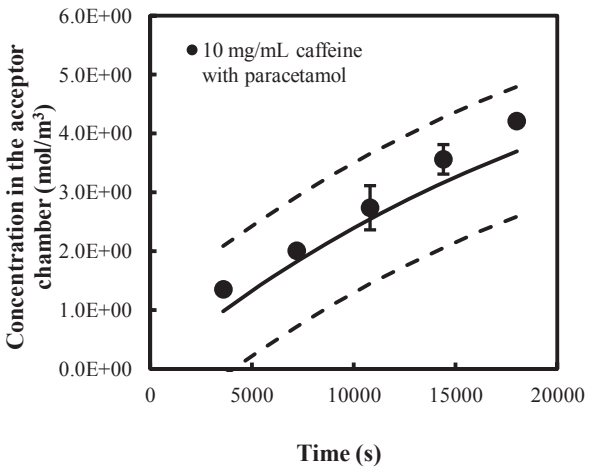

(b)

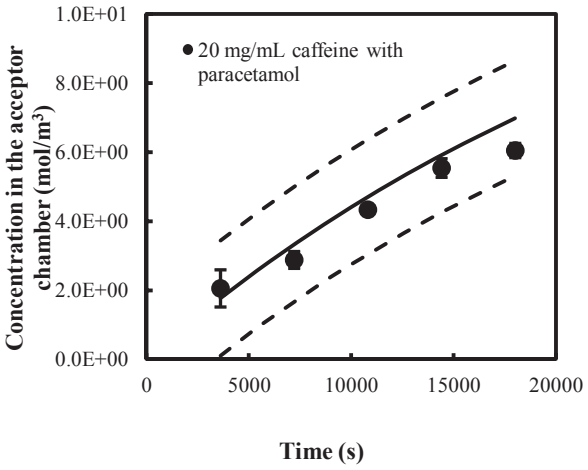

(c)

Figure 5.16 The diffusion of (a) 1 mg/mL caffeine with paracetamol, (b) 10 mg/mL caffeine with paracetamol and (c) 20 mg/mL caffeine with paracetamol: the experiments were performed in triplicates and an average concentration of caffeine in the acceptor chamber was plotted against time with standard errors. The diffusion data (in filled squares) was fitted with continuous diffusion model (in solid line) with 95 % confidence intervals (in dash lines).

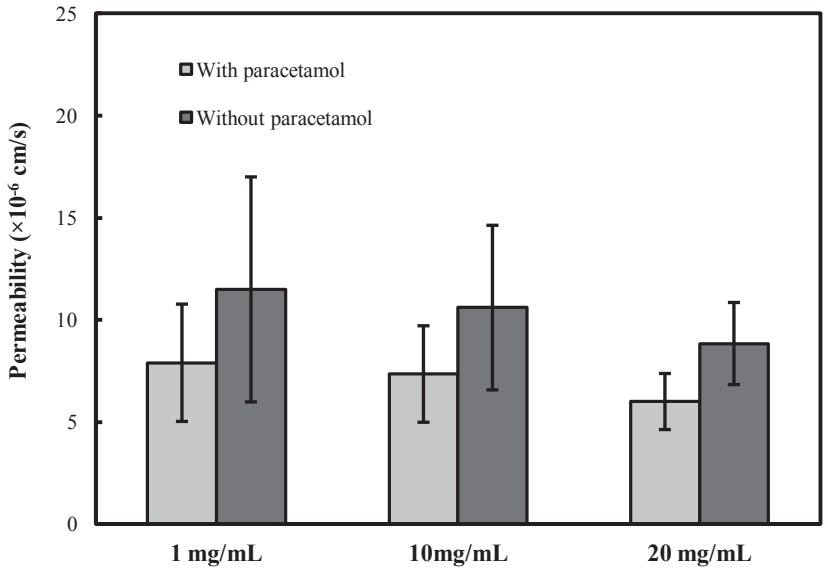

Figure 5.17 The permeability of 1, 10 and 20 mg/mL caffeine with paracetamol obtained from the fittings in Figure 5.16. The error bars are the 95 % confidence intervals of three repeats.

5.3 SUMMARY

In this chapter, the results of an investigation of potential physicochemical enhancement of molecular diffusion are described and can be summarised as:

- The permeabilities of five model diffusants were measured using the continuous method developed for caffeine.
- The physicochemical enhancement of the diffusion was carried out by adding ethanol and DMSO into the pre-treatment and donor solution: 40 % ethanol significantly promoted the diffusion of caffeine and theophylline by 58.3±9.0 % and 43.8±2.9 %, with a moderate enhancement of the other diffusants. In the case of 30 % DMSO, the permeability of paracetamol was increased by 14.0±0.1 % while it had no significant impact on the other diffusants.

- The mechanical properties of the liposome with and without ethanol and DMSO were measured by AFM and 30 % DMSO decreased both the Young's Modulus and hardness of the liposome while ethanol had no significant effect. The size and size distribution of the liposome with ethanol showed no significant difference indicating that the liposome remained intact.
- The diffusion of paracetamol with caffeine was carried out to investigate a possible synergetic effect of the two diffusants. The results showed that caffeine retarded the diffusion of paracetamol and the decrease of the permeability depended on the concentration of the retardant. In contrast, paracetamol had no significant effect on the diffusion of caffeine.

CHAPTER 6: THE DIFFUSION OF THE TPS THROUGH THE LIPOSOME MEMBRANE

6.1 INTRODUCTION

Tea polyphenols including Epicatechin (EC), epigallocatechin (EGC), epicatechin gallate (ECG) and epigallocatechin gallate (EGCG) are of growing interest, especially EGCG due to its unique health benefit of anti-bacteria, anti-oxidant and anti-cancer activity. However, they suffer from poor bioavailability if taken orally and the specific mechanisms involved with the health benefit still remain unclear. Hashimoto *et al*. investigated the interaction of TPs with lipid bilayers by using a liposome suspension (Hashimoto, Kumazawa et al. 1999), and a high affinity of ECG and EGCG to the lipid molecule such that it was suggested that they may perturb the membrane structure. Molecular dynamics simulation showed that EGCG has the strongest affinity to the lipid bilayer among all the TPs (Sirk, Brown et al. 2008; Sirk, Brown et al. 2009). These findings demonstrate that the health benefit and poor bioavailability of the TPs could be attributed to their interactions with the lipid bilayer and it is of great interest and importance to investigate the permeability of TPs through such membranes. There has been no such research on the diffusion of these TPs through cell artificial membranes. Here an investigation of the permeability of the tea polyphenols through the liposome membrane is described including the interactions between EGCG and the lipid bilayer, which provides an *in vitro* tool for developing diffusion enhancement of EGCG. The absorption isotherms and absorption kinetics of the TPs were measured and also the permeabilities of the TPs using the continuous diffusion protocols established in Chapter 4. In addition, ethanol and DMSO were

selected as potential diffusion enhancers. The pH of the system was also adjusted in order to alter the ionisation state of the diffusant in an attempt to improve the permeability. Raman spectroscopy and AFM were used to investigate the interactions between EGCG and the phosphatidylcholine.

6.2 RESULTS

6.2.1. UV calibration of the TPs

The λ_{max} of the TPs in the UV spectrophotometer corresponded to 273, 276, 200 and 195 nm for EGCG, ECG, EC and EGC. A plot if the absorbance as a function of concentration is shown in Figure 6.1. The absorptivity of the TPs was then obtained by linear fitting as listed in Table 6.1. The coefficient of determination (R^2) are > 0.99.

6.2.2. The absorption of the TPs by the liposome membrane

The absorption of the TPs was carried out by immersing 10 of the liposome membranes in 2 mL of each TP solution. The initial concentration of the TP solutions are: 1.0 mg/ml for EGCG, 1.0 mg/mL for ECG, 1.0 mg/mL for EC and 0.5 mg/mL for EGC. An aliquot of 2 μL of the solution was sampled at 600, 1200, 1800, 3600, 5400, 7200 s and then at intervals of 3600 s up to 18000 s. Figure 6.2 shows the amount (mol) of the absorbed TPs per mg of liposome within 5 h. The absorption of ECG and EGCG had the largest values: 5.30±0.78 and 4.46±0.08 $\times 10^{-8}$ mol were absorbed respectively after 5 h. There was a moderate absorption of the EC (1.99±0.01 $\times 10^{-8}$ mol) for the same time period, which was ~ 37.5 % of

the amount of ECG absorbed. There was no significant absorption of EGC by the liposome membrane.

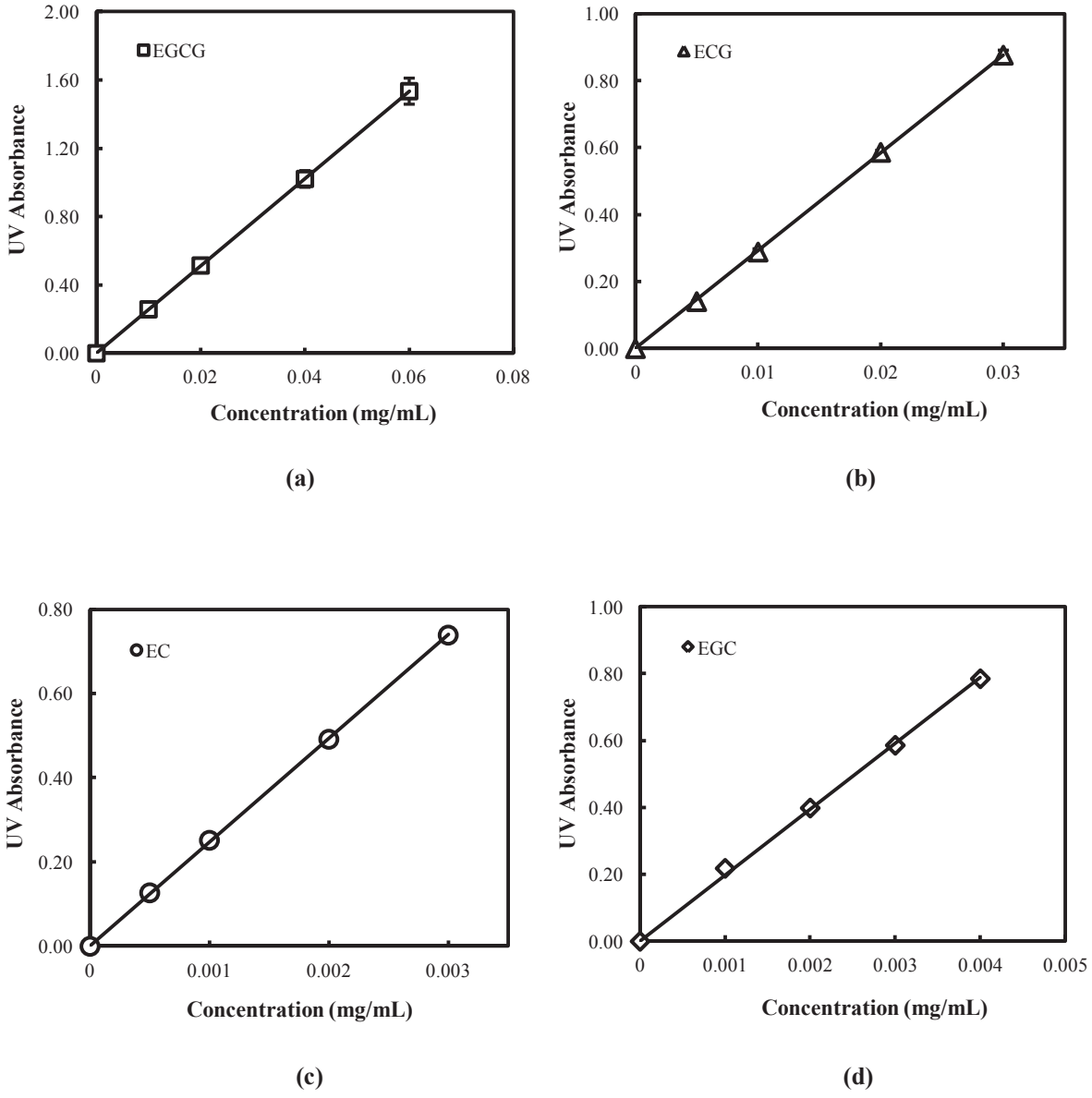

Figure 6.1 UV calibration of (a) EGCG, (b) ECG, (c) EC and (d) EGC. All the measurements were performed in triplicates and the average UV absorbance was plotted against time with standard errors.

The absorption kinetics for those molecules that exhibited significant absorption, i.e. ECG, EGCG and EC, were measured to obtain the absorption rate constant, k_a, where first order kinetics was assumed. The absorbed TPs were fitted to Equation 3.12 as shown in Figure 6.3 with $R^2 \geq 0.87$. The first order absorption rate constants for EGCG, ECG and EC are listed in Table 6.2, where statistically, k_{EGCG} and k_{EC} is 60 ± 9 % greater than k_{ECG} while there was no significant difference between k_{EGCG} and $k_{EC;}$ the subscripts refer to the particular TPs. Thus the absorption of EGCG and EC by the liposome membrane is more rapid than that of ECG.

Table 6.1 The UV absorptivity of the four TPs and their coefficient of determination (R^2).

	EGCG	ECG	EC	EGC
UV absorptivity	25.6	29.2	246.7	197.2
Coefficient of determination (R^2)	0.99	0.99	0.99	0.99

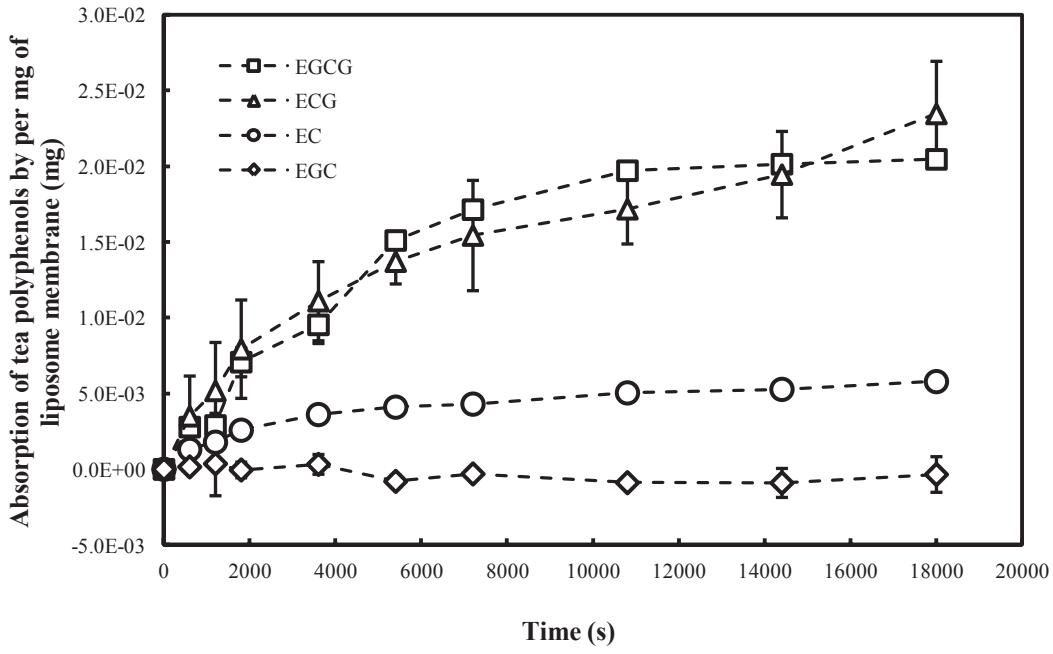

Figure 6.2 The absorption of the four tea polyphenols by per mg of liposome membrane within 5 hours. 10 liposome membranes were placed in the 2 ml solution of each tea polyphenol. Error bars represent standard error of three repeats.

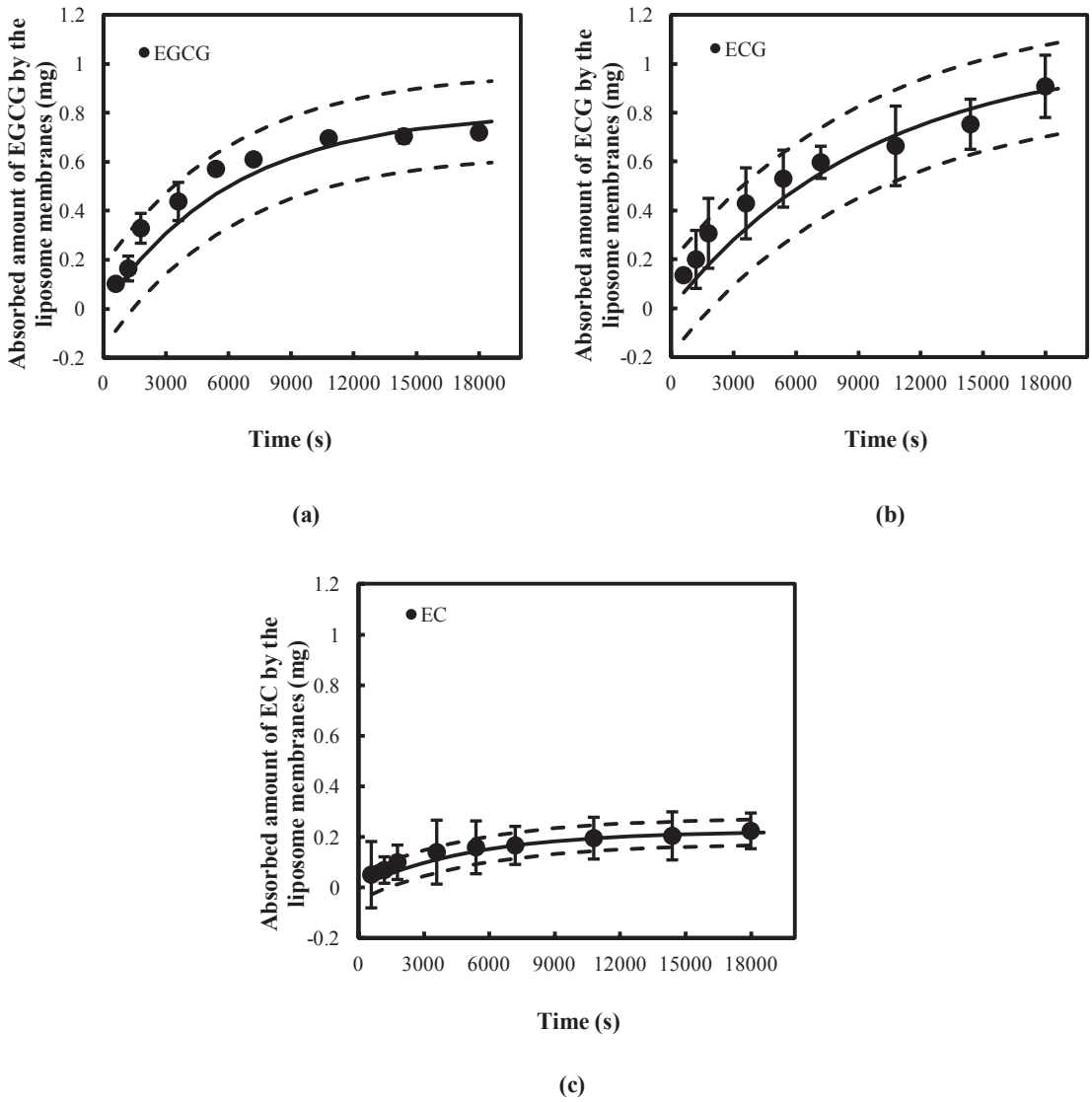

Figure 6.3 The absorption kinetics of (a) EGCG, (b) ECG and (c) EC: the absorbed amount of the three TPs from Figure 6.2. The solid lines are the best fits to Equation 3.12 with the 95 % confidence intervals shown as the dash lines.

Table 6.2 The first order absorption constant k_a, partition coefficient K in *n*-Octanol/PBS system and the coefficient of determination R^2.

	ECG	EGCG	EC	EGC
k_a ($\times 10^{-3}$ s^{-1})	2.17 ± 0.17	3.50 ± 0.17	4.00 ± 0.50	/
K[1]	23.90 ± 0.3	16.00± 0.2	1.40± 0.2	0.5± 0.1
R^2	0.90	0.91	0.87	/

[1] partition coefficient data from (Hashimoto, Kumazawa et al. 1999)

6.2.3. The influence of the concentration of EGCG on its absorption isotherms

The absorption of EGCG by the liposome membrane was measured at different concentrations of 0.5, 0.8, 2.0 and 3.0 mg/mL. The experiments were performed as described previously in Section 6.2.2 by immersing the 10 liposome membranes in the EGCG solution and an aliquot of 2 μL the solution were sampled at time intervals of 600, 1200, 1800, 3600, 5400, 7200 s and then at intervals of 3600 s up to 18000 s. The absorbed EGCG per mg of liposome for each concentration is plotted as a function of time in Figure 6.4.

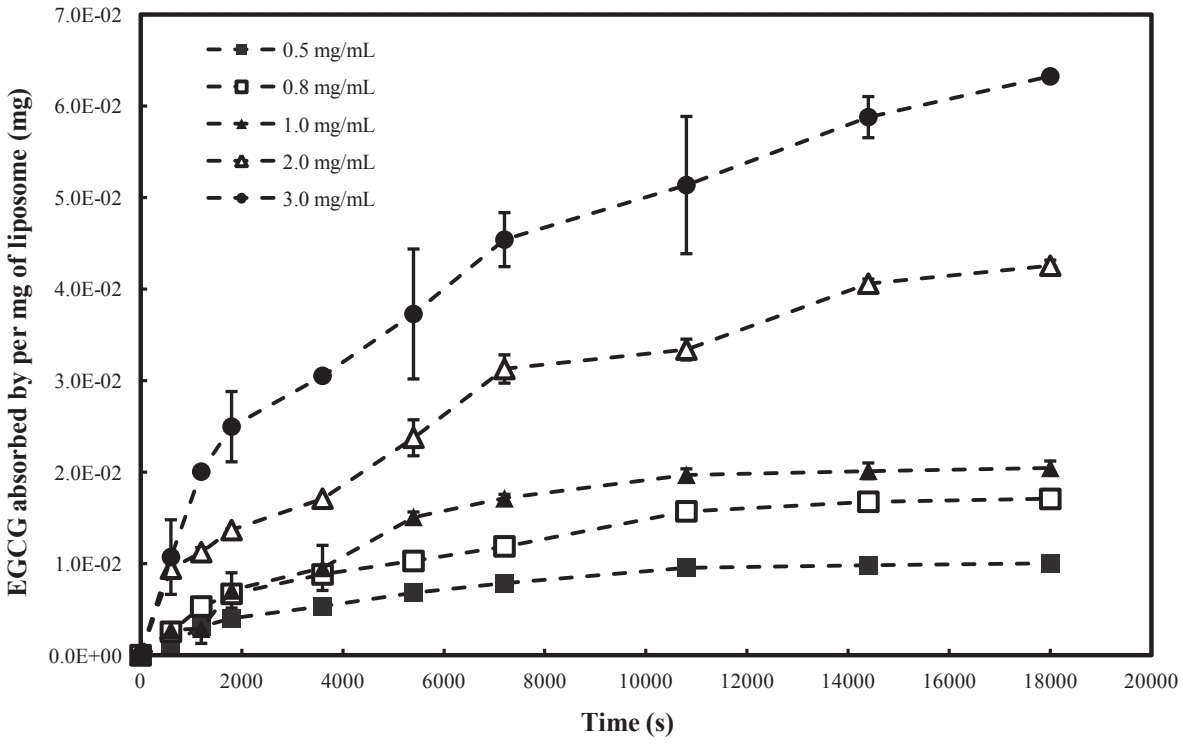

Figure 6.4 Absorption of EGCG at different concentrations by per mg of liposome membrane. 10 liposome membranes were immersed in the 2 ml solution of each EGCG solution. Error bars represent standard error of three repeats.

The absorption kinetics of the EGCG at different concentrations were carried out to obtain the absorption constant *k*, as described before. The absorbed EGCG were fitted to Equation 3.12 as shown in Figure 6.5 with $R^2 \geq 0.91$. The first order absorption constants of EGCG are listed in Table 6.3, where statistically there was no significant difference between the values at the different concentrations.

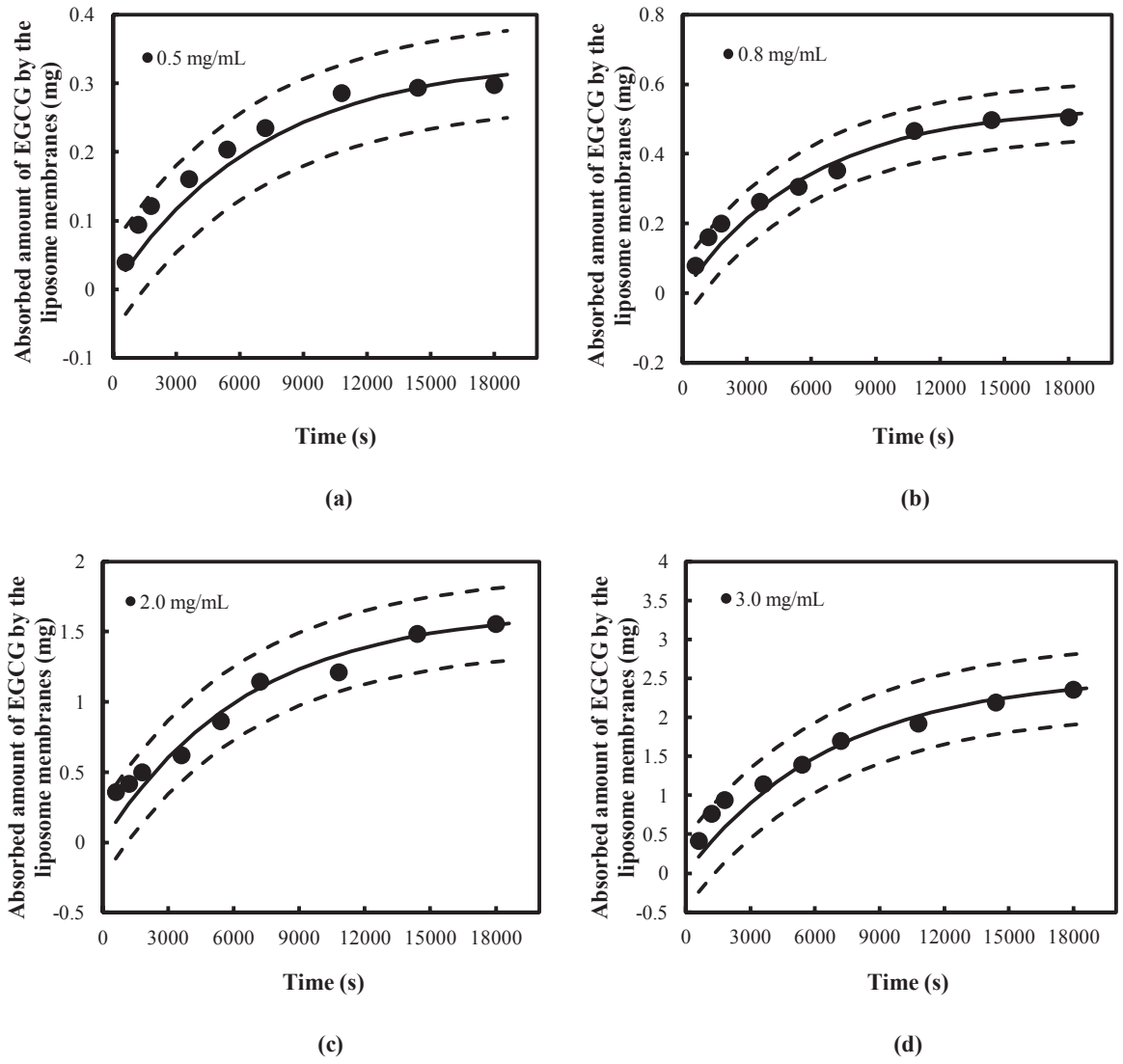

Figure 6.5 The absorption kinetics of EGCG at (a) 0.5 mg/mL, (b) 0.8 mg/mL (c) 2.0 mg/mL and (d) 3.0 mg/mL: the absorbed amount of the EGCG at different concentrations from Figure 6.4. The solid lines are the best fits to Equation 3.12 with the 95 % confidence intervals shown as the dash lines.

Table 6.3 The first order absorption constant *k* and the coefficient of determination R^2.

	0.5 mg/ml	0.8 mg/ml	1.0 mg/ml	2.0 mg/ml	3.0 mg/ml
k_a ($\times 10^{-3}$ s^{-1})	3.00 ± 0.33	3.67 ± 0.33	3.50 ± 0.17	3.33 ± 0.17	3.17 ± 0.17
R^2	0.92	0.95	0.91	0.94	0.91

6.2.4. The diffusion of ECG, EC and EGC through the liposome membrane

The diffusion of ECG was measured after the liposome membranes were immersed in the pre-treatment solution for 12 h with a concentration (1.0 mg/mL) equal to that to be used in the donor chamber. The concentrations in the acceptor chambers are plotted as a function of time in Figure 6.6. There was no obvious diffusion of ECG through the liposome membrane, since the concentrations of 5.25±1.82 $\times 10^{-2}$ mol/m^3 in the acceptor chambers correspond to the release of the ECG that was absorbed (5.45±0.15 $\times 10^{-2}$ mol/m^3) after the pre-treatment.

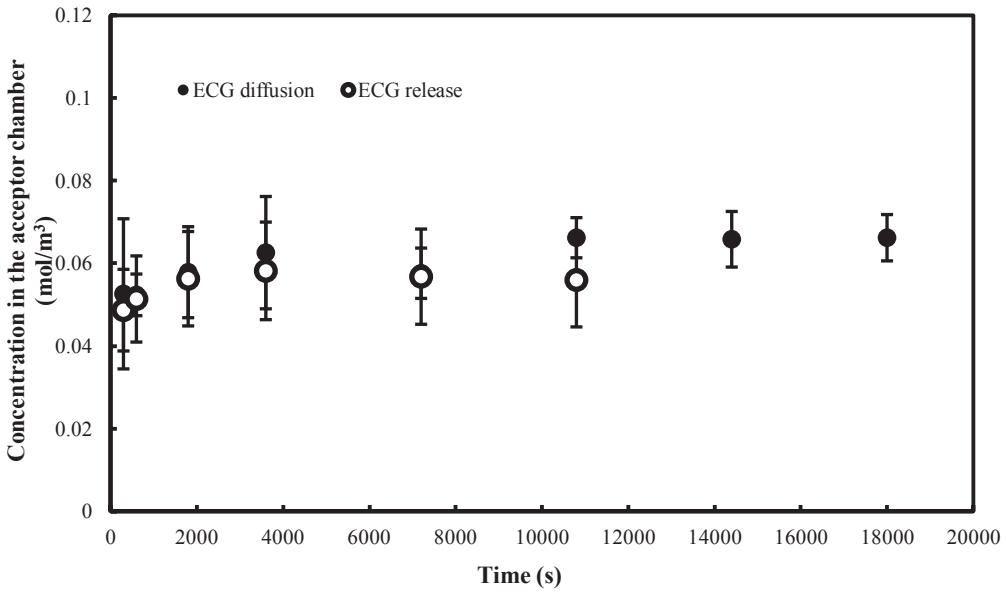

Figure 6.6 The diffusion and release of ECG after the liposome membrane was pre-treated with the 1.0 mg/ml ECG overnight. The experiments were performed in triplicates and an average concentration was plotted against time with standard error bars.

The diffusion of EC and EGC were measured in a similar way where the liposome membranes were pre-treated for 12 h with the concentrations equal to that to be used in the donor chamber (1.0 mg/mL for EC and 0.5 mg/mL for EGC). The solutions in the acceptor chambers were sampled for time intervals in the range 2-7 h, which corresponded to concentrations that could be detected by the UV. Figure 6.7 shows the concentrations of the EC and EGC in the acceptor chambers and the data were fitted to Equation 3.6 with $R^2 \geq 0.90$. The permeability of EC from the fitting is 1.08±0.07 $\times 10^{-6}$ cm/s, which is 21 ± 2 % smaller than that of EGC with a permeability of 1.31±0.11 $\times 10^{-6}$ cm/s.

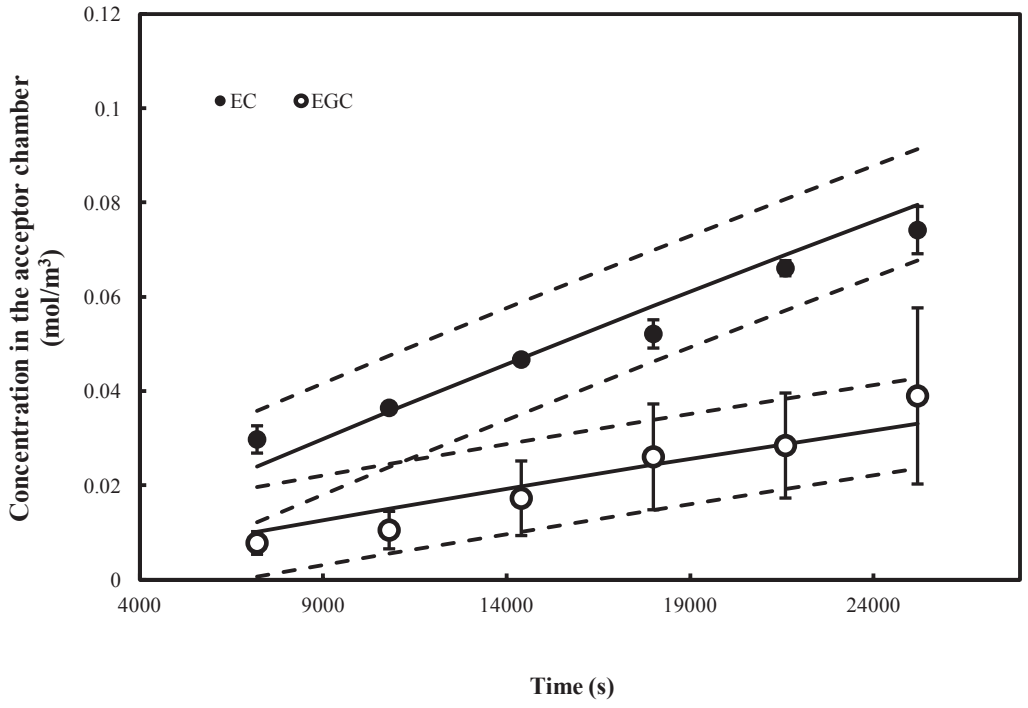

Figure 6.7 The diffusion of EC (filled circles) and EGC (open circles) through the liposome membrane after pre-treatment fitted by the continuous diffusion model (solid lines) with 95 % confidence intervals (dash lines). The error bars represent standard errors of three repeats. The solid lines are the best fits to Equation 3.6 with the 95% confidence intervals shown as the dash lines.

6.2.5. The diffusion of EGCG through the liposome membrane

The diffusion of EGCG was also measured using a similar method to that for EGCG where the liposome membranes were immersed in the pre-treatment solution for 12 h with a concentration (10.0 mg/mL), which is equal to that in the donor chamber. The concentrations in the acceptor chambers are plotted as a function of time in Figure 6.8. Similarly to ECG, there was no significant diffusion of EGCG through the liposome membrane, and the concentrations of 9.90±0.43 $\times 10^{-2}$ mol/m^3 EGCG in the acceptor chambers also corresponded to the release of the EGCG that was absorbed after the pre-treatment (8.44±0.73 $\times 10^{-2}$ mol/m^3). This result is consistent with the low bioavailability of EGCG, as it has an extremely limited diffusing rate through the lipid membranes.

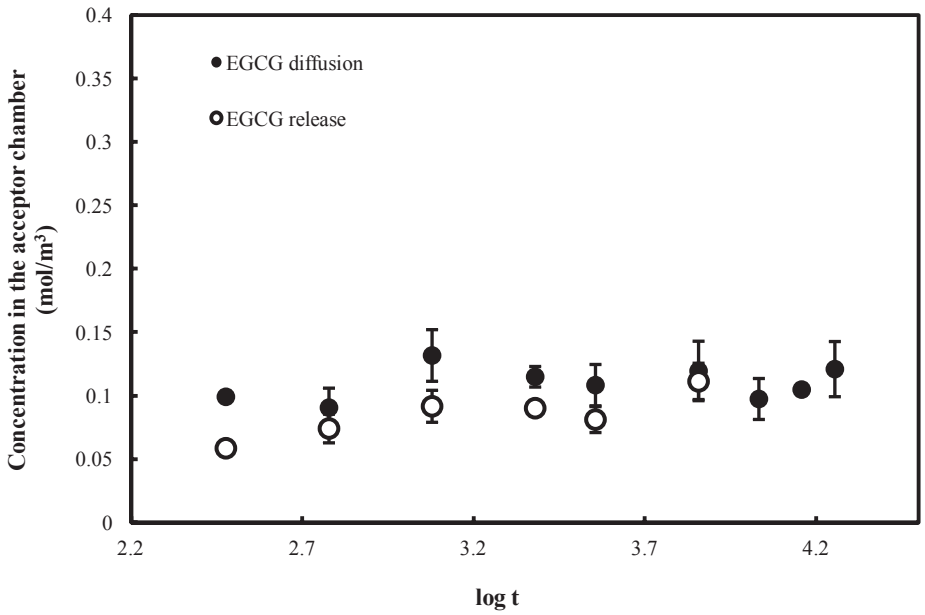

Figure 6.8 The diffusion of the EGCG after the liposome membrane was pre-treated with the 10.0 mg/ml EGCG for 12 h as shown in filled circles and the release of the EGCG that was absorbed by the lipsome membrane after the pre-treated. The experiments were performed in triplicates and an average concentration was plotted against time with standard error bars.

6.2.6. The physicochemical enhancement of the diffusion of EGCG through the liposome membrane

6.2.6.1. The physicochemical enhancement by DMSO and ethanol

Since EGCG did not diffuse significantly through the liposome membrane, attempts were made to enhance the diffusion by using ethanol and DMSO. The diffusion was carried out as described in the previous sections and the enhancers were added into both the pre-treatment solution and the donor solution.

As shown in Figure 6.9, 30% DMSO did not promote the diffusion of EGCG, but nearly 10.0 $\times 10^{-2}$ mol/m^3 more EGCG was released from the liposome membrane to the acceptor chambers although the variation was wide. A greater concentration of 50% DMSO showed no enhancement of the diffusion or a greater release of EGCG from the liposome membrane. As shown in Figure 6.10, neither ethanol nor 40% ethanol and 30% DMSO enhanced the diffusion of EGCG or promoted the release of EGCG from the liposome membrane.

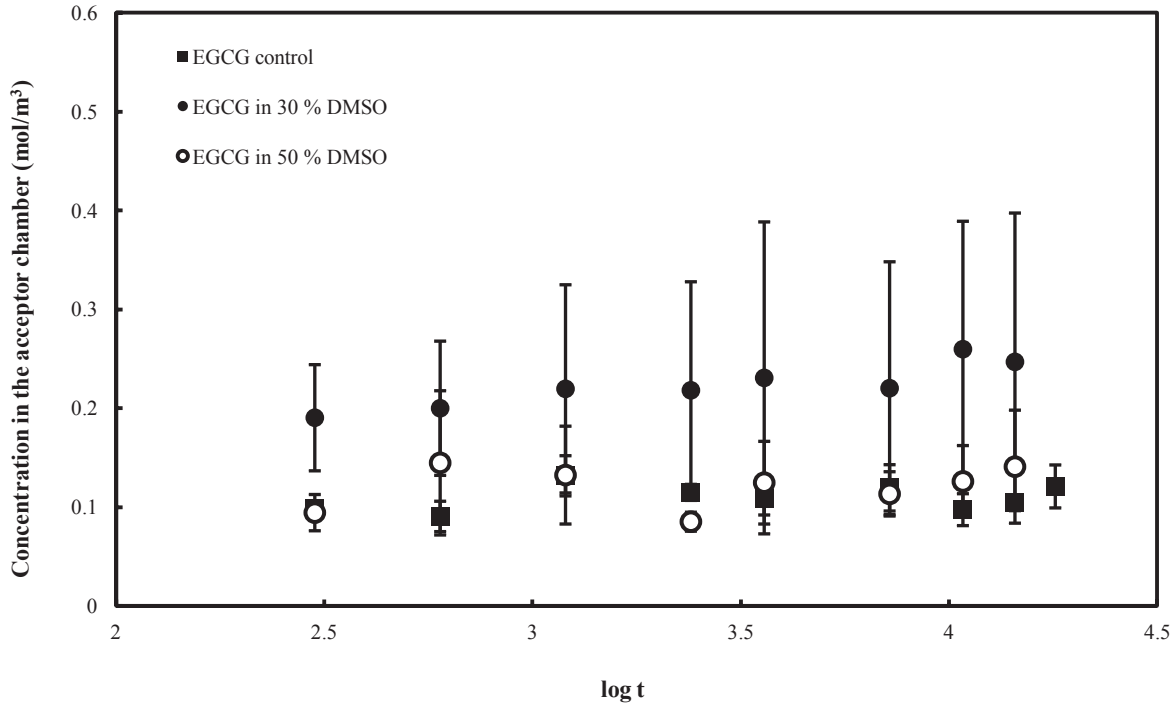

Figure 6.9 The diffusion of EGCG through the liposome membrane with DMSO. The experiments were performed in triplicates and an average concentration was plotted against time with standard error bars.

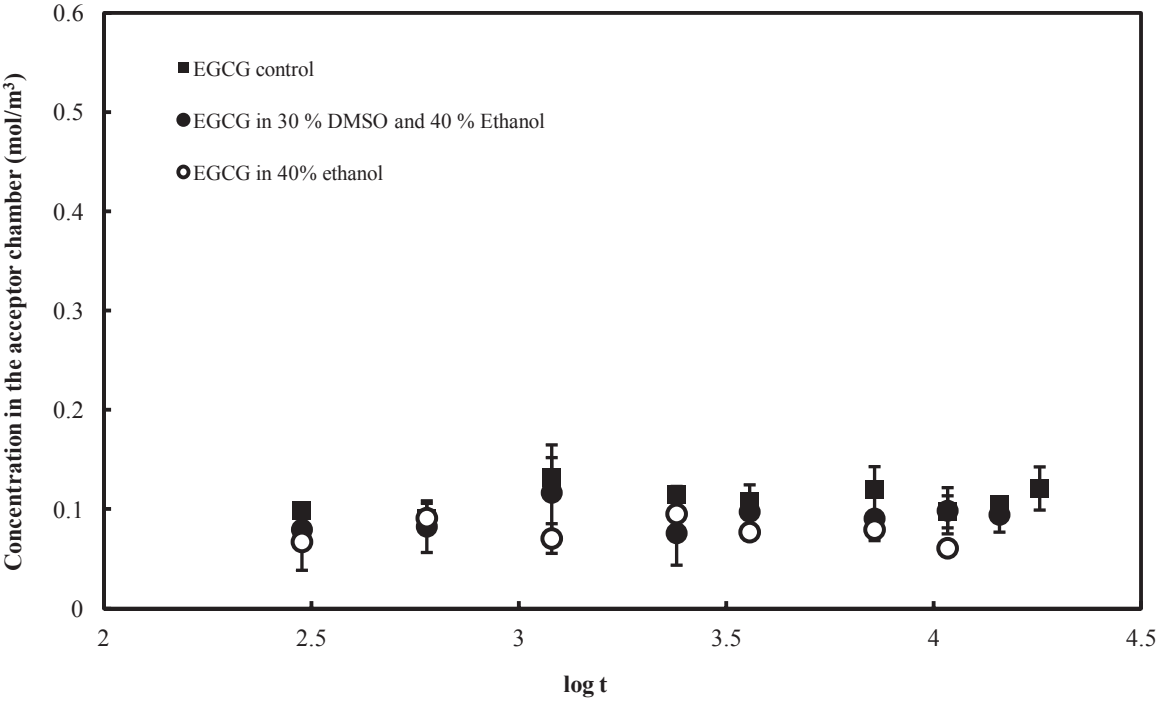

Figure 6.10 The diffusion of EGCG through the liposome membrane with ethanol and DMSO. The experiments were performed in triplicates and the mean concentration was plotted as a function of time with standard error bars.

6.2.6.2. The physicochemical enhancement by changing the pH

The pH of the donor and acceptor solutions were adjusted in order to change the ionisation state of the EGCG in the solution. The diffusion measurements were carried out as described previously and the pH in the pre-treatment and the donor solutions were adjusted to 2, 5 and 8 by HCl or NaOH. The experiment data are shown in Figure 6.11.

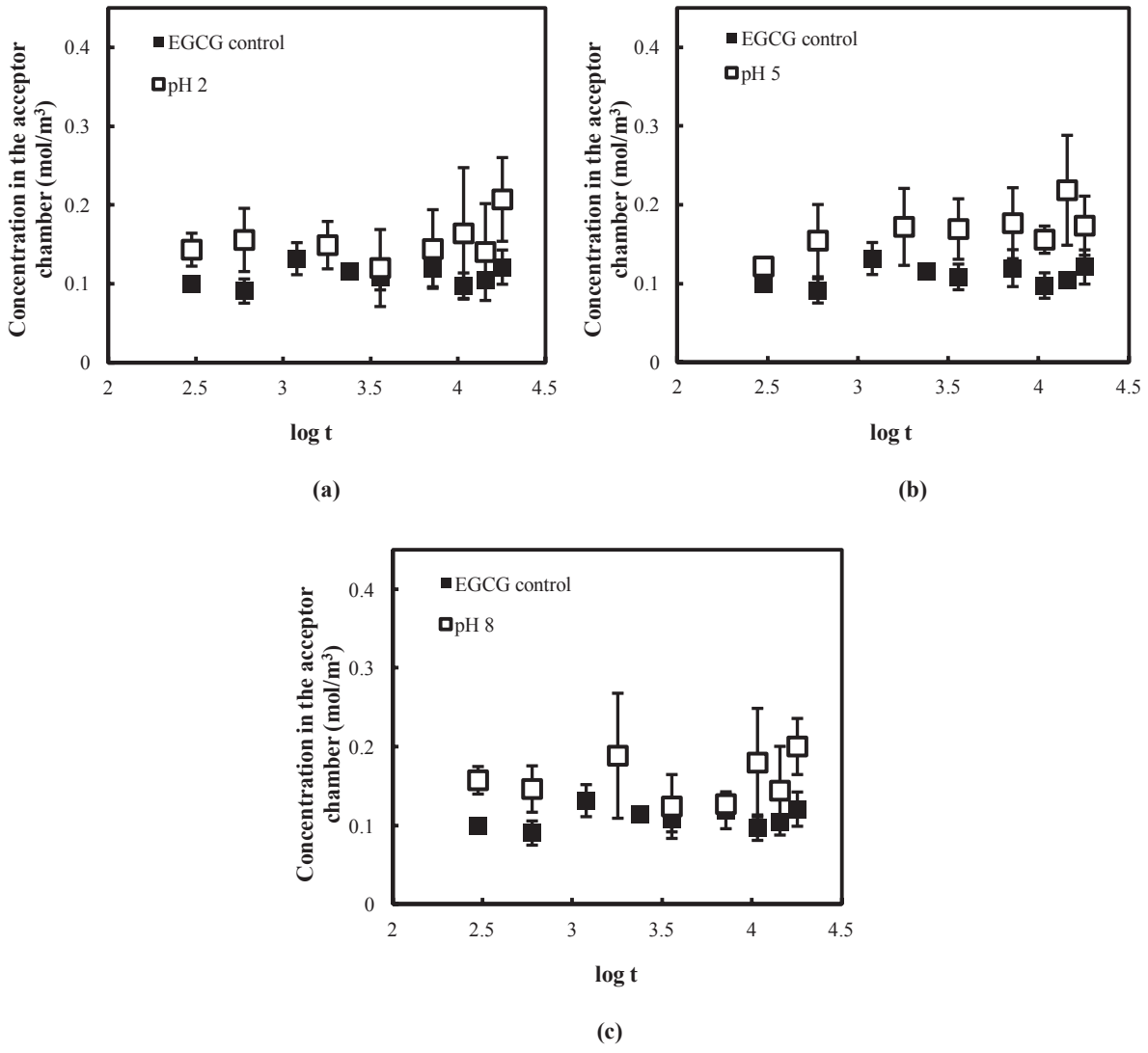

Figure 6.11 The diffusion of EGCG through the liposome membrane by changing the pH to 2 (a), 5 (b) and 8 (c). The experiments were performed in triplicates and an average concentration was plotted against time with standard error bars.

Since the pK_a of EGCG is reported to be about 8 (Inoue et al. 2002), a pH smaller than this value should increase the concentration of the unionised EGCG and thus potentially increase the quantity of EGCG diffused. However, it is clear from the results shown in Figure 6.11 that the diffusion process is not affected by a change in the pH.

6.2.6.3. The interactions between EGCG and liposome by Raman spectroscopy

Molecular dynamics simulations suggest that strong hydrogen bonds are formed between EGCG and the lipid bilayers (Sirk, Brown et al. 2009). Thus, Raman spectroscopy may provide some insight to the interaction of EGCG when absorbed on the liposome membrane used in the current work. Figure 6.12 shows the Raman spectra of liposome suspension, EGCG solution and a mixture of them both.

From a comparison of the three spectra, the broad peak at about 3100 - 3210 cm^{-1} of the hydroxyl groups of EGCG is not visible in the spectra of the mixture of liposome and EGCG, indicating an interaction occurred between the hydroxyl groups with the phosphatidylcholine. Moreover the peak at 1880 cm^{-1} of the liposome is also not visible in the spectra of the mixture, this peak corresponds to the vibrational region of C=C bonds. It could be deduced that a hydrogen bond is formed between the highly active hydroxyl groups of EGCG and the C=C of the phosphatidylcholine.

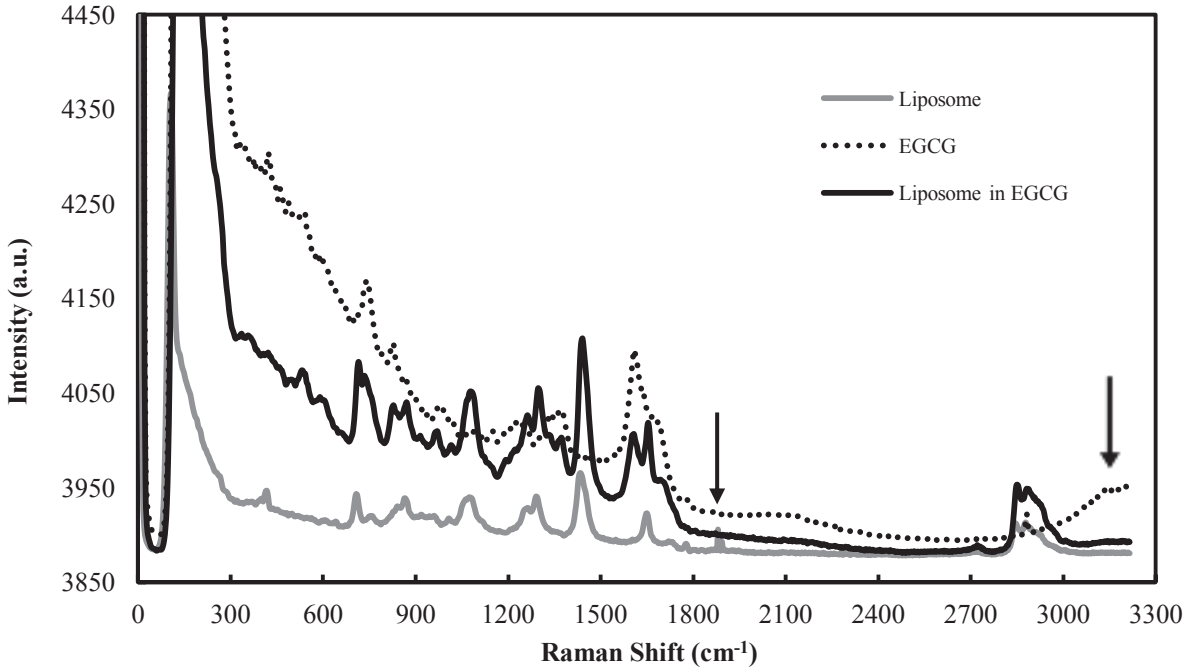

Figure 6.12 The Raman spectra of liposome suspension (grey line), EGCG solution (dash line) and a mixture of both (solid line).

6.2.6.4. The interactions between EGCG and liposome by AFM

The interactions between EGCG and phosphatidylcholine were further investigated by AFM. The Young's modulus and hardness of the liposome in the membrane with EGCG at pH 2, 7 and 8 are shown in Figure 6.13. EGCG does not significantly influence the Young's modulus or the hardness of the liposome at these pH values but the variation of the measured Young's modulus is wider than that of the control liposome.

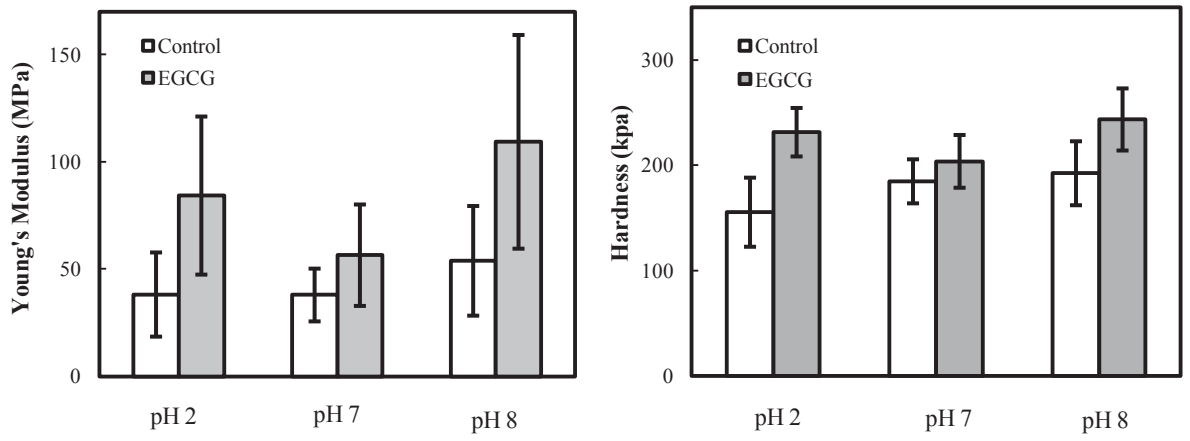

Figure 6.13 The Young's modulus and hardness of the liposome with EGCG at pH 2, 7 and 8 tested by AFM. 25 measurements were performed and the errors bars represent the 95 % confidence intervals.

6.3 SUMMARY

In this chapter, the absorption and the diffusion of the TPs through the liposome membrane were measured using the protocol developed for caffeine. A further investigation was focused on the physicochemical enhancement of EGCG and its interactions with the phosphatidylcholine. The results are summarised as follows:

- The absorption kinetics of the TPs has been studied and while EGC was not absorbed by the liposome membrane, EGCG and EC were absorbed with first order absorption rate constants of 3.50±0.17 and 4.00±0.50 $\times 10^{-3}$ s^{-1}, which are about 60% greater than that for ECG with a value of 2.17±0.17 $\times 10^{-3}$ s^{-1}.
- The absorption of EGCG was further investigated at different initial concentrations: the first order absorption rate constants at 0.5, 0.8, 1.0, 2.0 and 3.0 mg/mL were not statistically different with a mean value of 3.33±0.17 $\times 10^{-3}$ s^{-1}.

- The permeability of ECG was negligibly small while the values for EC and EGC are $1.08\pm0.07 \times 10^{-6}$ cm/s and $1.31\pm0.11 \times 10^{-6}$ cm/s, respectively.
- The small permeability of EGCG is consistent with its low bioavailability. The diffusion was not enhanced by ethanol or DMSO, nor by changing the pH to 2, 5 or 8.
- Raman spectroscopy was used to investigate the possible interactions between EGCG and the phosphatidylcholine. It was concluded that hydrogen bonding could be formed between the hydroxyl groups of EGCG and the C=C of the phosphatidylcholine. However, the mechanical properties of the liposome in the membrane with EGCG were not significantly different from the liposome without EGCG.

CHAPTER 7: ENCAPSULATION OF EGCG

7.1 INTRODUCTION

As discussed in the Chapter 2, EGCG is believed to have considerable health benefits, for example, it is widely studied for its anti-oxidant and anti-cancer activity. However, it is sensitive to the surrounding environment including pH, heat and light exposure. Microencapsulation can be a suitable technique to protect the active ingredient from degradation and achieve a long shelf life of the functional ingredient of green tea. Natural products are preferable wall/carrier materials for EGCG, since the challenge of encapsulating such a 'fragile' food ingredient lies in the safety of the protecting material with an acceptable bioavailability and no interference with the final products (Mellema 2007).

Edible waxes including beeswax have been used as carriers for various types of drugs (Raghuvanshi, Tripathi et al. 1992; Uner, Gonullu et al. 2005; Gowda, Ravi et al. 2009). It is hydrophobic, ductile without cracks and stable at room temperature. The plate-like crystals in the waxes are very efficient in hampering the diffusion of small molecules (Donhowe and Fennema 1993). This feature has made beeswax a potential wall/carrier material for water soluble EGCG. Mellema et al. (Mellema, Van Benthum et al. 2006) proposed that the preparation of wax microspheres as encapsulates should be a low cost, while the size should be such that it is not sensed in the mouth. They introduced two simple preparation techniques for wax capsules as shown in Figure 7.1: a 'solid' method involving the deposition of hot wax with the ingredient on a plate with size over 1 mm and a 'liquid' method where hot wax

with the ingredient is injected into cold oil with a high-shear mixer, giving particles in the range 150-500 μm. The present work has adapted a similar method developed from the technique in Gowda's work (Gowda, Ravi et al. 2009): this involves an emulsified cooling induced solidification as introduced in Chapter 2, where EGCG was dispersed in the beeswax matrix as microspheres.

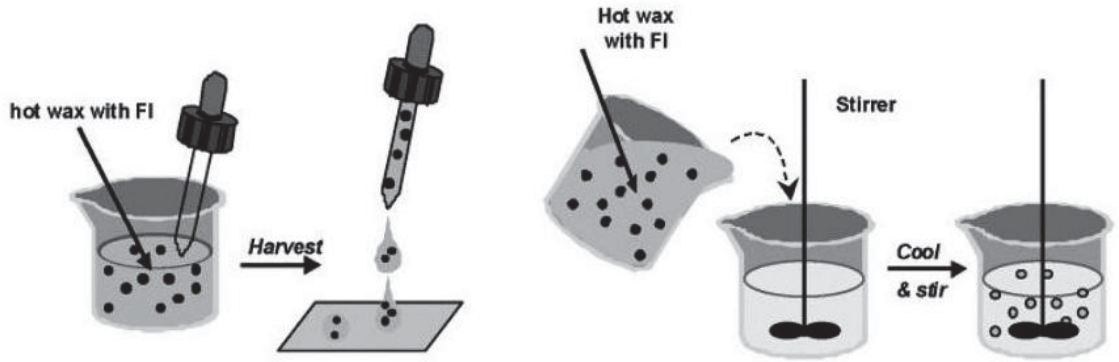

Figure 7.1 Schematic drawing of (a) a solid method involving deposition on a plate of hot wax with the encapsulated compound. and (b) a liquid method involving stirring hot wax with the encapsulated compound in hot vegetable oil followed by cooling (Mellema, Van Benthum et al. 2006).

To evaluate the release kinetics and mechanism of the EGCG released from the beeswax microspheres, the release profile data was fitted with a mathematic model. In a matrix system, when the drug has a limited solubility in the carrier solid and is mostly dispersed as particulates, it is called a monolithic dispersion. The mechanism of drug release from a non-swellable and non-erodible wax matrix system is primarily by diffusion, which is similar to a desorption process (Cheboyina and Wyandt 2008). The release kinetics developed by Higuchi (1963) and Baker (1974) has been widely used to fit a diffusion-controlled release model.

This chapter describes the encapsulation of EGCG using beeswax as microspheres based on the emulsified cooling induced solidification method. The morphological properties of the microspheres were observed by optical microscopy and the size distributions were also measured. The encapsulation efficiency was calculated for the four formulations employed in this study. *In vitro* release and long term leakage of the EGCG from the beeswax microspheres were measured and the data were fitted to wax matrix release kinetics.

7.2 MATERIALS AND METHODS

7.2.1. Materials

Beeswax (Refined with a melting point at 65^{o}C) and Tween 80 (viscous liquid) were purchased from Sigma UK were purchased from Sigma UK. EGCG was kindly provided by Unilever, U.K. A Rushton 6-blade impeller (Mechanical Engineering at University of Birmingham) and a beaker with 4 buffering bars (Glassblowing facility at School of Chemistry, University of Birmingham) were used to enhance the mixing.

7.2.2. The method of making beeswax microsphere of EGCG

As illustrated in Figure 7.2, to prepare the beeswax microspheres of EGCG, the beeswax was firstly melted in the beaker in a water bath at 70 ^{o}C as a carrier for EGCG and the oil phase in the emulsion system. At the same time, 10.0 g of Tween 80 was dissolved in 200 mL distilled water (5 %) and preheated to 70 ^{o}C to serve as the water phase. EGCG was then well dispersed in the melted beeswax for 10 min using an overhead stirrer (EUROSTAR Power, IKA) fitted with a Rushton 6-blade impeller at an agitation speed of 500 rpm. The preheated

solution of Tween 80 was then added into the mixture of the beeswax and EGCG to form an O/W emulsion under the same agitation speed of 500 rpm. Finally the emulsion was moved from the hot water bath into an ice bath to solidify the emulsified beeswax microspheres, under an agitation rate of 500 rpm for 20 min. The microspheres were then washed by distilled water followed by vacuum filtered using a Buchner funnel and air dried over night. The six formulations of the beeswax microspheres as listed in Table 7.1 were used to investigate the impact of agitation time (during the emulsification) and the loading on the properties of microspheres.

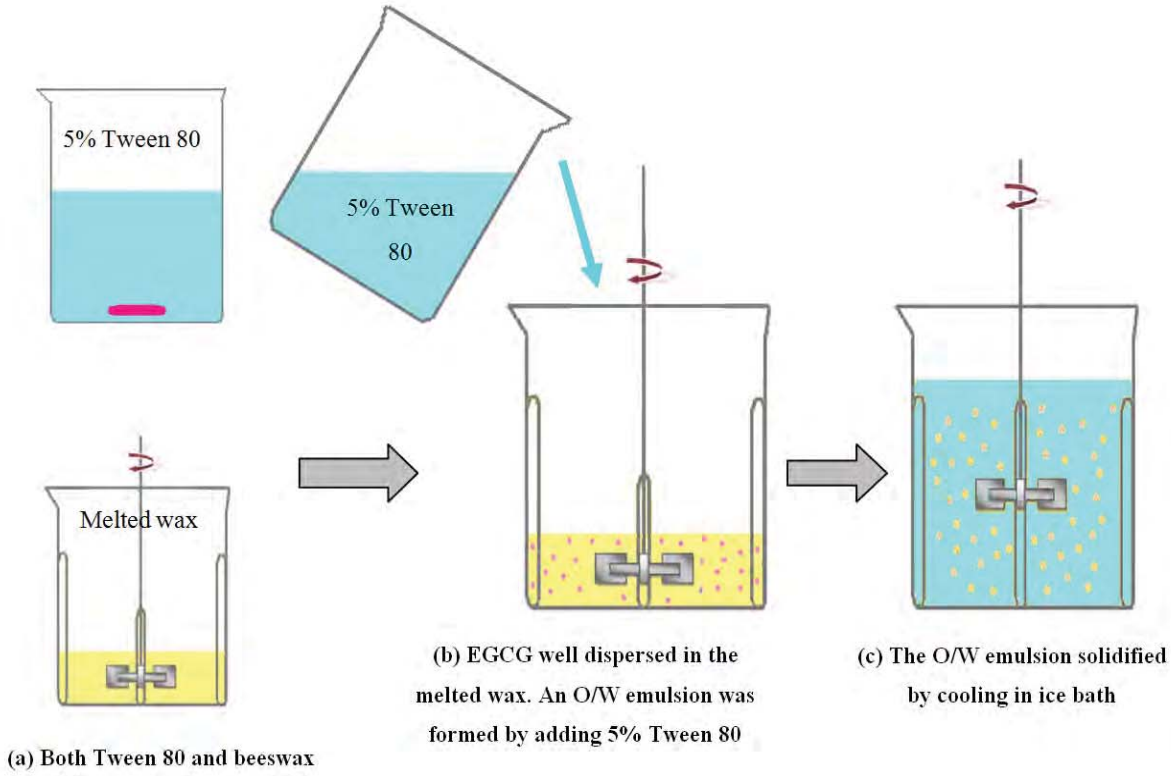

Figure 7.2 The preparation of the beeswax microspheres of EGCG: (a) 5 % Tween 80 and beeswax were both preheated to 70°C (b) EGCG was well dispersed in the melted beeswax by mixing, and an O/W emulsion was formed by vigorous mixing with the Tween 80 solution at 70°C (c) The beeswax microspheres were solidified by cooling in an ice bath.

Table 7.1: Formulation of the beeswax microspheres of EGCG.

Formulations	A	B	C	D	E	F
Beeswax (g)	8.0	8.0	8.0	8.0	8.0	8.0
EGCG (g)	0.2	0.2	0.2	0.4	0.1	0.8
Agitation time (min)	2	5	10	2	2	2

7.2.3. Characterisation of the beeswax microsphere

7.2.3.1. Optical microscope observation of the beeswax microsphere

A small sample of the beeswax microspheres of EGCG was mounted onto a glass slide to be observed by an optical microscope (Leica DM RBE, Leica Microsystems GmbH, Germany) equipped with Leica QWin Pro V2.8 software (Leica Microsystems Imaging Solutions Ltd., UK).

7.2.3.2. Size and distribution of the microsphere

The size distribution of the microspheres was measured by a Malvern Mastersizer (APA2000, Malvern Instruments Ltd., UK). It is based on a principle that the particles passing through a laser beam will scatter light at an angle that is directly related to their sizes: the intensity of the scatter light diminishes and the angle narrows with an increasing size, and the pattern is solved by Mie Theory for the calculation of particle size distributions based on Maxwell's electromagnetic field equations. It is capable of measuring a broad size range from 0.02 to 2000 μm, which is suitable for the size measurement of the beeswax microspheres in this work. The refractive index of the beeswax is 1.44 (Feldstein 1912), which is required to

determine the absolute size of the microspheres with this equipment. The mean size distribution of three repeat measurements was calculated.

7.2.4. Encapsulation efficiency of the beeswax microspheres of EGCG

To calculate the encapsulation efficiency of the beeswax microspheres of EGCG, the concentration of EGCG in the water phase of the o/w emulsion and the washing solution measured using a UV spectrophotometer. The encapsulation efficiency was calculated using the following expression:

$$EE = \frac{Mass_{total} - Mass_{recovered}}{Mass_{total}} \tag{7.1}$$

where $Mass_{total}$ is the total EGCG input and $Mass_{recovered}$ is the EGCG recovered from the water phase and the filtrate after the microspheres were washed.

7.2.5. *In vitro* release of the EGCG from the beeswax microsphere

The release of the EGCG from the beeswax microsphere was carried out in a sealed beaker with 200 mL distilled water maintained at 37 ^{o}C with a magnetic stirrer (RCT basic IKAMAG) at 200 rpm. An aliquote of 2 mL of the liquid phase was sampled at intervals of 1 h and filtered using a syringe filter (Fisher Scientific, UK) before being analysed by a UV spectrophotometer. The experiments were performed in triplicates and the mean value of the

amount released percentage was plotted as a function of time with standard errors. The release data was then compared pair wise using a similarity factor approach, where f_2 is defined as (Shah, Tsong et al. 1998; Cheboyina and Wyandt 2008):

$$f_2 = 50 \log\left\{\left[1 + \frac{1}{n}\sum_{1}^{n}(R_t - T_t)^2\right]^{-0.5} \times 100\right\} \quad (7.2)$$

where R_t and T_t are the cumulative percent releases at time t, for any two release profiles. A value of f_2 in the range 50 - 100 suggests that the two release profiles are similar.

In Higuchi release kinetics (Higuchi 1963), the release of a water soluble drug from a slab of solid matrix is proportional to square-root of time:

$$M_t = [D\,(2C_0\text{-}C_s)C_s t]^{1/2} \quad (7.3)$$

where M_t is the amount of drug released at time t, C_0 is the initial concentration of the drug in the matrix, C_s is the saturation solubility of the drug in the matrix and D is the diffusion coefficient of the drug in the matrix.

Baker-Lonsdale adapted the Higuchi model (Higuchi 1963; Baker 1974) for describing the release of a drug from a spherical matrix as:

$$\frac{3}{2}\left[1-\left(1-\frac{M_t}{M_0}\right)^{\frac{2}{3}}\right]-\frac{M_t}{M_0}=\frac{3DC_s}{r^2C_0}t \tag{7.4}$$

where M_t/M_0 is the release percentage at time t and r is the radius of a homogenous monolithic sphere. By solving Equation 7.4:

$$\frac{3}{2}\left[1-\left(1-\frac{M_t}{M_0}\right)^{\frac{2}{3}}\right]-\frac{M_t}{M_0}=kt+c \tag{7.5}$$

where k is a release rate constant corresponding to the slope of the fitting line and c is a constant corresponding to the intercept of the fitting line (Cheboyina and Wyandt 2008). The release data of the six formulations of EGCG from beeswax microspheres were fitted to Equation 7.5.

7.2.6. Leakage of the EGCG from the beeswax microsphere

The use of beeswax to make microspheres of EGCG for long term storage was evaluated by leakage experiments for up to 35 days. The beeswax microspheres were stored in a glass bottle with 200 mL distilled water at room temperature. An aliquot of the liquid phase was sampled and filtered to be analysed by a UV spectrophotometer. The leakage tests of the six formulations were performed in triplicates and the mean value of the leakage was plotted as a function of time with standard errors and fitted to Equation 7.5.

7.3 RESULTS

7.3.1. Encapsulation efficiency of the beeswax microspheres of EGCG

Figure 7.3 shows the impact of agitation time on the encapsulation efficiency of the beeswax microspheres of EGCG using the emulsified cooling induced solidification method. Statistically, with 95% confidence there was no significant difference in the encapsulation efficiency for formulations A and B; the mean value of the residual EGCG in the microspheres is 55.8±1.1 %. This suggests that within 5 min the agitation time had no impact on the encapsulation efficiency. When the agitation was increased to 10 min, there was a considerable decrease in the encapsulation efficiency with only 22.3±1.7 % of the EGCG was trapped in the wax.

Figure 7.4 shows the impact of an increasing loading of the EGCG in the beeswax on the encapsulation efficiency. When the loading was increased from 1.25 to 5 %, the encapsulation efficiency did not increase significantly with a mean value of 57.4±2.7 %. A

further loading of EGCG into the beeswax by 10 % yielded a significant reduction of the encapsulation efficiency to only 25.4±2.2 %.

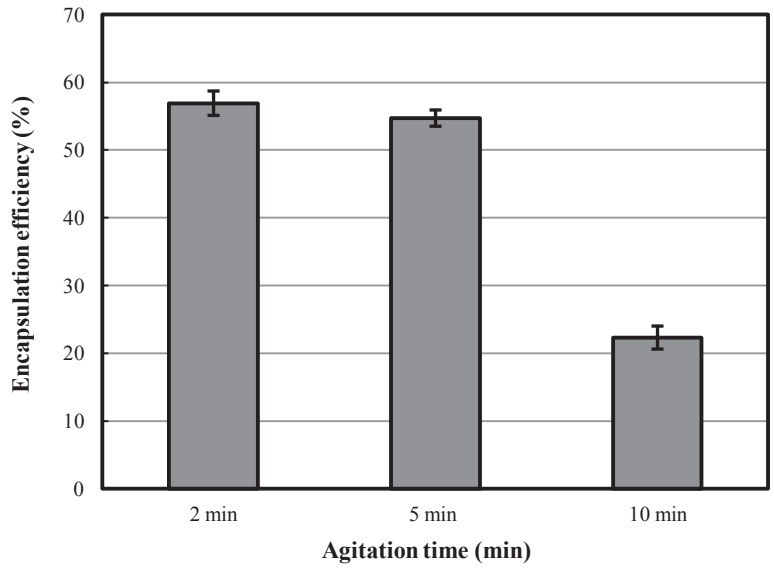

Figure 7.3 The impact of agitation time on the encapsulation efficiency of the beeswax microspheres of EGCG. The experiments were performed in triplicates and an average value was plotted with 95 % confidence intervals.

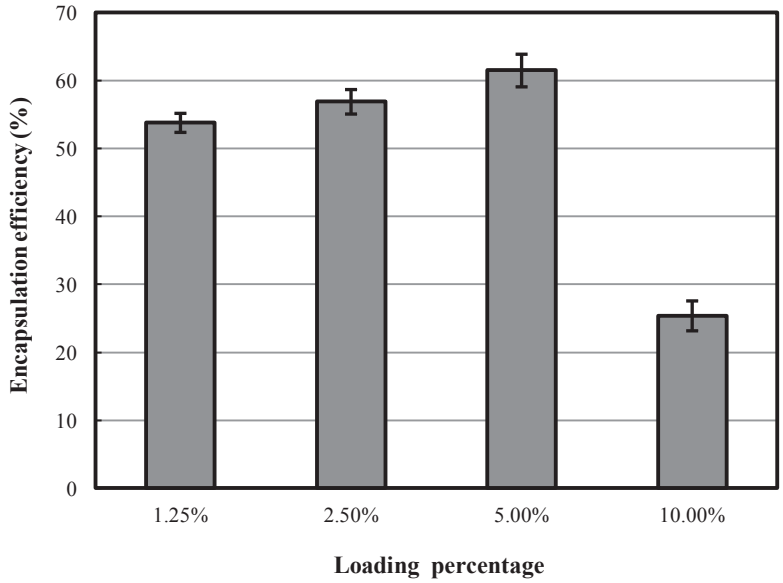

Figure 7.4 The impact of loading on the encapsulation efficiency of the beeswax microspheres of EGCG. The experiments were performed in triplicates and a mean value was plotted with 95 % confidence intervals.

7.3.2. Size distributions of the beeswax microspheres of EGCG

The impact of agitation time on the size distributions is shown in Figure 7.5 and the volume moment mean sizes (D [4, 3]) with their spans are listed in Table 7.2. A prolonged agitation time during the emulsification resulted in slightly smaller microspheres: also there was a reduction of 18.2±0.4 % with a narrower distribution when the agitation time was increased by a factor of five.

Figure 7.6 shows the impact of the loading on the sizes of the beeswax microspheres. There was a slight increase of 9.4±0.3 % when the loading was increased from 1.25 to 10.00 %.

Table 7.2 The agitation time, loading, D [4, 3] and span of the beeswax microspheres of EGCG measured by Malvern Mastersizer. All the measurements were performed in triplicates.

Formulations	A	B	C	D	E	F
Agitation time (min)	2	5	10	2	2	2
Loading percentage (%)	2.50	2.50	2.50	5.00	1.25	10.00
D [4, 3] (μm)	176.4±3.5	151.9±3.3	144.2±2.2	173.9±2.8	169.4±3.1	185.4±5.8
Span	1.77±0.21	1.67±0.19	1.47±0.13	1.75±0.16	1.77±0.26	1.75±0.24

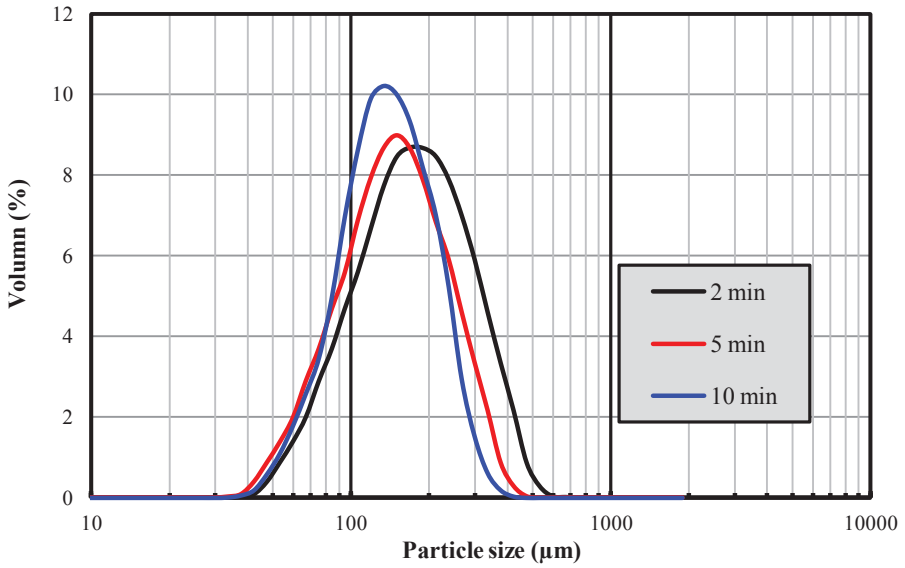

Figure 7.5 The impact of agitation time on the size distribution of the beeswax microspheres of EGCG. The measurements were performed in triplicates and the mean volume distributions are plotted.

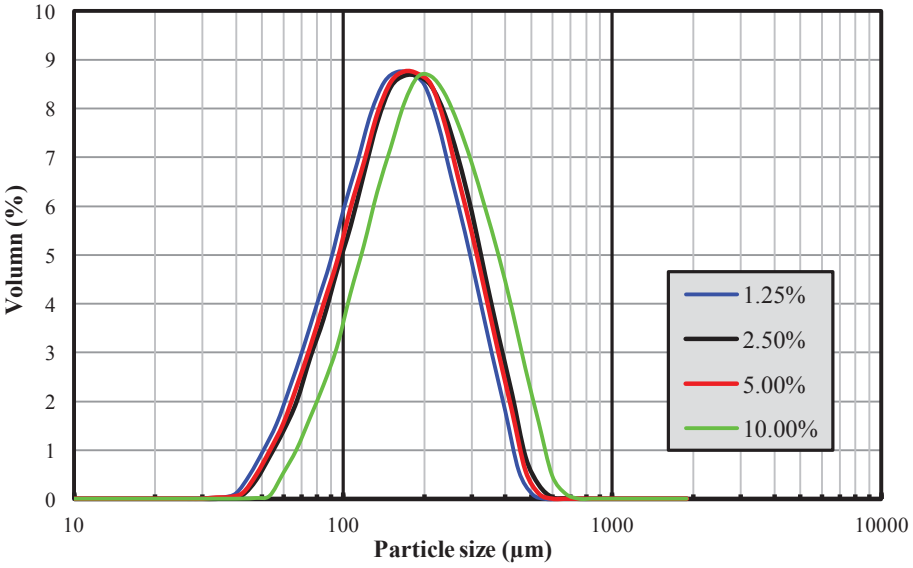

Figure 7.6 The impact of loading on the size distribution of the beeswax microspheres of EGCG. The measurements were performed in triplicates and the mean volume distributions are plotted.

7.3.3. Optical microscope observation of the beeswax microsphere of EGCG

The beeswax microspheres of EGCG were observed under microscope as shown in Figure 7.7.

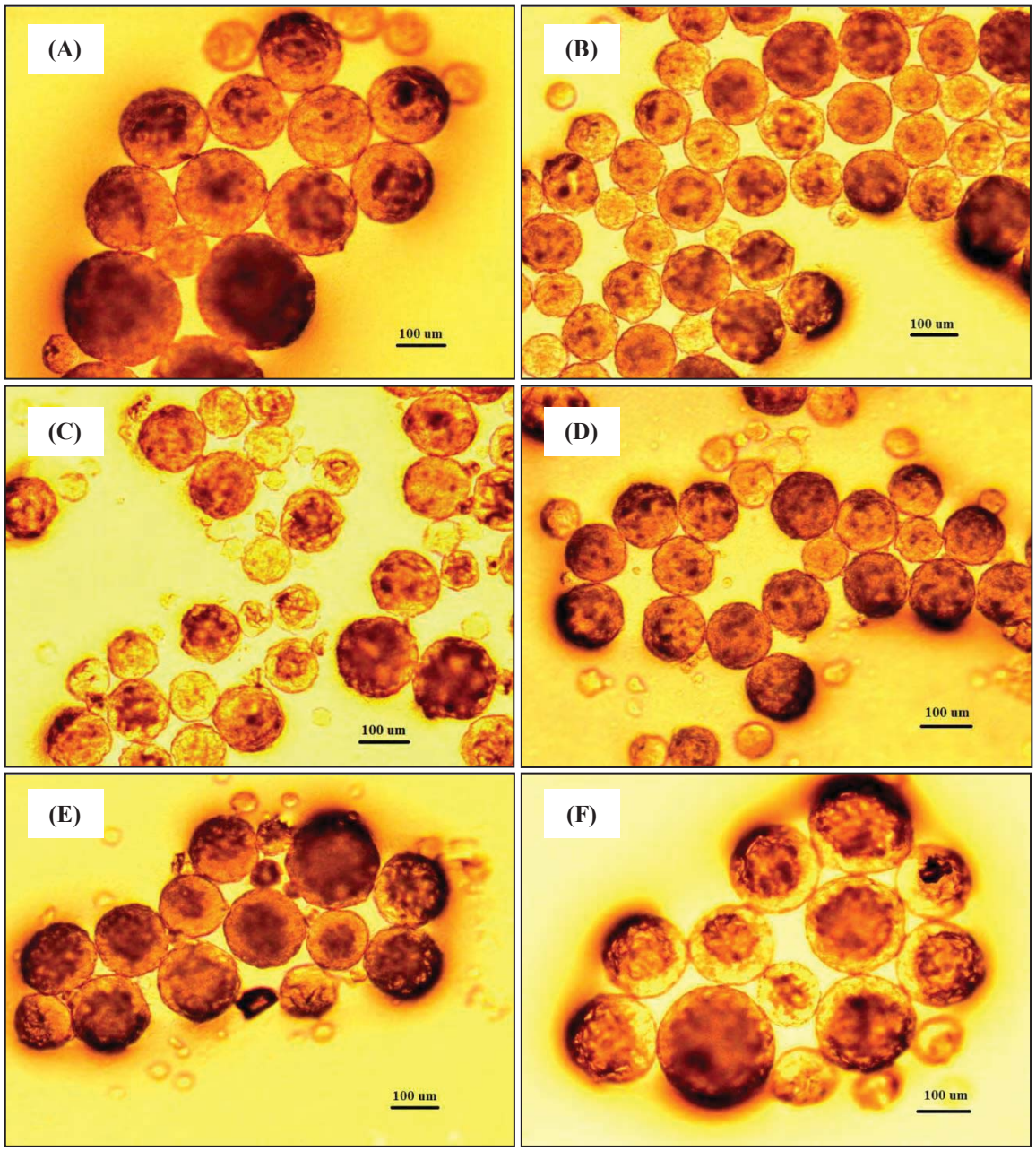

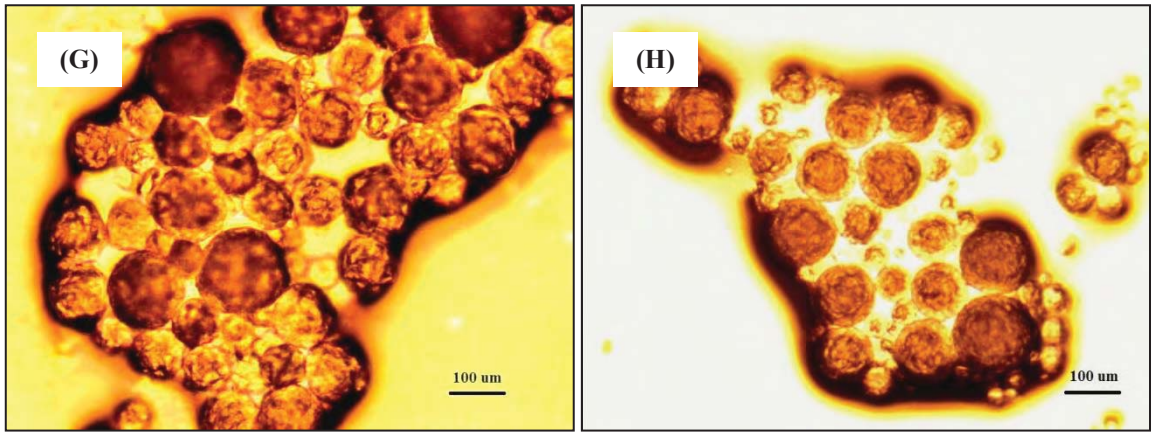

Figure 7.7 Optical microscopy observation of the beeswax microspheres of EGCG: (A) formulation A, (B) formulation B, (C) formulation C, (D) formulation D, (E) formulation E, (F) formulation F, (G) typical aggregated beeswax microspheres when agitation is under 500 rpm (H) typical aggregated beeswax microsphere when Tween 80 is absent.

The formulation of making the beeswax microsphere of EGCG was optimised in the preliminary experiment that aggregated microspheres with irregular shapes as shown in Figure 7.7 (G) and (H) (due to a low agitation speed and the absence of the surfactant Tween 80) were eliminated. There was no visible difference in the morphological properties of the six optimised formulations, and the beeswax microspheres were regular in shape with rough surface as seen in Figure 7.7 (A)-(F). The dark shadows could be the dispersed EGCG particulates which were visible in some microspheres, indicating that the distribution of EGCG may not be uniform. There were no visible cracks on the surfaces of the microspheres.

7.3.4. *In vitro* release of EGCG from the beeswax microspheres

The release profiles of EGCG from the beeswax microspheres with a prolonged agitation time during emulsification are shown in Figure 7.8. It was observed that further agitation had

no impact on the release profile as indicated by the values of f_2 listed in Table 7.3. The release of EGCG from the microspheres within 8 h are very limited, with only an average of 2.3±0.8 % released at the end of the experiments.

The release profile of EGCG from the beeswax microspheres with an increasing loading percentage is shown in Figure 7.9. The values of f_2 listed in Table 7.4 suggest that the release profiles of the four formulations are not significantly different. The mean release of the four formulations after 8 h was 3.1±0.7 %

The release result data has demonstrated that beeswax is very efficient in hampering the diffusion of the trapped EGCG into a water phase, and a smaller size microspheres and a higher loading percentage did not result in a faster release of the encapsulated EGCG. Since there was no significant difference in all of the release profiles, the release profile of formulation D was fitted to Equation 7.5 as an example as shown in Figure 7.10. The determination coefficient R^2 of the fitting was 0.99, indicating that the release profile of EGCG from the beeswax matrix fits the Higuchi spherical matrix release kinetics and thus the release mechanism could be diffusion-controlled. The obtained release rate constant k was $7.78\pm0.58 \times 10^{-9}$ s^{-1}.

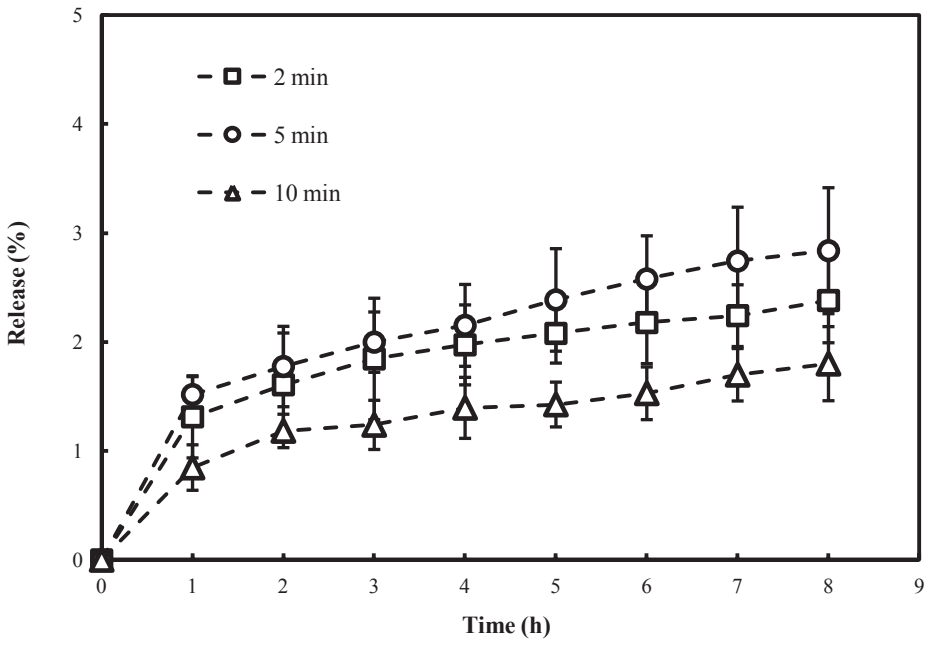

Figure 7.8 The impact of agitation time on the release profile of EGCG from the beeswax microspheres in PBS (pH 7.4) at 37°C. The experiments were performed in triplicates for each formulation and an average release percentage was plotted as a function of time with standard errors.

Table 7.3 Similarity factor (f_2) of the release profiles of the three formulations (formulation C as a reference).

Formulations	A (2min)	B (5 min)	C (10 min)
f_2	96.97	93.82	100.00

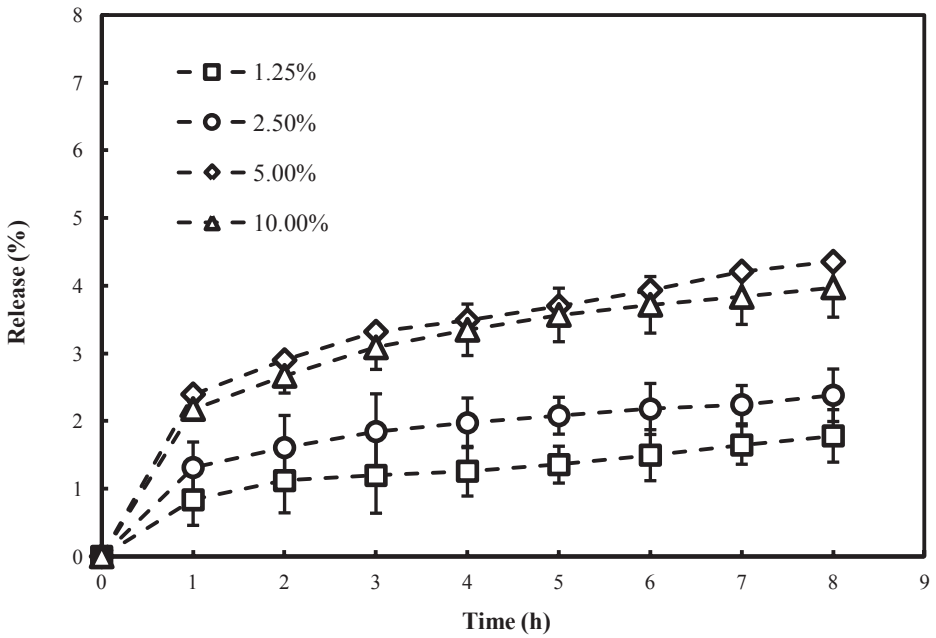

Figure 7.9 The impact of the loading on the release profile of EGCG from the beeswax microspheres in PBS (pH 7.4) at 37°C. The experiments were performed in triplicates for each formulation and an average release percentage was plotted as a function of time with standard errors.

Table 7.4 Similarity factors (f_2) of the release profiles of the four formulations (formulation E as a reference).

Formulations	A (2.50%)	D (5.00%)	E (1.25%)	F (10.00%)
f_2	96.44	80.61	100.00	82.64

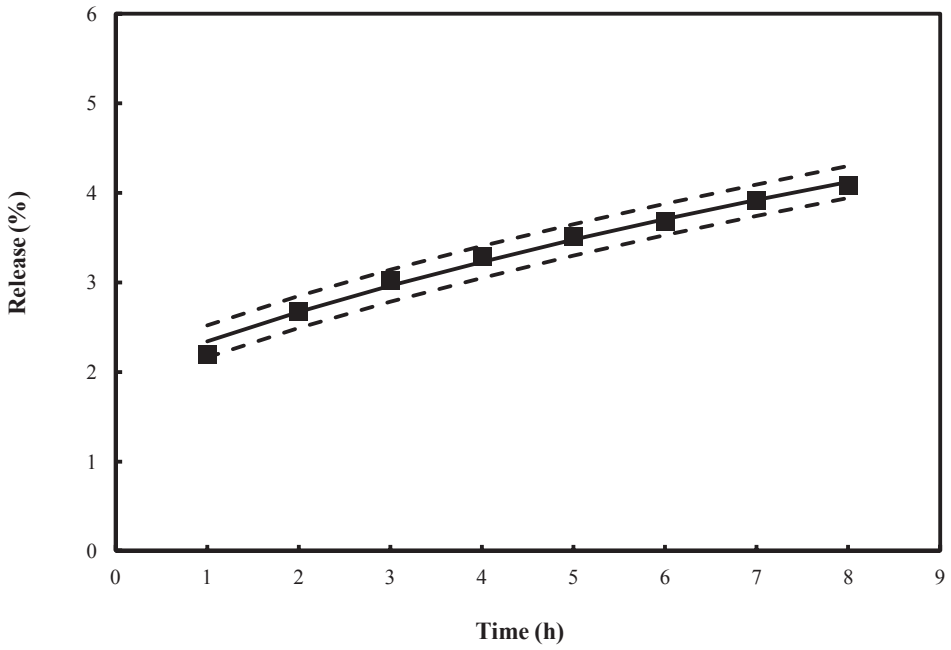

Figure 7.10 The release data of EGCG from the beeswax microspheres fitted by Higuchi spherical matrix release kinetics (solid line) with 95 % confidence intervals (dash lines).

7.3.5. Leakage of EGCG from the beeswax microspheres

The leakage of EGCG with a prolonged agitation time from the beeswax microspheres is shown in Figure 7.11. The agitation time during the emulsification had no significant effect as indicated by the values of f_2 in Table 7.5. There was a relatively fast leakage in the first 5 days with a mean value of 7.8±0.8 % of the encapsulated EGCG leaked into the water phase. After 35 days, a total of 10.4±0.8 % EGCG leaked, indicating that beeswax is a potential carrier material for the long term preservation of EGCG.

The leakage of EGCG with increasing loading of the microspheres is shown in Figure 7.13. They show a similar behaviour to the leakage of EGCG with a prolonged agitation time that it

is relatively fast in the first 5 days and then decreases. The total release for 5.00 % loading was slightly greater than that at 1.25 % (13.6±0.8 % leaked compared with 8.9±0.4 %). The leakage profiles of the four formulations were not significant different as indicated by the values of f_2 in Table 7.6. This is further evidence that beeswax is a potential carrier material for long term preservation of EGCG.

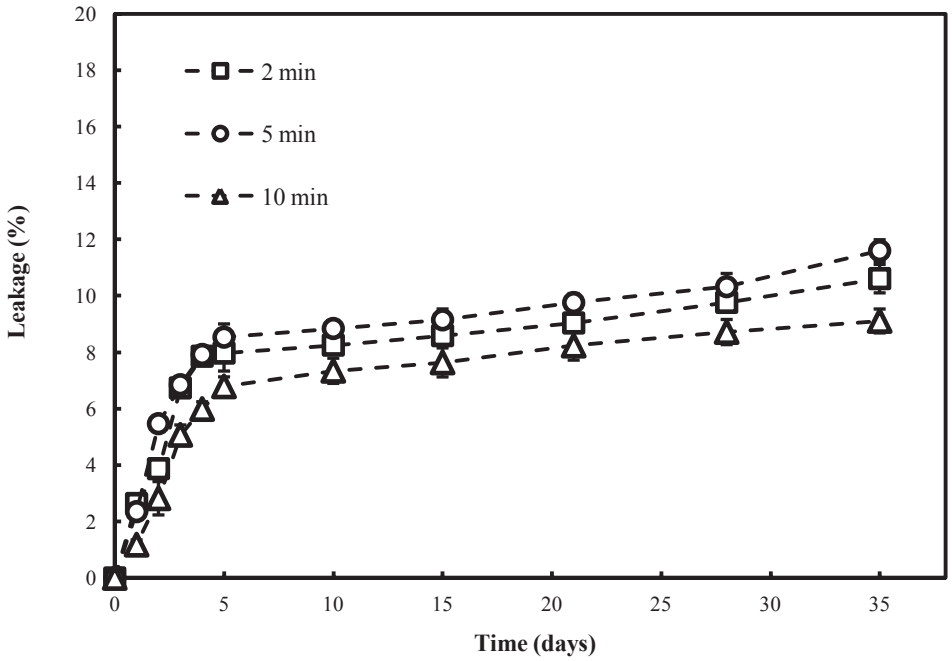

Figure 7.11 The impact of agitation time on the leakage of EGCG from the beeswax microspheres as a function of time. The experiments were performed in triplicates and an average leakage was plotted with standard errors.

Table 7.5 Similarity factors (f_2) of the leakage of the three formulations (formulation C as a reference).

Formulations	A (2 min)	B (5 min)	C (10 min)
f_2	98.59	96.96	100.00

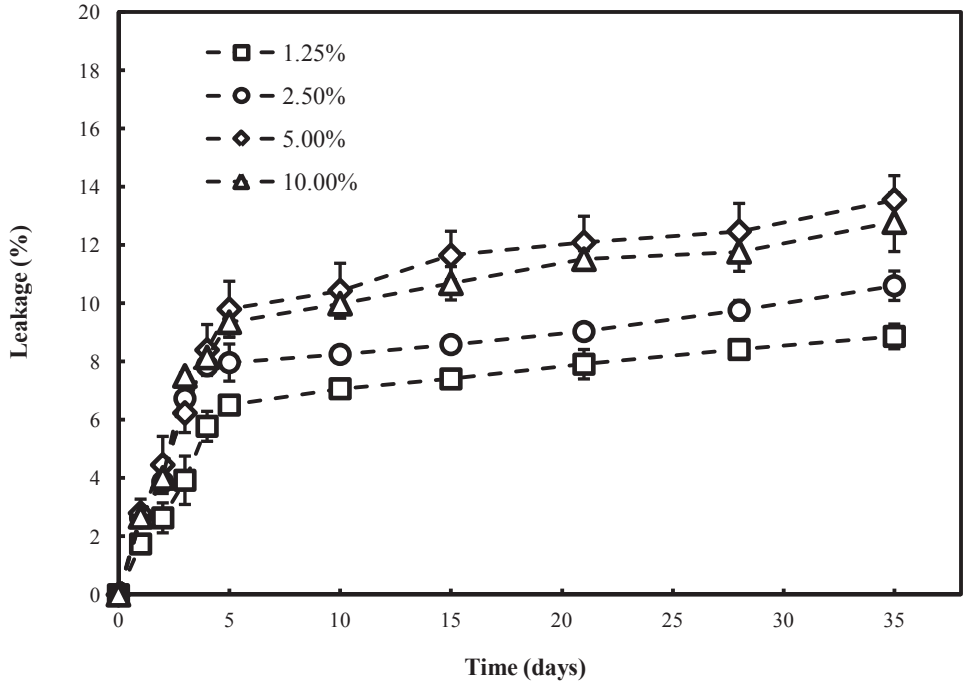

Figure 7.12 The impact of the loading percentage on the leakage of EGCG from the beeswax microspheres as a function of time. The experiments were performed in triplicates and an average leakage was plotted with standard errors.

Table 7.6 Similarity factors (f_2) of the leakage profiles of the four formulations (formulation E as a reference).

Formulations	A (2.50%)	D (5.00%)	E (1.25%)	F (10.00%)
f_2	84.44	70.54	100.00	73.00

Since the leakage profiles were similar, the leakage date of EGCG from the beeswax microspheres in formulation D was fitted to Equation 7.5 of the Higuchi spherical matrix release kinetics as an example in Figure 7.13. The determination coefficient R^2 of the fitting was 0.75, indicating that the leakage profile could also follow a diffusion-controlled release mechanism; the release rate constant, k, from the fitting is $9.53 \pm 1.47 \times 10^{-10}$ s^{-1}.

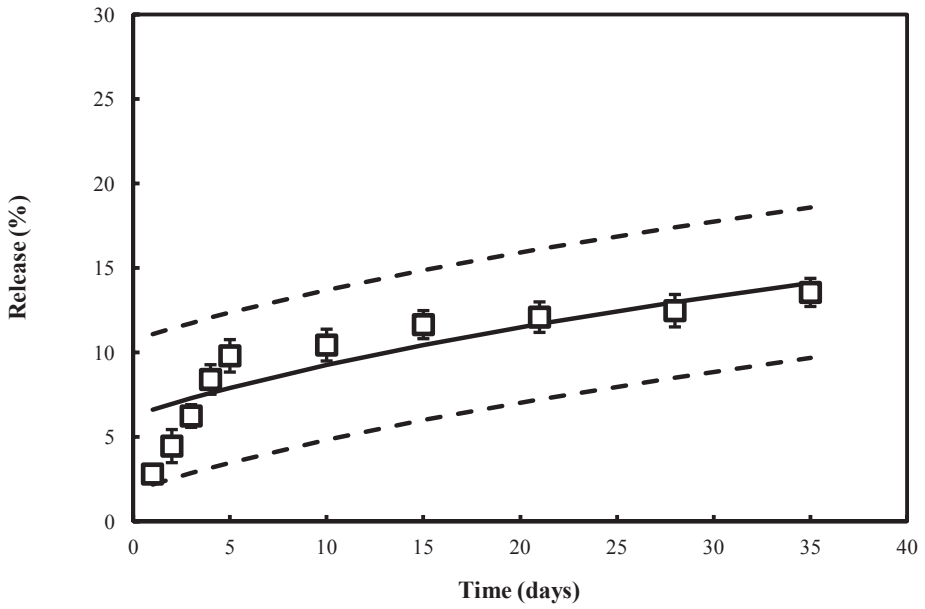

Figure 7.13 The leakage data of EGCG from the beeswax microspheres fitted by Higuchi spherical matrix release kinetics (solid line) with 95% confidence intervals (dash lines).

7.4 DISCUSSION

The beeswax was selected as the carrier material since it is a natural inert material that is highly hydrophobic so that it could serve as an excellent moisture barrier (Mellema 2007) particularly since no surface cracks are generally observable. A simple and low cost method of making beeswax microspheres containing EGCG was optimised by adjusting the loading, the volume of the water phase, the choice and quantity of surfactant, agitation speed and time of emulsification. It was found that the spherical, discrete wax microspheres could only be produced by using the 5% (v/v) Tween 80 in the water phase and an agitation speed of 500 rpm, otherwise aggregates of irregular wax would form after solidification. When the agitation time during the emulsification increased, so that more molten beeswax got cut by the impeller blade, the size of the microspheres decreased slightly. However, a prolonged

agitation time also allowed more EGCG to escape from the wax into the water phase, which resulted in a considerable reduction in the encapsulation efficiency.

When the loading of the EGCG was increased from 1.25 (E) to 2.50 (A) and 5.00 (D) %, there was no significant increase in the encapsulation efficiency of the beeswax microspheres. However, for a further loading of the EGCG powder into the molten wax up to 10.00 % (F), the encapsulation efficiency decreased from 57.4 to 25.4 %; the actual amount of EGCG encapsulated in the beeswax in formulation F was equal to that of D as listed in Table 7.7. This has demonstrated that under the current emulsification conditions, 0.22±0.01 g EGCG was the maximum amount that could be encapsulated in the beeswax by this method. This may be explained on the basis that since natural beeswax consists of esters of long-chains alcohols and fatty acids (Mellema, Van Benthum et al. 2006), the highly water soluble EGCG is poorly soluble in the liquid beeswax and is thus rather dispersed as a suspension under agitation during the preparation process. When being emulsified, the EGCG partitioned into water phase rapidly; in the optimum condition this corresponded to nearly 40 % of the EGCG diffusing from the wax into the water. Therefore, it is important to control the time during the emulsification to avoid the partitioning of EGCG into the water phase, as well as optimising the loading of EGCG in order to avoid low encapsulation efficiency.

The *in vitro* release of EGCG from the beeswax microspheres was very limited with less than 5 % being released after 8 h. Neither a prolonged agitation time, i.e. smaller microspheres, nor a higher amount of EGCG loaded in the wax resulted in a faster release. This demonstrated that although beeswax is an ideal carrier material for protecting EGCG from

the surrounding environment and effectively prevented its releasing; the release in human intestinal tract is predicted to be poor based on the observed *in vitro* data. There was a report that a burst release of indomethacin-beeswax occurred within 1 h in a pH 7.2 phosphate buffer solution, however the result of this work showed a rather slow release and it was in accordance with the 3% release of the theophylline from beeswax pellets matrix system (Cheboyina and Wyandt 2008), compared with a release of 97 % theophylline from cetyl ester wax, which is more hydrophilic than beeswax.

Table 7.7 The amount of the encapsulated EGCG in the beeswax microspheres calculated from their encapsulation efficiency (%) in section 7.3.1.

Formulations	A	B	C	D	E	F
Encapsulation efficiency	56.9±1.8	54.7±1.2	22.3±1.7	61.5±2.4	53.8±1.4	25.4±2.2
Encapsulated EGCG (g)	0.11±0.00	0.11±0.00	0.04±0.00	0.23±0.01	0.05±0.00	0.20±0.02

The total leakage of the encapsulated EGCG from the beeswax microspheres for all the formulations was no more than 11 %, which corresponds to the leakage resulted obtained by Mellema (Mellema, 2006). On this basis beeswax is potentially a long term preservation carrier for EGCG.

Cheboyina (Cheboyina, 2008) described the three steps for the release from a wax matrix as: (1) penetration of the dissolution medium into the wax matrix, (2) dissolution of the dispersed drug particles and (3) diffusion of the dissolved drug through the wax matrix. The fittings of the release and leakage profile by the Higuchi spherical matrix release kinetics/Baker-

Lonsdale model suggest that the mechanism was probably a diffusion-controlled and that the diffusion of EGCG in the wax matrix was the rate-determining step. However, since the release of the EGCG from the beeswax microspheres is very limited, it was more desirable to carry out a further investigation on the release mechanism with more release data. From the measured release constant, k, the diffusion coefficient of EGCG in the beeswax could be calculated from $\frac{3DC_s}{r^2C_0}$ in Equation 7.4 if C_s can be obtained.

7.5 CONCLUSIONS AND FUTURE WORK

An effective protection of EGCG against the environment was achieved by the preparation of beeswax microspheres as a carrier. The microspheres were produced by an emulsified cooling induced solidification process and were of the matrix type that does not require any additional coating. The beeswax microspheres were regular in shape with rough surfaces and a volume moment mean size of < 200 μm. Prolonged agitation resulted in slightly smaller microspheres and a higher loading percentage resulted in larger diameters. Neither the agitation time nor the loading had a significant impact on the encapsulation efficiency. Due to the highly hydrophobic nature of beeswax, the optimised formulation yielded 52.4±2.7 % encapsulation efficiency. The *in vitro* release profile of EGCG from the beeswax microspheres at 37^{o}C was less than 5 % after 8 h, and the leakage of EGCG in the water solution at room temperature was < 11 % after 35 days. The fittings of the release and leakage profiles by the Higuchi spherical matrix release kinetics/Baker-Lonsdale model indicated a diffusion-controlled mechanism. However, more release data are requirerd to confirm the release mechanism. These results have demonstrated that beeswax could be used as a carrier matrix material for EGCG and more preferably a long term preservation carrier.

In future work, different edible waxes could be selected for a formulation with improved *in vitro* release, and a different form of the formulation such as tablets could be also explored. More investigation on the release and leakage profile could be carried out for a better understanding on the release mechanism of the wax system.

CHAPTER 8: DISCUSSION

8.1 CHARACTERISATION OF THE LIPOSOME MEMBRANE

The major absorption barrier of the GI tract is the simple columnar epithelium (the cells in the outer layer) with goblet cells, which are located at the base membrane that is attached to the connective tissues and blood capillaries for transporting absorbed nutrition (Caceci 2008) as described in Chapter 2. Liposomes have been widely studied for mimicking cells because of the unique lipid bilayer-enclosed vesicle structure. The liposome membrane is shown for the first time using cryo-SEM (Chapter 4).

As described by Flaten (Flaten, Dhanikula et al. 2006), two different sizes of liposome could be achieved by repeated extrusion through 800 nm and 400 nm filter membranes. It has been shown in the current work using cryo-SEM that the smaller liposomes have partially filled the pores of the membrane to ensure a robust support for the construction of a compact layer of the larger liposomes for mimicking biological cells. The permeability of caffeine through the different components of the liposome membrane including the blank substrate membrane was also measured here and will be discussed later. The deposition of the liposome into and onto the substrate membrane was achieved by a high speed centrifuge. An attempt was made to study the effect of prolonged centrifugal force on the deposition of the liposome by increasing the centrifuge time. Although a prolonged process made the liposome membrane less permeable for caffeine, it was found that there was a considerably greater possibility of

damage to the membrane, such as rupture and fracture, and the results are not described in the current work.

8.2 CONTINUOUS DIFFUSION THROUGH THE LIPOSOME WITH PRE-TREATMENT

8.2.1. Mass absorption and the molecular diffusion with pre-treatment

The liposome membrane model has been developed from the work of Flaten *et al*. (Flaten, Bunjes et al. 2006; Flaten, Dhanikula et al. 2006; Flaten, Skar et al. 2007; Flaten, Luthman et al. 2008) since it can provide rapid and improved prediction of human absorption by successfully depositing the liposome in a substrate membrane. The diffusion of caffeine was first measured according to their incremental method (Flaten, Dhanikula et al. 2006) and the permeability without pre-treatment ($5.3\pm0.2 \times10^{-6}$ cm/s) is smaller than the reported value ($12.54\pm0.98 \times10^{-6}$ cm/s) (Flaten, Dhanikula et al. 2006) by a factor of about two probably due to small differences in the procedures and chemicals used in the two laboratories. The result showed a lag time in the first 2 h and only after 3 h was a constant diffusion rate observed. Pre-treatment of the membrane with a caffeine solution with the same concentration as the donor solution reduced or even eliminated the lag time after total immersion.

In principle, the permeability should be a constant, if there is no physical or chemical change in the membrane. The observed lag time is actually the time during which the diffusant partitions from the bulk solution in the donor chamber into the liposome until the concentrations in the donor side and in the liposome membrane equilibrate. When the

membrane was pre-treated on both sides, there was a maximum rate of diffusion since the diffusant had partitioned into the liposome membrane and the concentration reached equilibrium with the pre-treatment solution. As a result of these observations, the mass absorption (partitioning) by the liposome membrane was investigated.

An equilibrium amount of 1.52±0.05 $\times 10^{-7}$ mol caffeine was absorbed in the liposome membrane within 1 h, which means that remarkably 20±1 % of the diffusant in the 0.1 mL donor solution was absorbed by the liposome membrane. This result is comparable to the difference in the amount of the diffused caffeine when the liposome membrane was pre-treated and untreated. This accounts for the 2 h of lag time with the incremental method viz., the caffeine partitioned into the membrane by being absorbed and retained with a minor release into the acceptor chamber over the same time period. The release rate of caffeine increased gradually with an increasing amount absorbed by the liposome membrane, until an equilibrium concentration was achieved. The current work has shown that the permeability of caffeine through the liposome membrane without pre-treatment is only about half of that with pre-treatment, indicating the importance of a pre-treatment of the liposome membrane. It also indicated that the measurement of permeability without pre-treating the membrane is particularly difficult for compounds having a high partition coefficient since it can result in a false 'zero' value due to a large proportion of the compound being absorbed by the membrane.

The authors of the incremental method (Bangham, Hill et al. 1974; Flaten, Bunjes et al. 2006; Flaten, Dhanikula et al. 2006; Flaten, Skar et al. 2007; Flaten, Luthman et al. 2008) assumed

a steady-state diffusion after a 3 h lag time since the measurements were considered to be consistent with sink conditions i.e. the concentrations in the donor chambers are assumed to remain constant and those in the acceptor chambers are assumed to be always zero. However, the determination of the lag time was ill-defined and the concentration in the donor chamber decreased significantly due to absorption and diffusion. This results in a smaller permeability with a reduced driving force when applying Equation 3.7. A continuous procedure was thus carried out to ensure that the concentrations could be measured by a UV spectrometer and, instead of assuming steady-state, a mathematical model based on the time-dependent concentrations in the donor and acceptor chambers was employed to calculate the permeability values. The model assumed that the solutions in both the donor and acceptor chambers were well mixed so that the boundary concentration at the membrane interface is equal to the bulk concentration. This assumption was validated by measuring the permeability under the same conditions except that the chambers were agitated with a shaker.

It was found that the permeability of caffeine through the liposome membrane was independent of (a) the pre-treatment time, for times >1 h, and (b) the concentration of the donor solution. Important factors were that the membrane was saturated with the diffusant after 1 h and that there was no evidence of a loss in integrity and stability under these conditions. Consequently, this has established the suitability of the continuous method for obtaining values of the permeability.

The diffusion coefficient could be obtained from the permeability values if the partition coefficient of the diffusant between the liposome and water phase is known. Thus this

method could offer useful means of understanding the role of molecular architecture and polarity in addition to predicting human absorption.

8.2.2. The impact of the desorption on the permeability

Pre-treating the membrane can effectively reduce or eliminate the underestimation of the permeability; however, any possible overestimation should be considered. The MATLAB modelling suggests that a rapid desorption may result in a larger permeability calculated from Equation 3.8 thus there can be an overestimation of the permeability if the desorption is ignored. It was analysed that the permeability of caffeine was not significantly influenced by the desorption of the caffeine. Although the values of K for the molecules studied here are unknown, except for caffeine, on the basis of their partition coefficients between a water/octane system (Table 8.1), it was calculated that the permeabilities were not affected significantly by estimating their A and B values based on the values of caffeine (Table 8.2). The partition coefficient for caffeine in Table 8.1 is ~ 1, which is less than the value (2.2) obtained in the current work from the absorption data. However, similar permeabilities were obtained for both values of the partition coefficient. Thus it can be concluded that the desorption of the diffusants from the membrane was not a significant factor in determining permeability results.

Table 8.1 The published octane-water partition coefficients of the diffusants (Zhu, Jiang et al. 2002; Corti, Maestrelli et al. 2006)

	Paracetamol	Theophylline	Caffeine	Acyclovir	Nadolol	Amphotericin B
Partition coefficient	3.02, 3.23	0.56	0.85, 1.05	0.02	5.13	0.03

Table 8.2 Permeability values (normalised by the value of caffeine)

	[a]Continuous model	[b]Continuous model with desorption
Paracetamol	0.39±0.00	0.37±0.01
Theophylline	1.29±0.32	0.93 ±0.30
Caffeine	1.00±0.11	0.94±0.12
Acyclovir	0.40±0.03	0.36±0.03
Nadolol	0.52±0.15	0.45±0.13
Amphotericin B	0.19±0.14	0.19±0.09

[a] Data fitted to Equation 3.6.

[b] Data fitted to Equation 3.8 using MATLAB.

8.2.3. A comparison of the permeability obtained from the *in vitro* assays with F_a

The human absorption values (F_a %) of the six model diffusants are plotted as a function of the caffeine normalised permeability in Figure 8.1, which was obtained in the current study from the improved procedure. Plots based on data published using the PAMPA model (J. A. Ruell 2002; Avdeef and Tsinman 2006), the solution based PAMPA with a hydrophilic filter (Zhu, Jiang et al. 2002), the lipid/oil/lipid tri-layer PAMPA model (Chen, Murawski et al. 2008) and the cell based caco-2 model are also shown for comparison purposes.

PAMPA models have been proved to be a very successful predictive assay, being high-throughput and low-cost. However, the conventional method with the hydrophobic membrane which was coated with 10% (w/v) egg lecithin dissovled in n- dodecane, failed to give a correct prediciton of well absorbed molecules such as caffeine and theophylline as shown in Figure 8.1 (b). It has been proposed that the excess solvent used in this method could retain molecules with a high partition coefficient, and for polar molecules, more energy is required to permeate through an alkane barrier due to the lack of hydrogen bonding in the solvent

(Avdeef and Tsinman 2006). The data obtained using the PAMPA-hydrophilic and PAMPA-trilayer models are shown in Figure 8.1 (c) and (d); they are improved PAMPA models where the first one used a hydrophilic substrate membrane to avoid the additional barrier of a hydrophobic membrane; while the second ensures that there is a lipid bilyer in the substrate membrane without excess of solvent. The prediction of the human absorption is clearly improved compared with the traditional PAMPA method, nevertheless, the methods underestimated the permeability of certain molecules that can give false zero values.

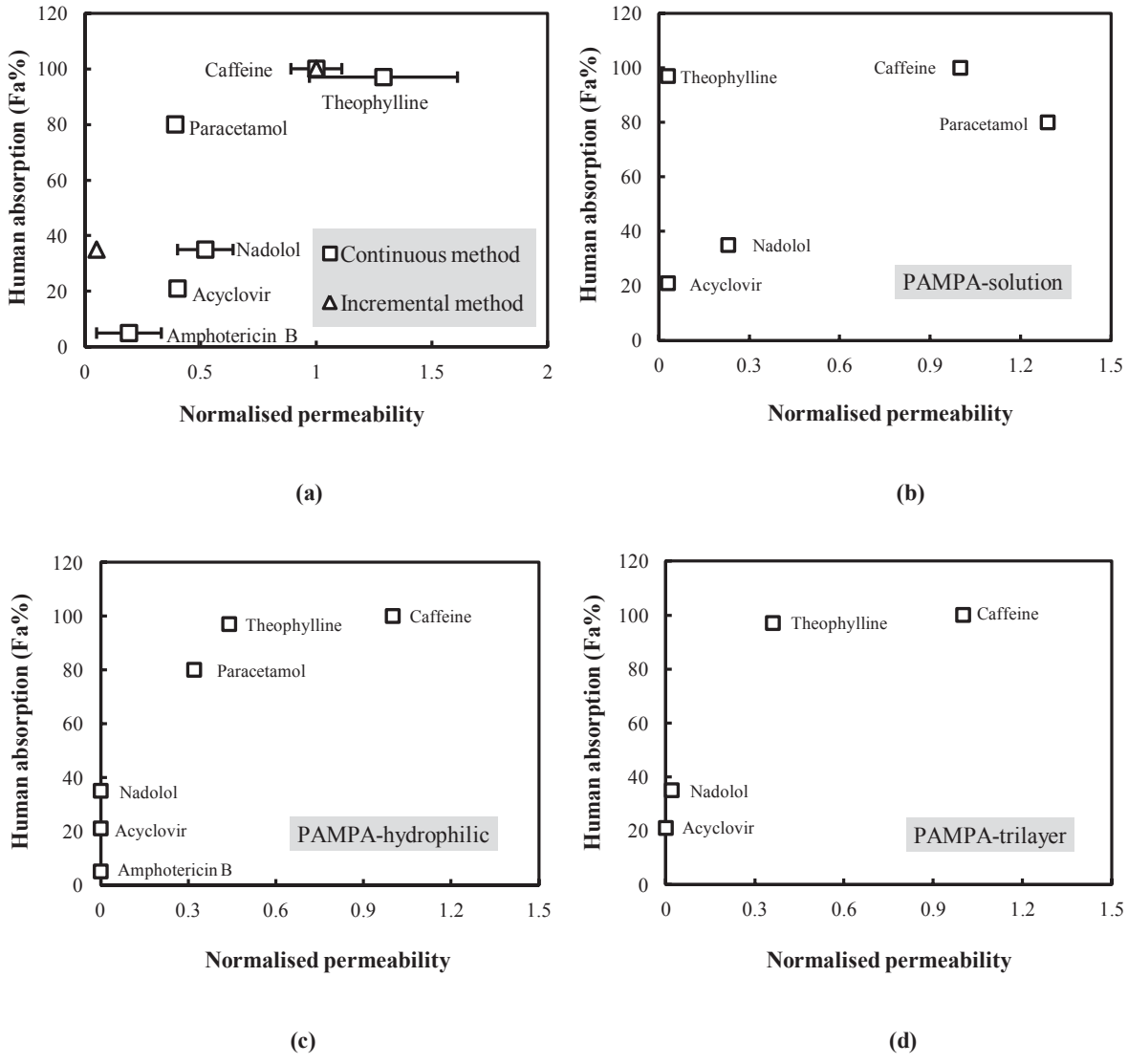

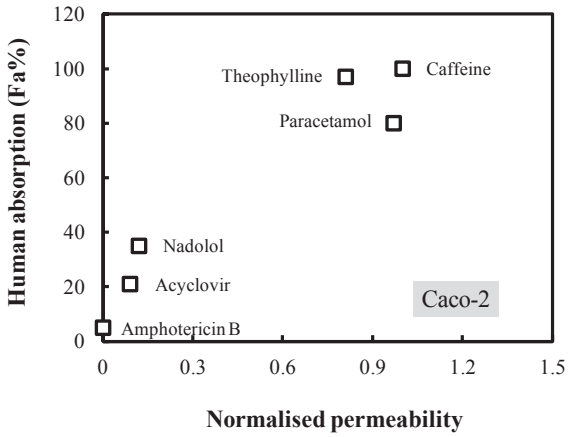

(e)

Figure 8.1 Correlation between human absorption and normalised permeability obtained from the following *in vitro* models: (a) incremental (Flaten, Dhanikula et al. 2006) and continuous methods; (b) solution based PAMPA (J. A. Ruell 2002; Avdeef and Tsinman 2006); (c) PAMPA with hydrophilic filter (Zhu, Jiang et al. 2002); (d) tri-layer PAMPA (Chen, Murawski et al. 2008); (e) Caco-2 cell model (Yazdanian, Glynn et al. 1998; Yamashita, Furubayashi et al. 2000; Siissalo, Laine et al. 2010).

The current liposome membrane, which involves no solvent in the membrane, shows a close correlation with human absorption. However, the incremental model does not separate those those molecules with a moderate and a poor human absorption (F_a%), which are considerably underestimated. In Figure 8.1 (a), the continuous liposome method achieved a closer prediction for the molecules with small values of the permeability such as nadolol, acyclovir and amphotericin B. This is largely due to the pre-treatment of the liposome membrane which saturates the liposome to reach the eqilibrium concentration of the donor chamber and in the liposome. Moreover, the permeabilities of these molecules are underestimated by the other established models (J. A. Ruell 2002; Avdeef and Tsinman 2006; Zhu, Jiang et al. 2002;

Chen, Murawski et al. 2008) to the extent that most of them suggest that the permeability is approximately zero but the *in vivo* data show that this should not be the case.

The Caco-2 model is a monolayer of intestinal epithelial cell lines that predicts different pathways of the drug transport. As the model diffusants were known to diffuse passively via the cell membrane, the results of the improved liposome membrane were comparable with those from the Caco-2 (Yazdanian, Glynn et al. 1998; Yamashita, Furubayashi et al. 2000; Siissalo, Laine et al. 2010) as shown in Figure 8.1 (e). Given the difficulty of the cell cultivation and the relatively high cost of carrying out a Caco-2 experiment, the much simpler and lower-cost liposome membrane model is a significant improvement as a first stage *in-vitro* assay before a further more complicated method is carried out based on human absorption prediction.

8.3 THE PHYSIOCHEMICAL ENHANCEMENT OF THE MOLECULAR DIFFUSION THROUGH THE LIPOSOME MEMBRANE

8.3.1. The impact of ethanol on the diffusion through the liposome membrane

Ethanol is a widely used diffusion enhancer different mechanisms have been proposed (Moser, Kriwet et al. 2001): in particular it can enhance the diffusion coefficient, the apparent partition coefficient of the diffusant and the solubility in the membrane (Inada, Nakagawa et al. 1990; Pershing, Silver et al. 1992). The perturbation of the lipid bilayers by ethanol was studied by Barry and Gawrisch (1994) and Koenig and Gawrisch (2005) who found that it could disrupt the molecular packing in the rigid region of the glycerol backbone, which

resulted in a lateral expansion of the bilayer, and that could significantly disorder the entire acryl chain, leading to fluidisation of the membrane lipids. Furthermore, molecular dynamics (MD) (Chanda and Bandyopadhyay 2006; Gurtovenko and Anwar 2009) revealed that ethanol interacts strongly with the phosphocholine headgroups, reorienting them toward the aqueous layer, which modifies the dynamic behaviour of both the lipid and the water molecules. The physiochemical enhancement of nearly 60 % of the diffusion for caffeine by ethanol is thus an outcome of these molecular interactions between ethanol and lipid bilayer which makes the liposome membrane more fluid and permeable for molecular diffusion (Patra, Salonen et al. 2006). This suggests that a formulation of highly concentrated ethanol or a strong alcoholic drink would have a considerable impact on biological membranes and hence the GI absorption. Interestingly, ethanol was reported to have a concentration-dependant enhancement on its enhancement of the diffusion (Kuriharabergstrom, Knutson et al. 1990). And this was also observed in this work the enhancement of the diffusion increased with a growing concentration of ethanol.

It was observed in this study that ethanol is most potent in enhancing the diffusion of caffeine and theophylline, and it has only a modest effect on the diffusion of nadolol, acyclovir and amphotericin B. Although ethanol increases the solubility of paracetamol, there are no reports of it improving the *in-vivo* bioavailability, which is consistent with the current results. The physiochemical interactions between the lipid bilayer and different molecules are complex, and further investigation will be needed to understand the specificity of the action of ethanol.

It is important to ensure that the liposome is not disrupted at high concentrations of ethanol, which would lead to an artifactual values of the permeability. The current work established that the size distributions of the liposomes were not affected by ethanol. A similar finding was reported by Komatsu *et al* (Komatsu and Okada 1995) who observed that there was no significant aggregation or fusion in egg PC liposome compared with dipalmitoyl PC (DPPC) liposomes in the presence of ethanol. Therefore, there is strong evidence that the liposome membrane remains intact in the presence of ethanol, and the physiochemical enhancement of the molecular diffusion through the liposome membrane is a result of the molecular interactions between the lipid and ethanol as discussed above.

8.3.2. The impact of DMSO on the diffusion through the liposome membrane

The surface mechanical properties of the liposome membrane under different conditions were examined using colloid probe AFM rather than the conventional single vesicle method (Liang 2004). DMSO has been reported to reduce the area compressibility modulus and bending rigidity of lipid membranes (i.e. a reduction in rigidity) (Notman 2006; Gurtovenko and Anwar 2007), and the current AFM results confirmed this observation since it caused a significant reduction of the Young's modulus and hardness of the liposome. Despite being able to induce pore formation in the lipid bilayer and thus to promote the permeability (Gordeliy, Kiselev et al. 1998), the DMSO molecule interacts more intensively with water molecules than with the polar head groups of liposomes thus inducing some dehydration of these groups (Kiselev, Lesieur et al. 1999; Sum and de Pablo 2003), which could result in a tighter packing of the liposome bilayer. This could be possibly the reason for the limited enhancement of DMSO on the diffusion of the model diffusants.

8.3.3. The synergetic effect on the diffusion of paracetamol and caffeine

Potential synergetic effects on the diffusion of two diffusants carried out in artificial membrane assays have not been studied previously. Paracetamol and caffeine was explored in the current work as an example of an application of the improved liposome membrane method to the study of the diffusion of combination formulations.

It was reported that the inhibitory effect of paracetamol on cyclooxygenase (COX) would be more effective when combined with caffeine as a pain killer (Fiebich, Lieb et al. 2000), and it was proposed that the AIs act on different but distinct molecular targets in those multi-target combinations (Straube, Aicher et al. 2011). However, the results from the diffusion of paracetamol with increasing concentration of caffeine showed a decreasing permeability while the permeability of caffeine was not influenced by paracetamol, indicating that the negative synergy of caffeine could retard the absorption of paracetamol in the human GI tract. This influence of caffeine on the absorption of paracetamol should be considered in the combination formulations if the results are clinically confirmed.

8.4 THE DIFFUSION OF THE TPS THROUGH THE LIPOSOME MEMBRANE

There has no published work on the permeability of TPs through cell membranes or artificial membranes. Here, the diffusion of the TPs was investigated by using the established improved liposome membrane method. The absorption of the TPs by the liposome membrane was firstly measured due to their strong binding to the lipid bilayer (Hashimoto, Kumazawa et al. 1999; Sirk, Brown et al. 2009). The current results showed that EGCG and ECG have

the highest amount of absorption, which agreed with the reported results that those two TPs have the strongest affinity (incorporation) to the lipid bilayer (Hashimoto, Kumazawa et al. 1999; Kajiya, Hojo et al. 2004). The extent of absorption of the four TPs by the liposome membrane is in the order of their partition coefficients in a water/octane system. The results of the absorption of those TPs correlate closely with their health properties that ECG and EGCG have the highest radical scavenging activity (Henning, Fajardo-Lira et al. 2003) compared with EC and EGC, such as antioxidant and antitumor activities (Higdon and Frei 2003; Kuzuhara, Suganuma et al. 2008). It has been proposed that the interactions of the TPs with lipid bilayers is governed by the presence of a galloyl moiety as shown in Figure 8.2 since these functional groups have a stronger affinity for lipid bilayers (Kajiya, Hojo et al. 2004).

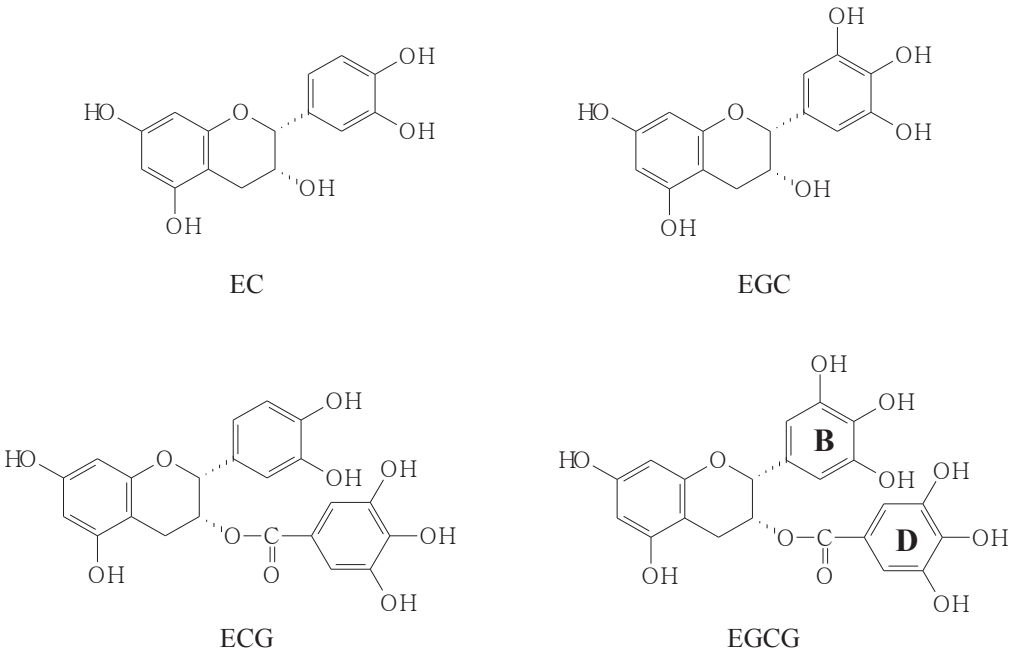

Figure 8.2 The chemical structures of the TPs with ring labels of EGCG (B and D ring).

The current absorption kinetics data reveal that EGCG has the highest absorption constant and thus the fastest interaction with the lipid bilayers. This is consistent with the result obtained from molecular dynamics by Sirk, T *et al*. (Sirk, Brown et al. 2008) that EGCG has the highest number of hydrogen bonds formed with lipid headgroups and a large number of those bonds were located at the B and D rings. This is in accordance with the current Raman spectroscopy results from which it was concluded there are strong interactions between the two molecules arising from the hydrogen bonds formed between EGCG and the lipid molecules.

Further molecular dynamics studies (Sirk, Brown et al. 2008) showed that since the TPs are bounded to the bilayer surface with a strong interaction, their diffusion along the bilayer was characterised by the formation and breaking of the hydrogen bonds. The current results have demonstrated that since EGCG and ECG have the strongest affinity to the lipid bilayer, their diffusion through the liposome membrane was retarded compared with EC and EGC. Moreover, neither the addition of a diffusion enhancer or a change of pH of the diffusion solution (as an attempt to decrease the number of ionised EGCG groups and so suppress hydrogen bonding) could improve the diffusion of EGCG. This suggests that the strong bonding between the lipid molecule and EGCG is rather difficult to break, which thus results in a low bioavailability of this TP.

CHAPTER 9: OVERALL CONCLUSIONS AND FUTURE WORK

9.1 OVERALL CONCLUSIONS

An artificial membrane system has been developed to avoid the high-cost and undesirable animal tests involved in an accurate prediction of human absorption: a lipid bilayer of liposomes resembles the walls of biological cells so that a liposome membrane is more representative of the barrier to absorption in the GI tract than the conventional PAMPA model in terms of morphology. Moreover, this approach avoids residual solvent in the test membrane, which is a problem with some *in vitro* methods since it may interfere with the diffusion. Consequently, the artificial liposome membrane model developed by Flaten and his coworkers (Flaten, Bunjes et al. 2006; Flaten, Dhanikula et al. 2006; Flaten, Skar et al. 2007; Flaten, Luthman et al. 2008) is an ideal basis for screening the biological availability of pharmaceutical drugs or nutritionally beneficial molecules. The procedure that they developed for measuring permeability has a number of limitations that are primarily associated with the absorption of the diffusant in the membrane. This introduces errors that were overcome in the present work by pre-treating the membrane with the diffusant and fitting the data to an appropriate model. A particular advantage of the modified method is that it allows an accurate measurement for diffusants with small values of the permeability and thus leads to an improved correlation with *in vivo* human absorption compared with existing methods.

The application of the improved liposome membrane can be extended to explore the physicochemical enhancement of molecular diffusion. The current result showed that 40 % ethanol has the most significant enhancement on the diffusion of caffeine and theophylline by nearly 60 % and also nearly 30 % for the other diffusants. It was also found that the enhancement of ethanol is concentration-dependant, and the size analysis of the liposomes in ethanol suggests that the physicochemical interaction did not cause any morphological changes to the liposome. Therefore further work is required to ascertain the exact mechanism of the enhancement. On the contrary, despite of its significant impact on the elastic properties of the liposome, DMSO did not result in any significant physicochemical enhancement of the diffusion, although it has been reported to induce pore formation in the lipid bilayers.

The application of the improved liposome membrane was further examined by investigating a potential synergetic effect on the diffusion of various compounds in a combination formulation, where caffeine and paracetamol was used as an example in this work. Paracetamol is often combined with caffeine for an enhanced medical benefit; however the results showed that caffeine has a negative synergy on the absorption of paracetamol to the extent that its permeability was only half of that without caffeine.

The diffusion of TPs through the liposome membrane was measured and attempts were made to enhance the permeability of EGCG due to its health benefits. A large quantity and a rapid absorption of EGCG by the liposome membrane was observed, and it cannot diffuse freely thus indicating a low bioavailability in the human GI tract. The absorption of the other TPs was in the order of their partition coefficient in a water/octane system, i.e.

ECG>EGCG>EC>EGC, which was consistent with published work on a similar system (Hashimoto, Kumazawa et al. 1999; Kajiya, Hojo et al. 2004). This result correlates closely to their health properties (Higdon and Frei 2003; Kuzuhara, Suganuma et al. 2008). The strong hydrogen bonding interaction between EGCG and the lipid bilayer was observed by the current Raman spectroscopy data, which is consistent with molecular dynamics simulations (Sirk, Brown et al. 2008). It may be concluded that this bonding is rather difficult to disrupt since attempts at using diffusion enhancers and changing the pH in the donor chamber did not affect the permeability values.

Finally, an effective protection of EGCG from the environment was achieved by the preparation of beeswax microspheres as a carrier. The microspheres were regular in shape without visible cracks and a mean size of less than 200 μm. The preparation involved an emulsified cooling induced solidification; the agitation time during the emulsification and a higher loading rate did not influence the encapsulation efficiency. An optimum of 52.4±2.7 % encapsulation efficiency was obtained due to the high hydrophobic property of the beeswax and the high solubility of the EGCG in the water phase. The *in vitro* release profile of EGCG from the beeswax microspheres at 37^{o}C was less than 5 % within 8 hours, and the leakage of EGCG in the water solution at room temperature was no more than 11 % within 35 days, indicating that beeswax could be used as a carrier matrix for long term uses. The fitting of the release and leakage data indicated a diffusion-controlled mechanism.

9.2 FUTURE WORK

In future work, the preparation of the membrane with different sizes of liposome could be explored to investigate the morphological impact of the liposome on the molecular diffusion. More model diffusants with a variety of physicochemical properties could be examined to establish a predictive correlation between the permeability and human absorption; and for a correlation between the permeability with molecular properties (Zhu, Jiang et al. 2002). The partitioning coefficient of the molecules in the liposome membrane could be studied to obtain their diffusion coefficient and other important parameters for MATLAB programming. The application of the liposome membrane could be extended to measure the permeability of various formulations, to test potential diffusion enhancers and retardants for a targeted release.

The absorption kinetic of the TPs was based on the partition coefficient in a water/octane system (Hashimoto, Kumazawa et al. 1999), and the result of the absorption constant *k* could be improved if the partition coefficient of the TPs between water and liposome was obtained, for example, by the use of HPLC with an immobilised liposome membrane column (Uekusa, Takeshita et al. 2008).

Different encapsulation processes and materials could be explored for application to EGCG, such as spray drying and liposome entrapment (Fang and Bhandari 2010). The leakage of the encapsulated EGCG from the beeswax microspheres could be extended to months or years to examine the further release and to determine whether EGCG is degraded even when it is still trapped in the wax. As mentioned previously, more release or leakage data is required for

fitting the mathematic models as a basis for an improved understanding of the release behaviour.

APPENDIX A

THE IMPACT OF THE DESORPTION ON THE PERMEABILITY

An example of the MATLAB programming:

```
function xdot=membrane(t,x);
xdot = zeros(1,1);
cd0=1.51; % intial conc in donor mg/ml
va=0.6; % acceptor volume, ml
A=3.1416/4*0.008^2; % membrane area, m^2.
vd=0.1; % donor volume, ml
mm0=29.52*10^(-3); % initial caffeine in membarne, mg
Kvm=0.02952/1.46572; % product of equilibrium constant and membrane volume,
ml
Km=11.49*10^(-6); % permeability in cm/s

%x(2)=(cd0*vd+mm0-x(1)/2*Kvm-x(1)*va)/(vd+Kvm/2) % concentration in donor
chamber at time t, mg/ml
%xdot(2)=(-xdot(1)/2*Kvm-xdot(1)*va)/(vd+Kvm/2)
%Mt=Kvm/2*(cd+x(1))*10^(-2.7552)/(7.62*10^-3)*(t/60)^0.2126;  % mg
if t<600
P2=2.653*10^-3/600/(7.62*10^-3)*Kvm/2*((cd0*vd+mm0-x(1)/2*Kvm-
x(1)*va)/(vd+Kvm/2)+x(1))% initial two points, mg/s
end
if t>=600
P2=Kvm/2*((cd0*vd+mm0-x(1)/2*Kvm-x(1)*va)/(vd+Kvm/2)+x(1))*10^(-
1.0153)*0.2126*(t)^(-0.7874)
end

xdot(1)=P2/va/2+Km*A/va*((cd0*vd+mm0-x(1)/2*Kvm-x(1)*va)/(vd+Kvm/2)-
x(1))*10^4;



t0=0;tf=18000;
x0=[0]'
[t x]=ode23('membranefinal',t0,tf,x0);
plot(t,x)
legend('x(1)')
title('C in the acceptor')
xlabel('t')
ylabel('Ca')
```

REFERENCES

Adson, A., T. J. Raub, et al. (1994). "Quantitative approaches to delineate paracellular diffusion in cultured epithelial-cell monolayers." Journal of Pharmaceutical Sciences **83**(11): 1529-1536.

Al-Awqati, Q. (1999). "One hundred years of membrane permeability: does Overton still rule?" Nature Cell Biology **1**(8): E201-E202.

Aminabhavi, T. M. and S. F. Harlapur (1997). "Sorption/desorption and diffusion kinetics of ketones and nitriles into fluoropolymer membranes." Journal of Applied Polymer Science **65**(4): 635-647.

Artursson, P. and J. Karlsson (1991). "Correlation between oral-drug absorption in humans and apparent drug permeability coefficients in human intestinal epithelial (Caco-2) cells." Biochemical and Biophysical Research Communications **175**(3): 880-885.

Artursson, P., K. Palm, et al. (2001). "Caco-2 monolayers in experimental and theoretical predictions of drug transport." Advanced Drug Delivery Reviews **46**(1-3): 27-43.

Avdeef, A., S. Bendels, et al. (2007). "PAMPA - Critical factors for better predictions of absorption." Journal of Pharmaceutical Sciences **96**(11): 2893-2909.

Avdeef, A. and O. Tsinman (2006). "PAMPA - A drug absorption in vitro model 13. Chemical selectivity due to membrane hydrogen bonding: In combo comparisons of HDM-, DOPC-, and DS-PAMPA models." European Journal of Pharmaceutical Sciences **28**(1-2): 43-50.

Baker, R. W., Lonsdale, H.K. (1974). Controlled release: mechanisms and rates. New York, Plenum Press.

Balentine, D. A., S. A. Wiseman, et al. (1997). "The chemistry of tea flavonoids." Critical Reviews in Food Science and Nutrition **37**(8): 693-704.

Balimane, P. V., S. H. Chong, et al. (2000). "Current methodologies used for evaluation of intestinal permeability and absorption." Journal of Pharmacological and Toxicological Methods **44**(1): 301-312.

Bangham, A. D., M. W. Hill, et al. (1974). Preparation and use of liposomes as models of biological membranes. Plenum Press.

Barry, J. A. and K. Gawrisch (1994). "Direct NMR evidence for ethanol binding to the lipid-water interface of phospholipid-bilayers." Biochemistry **33**(26): 8082-8088.

Bonting, S. L. and J. J. H. H. M. Pont (1981). Membrane transport, Elsevier/North-Holland Biomedical Press.

Bordi, F., C. Cametti, et al. (2000). "Ion permeation across model lipid membranes: A kinetic approach." Journal of Physical Chemistry B **104**(22): 5318-5323.

Bunge, A. L. and R. L. Cleek (1995). "A new method for estimating dermal absorption from chemical-exposure. 2. Effect of molecular-weigt and octanol water partitioning " Pharmaceutical Research **12**(1): 88-95.

Caceci, T. (August 2008). "Veterinary Histology." from http://www.vetmed.vt.edu/education/Curriculum/VM8054/VM8054HP.htm.

Cai, Y., N. D. Anavy, et al. (2002). "Contribution of presystemic hepatic extraction to the low oral bioavailability of green tea catechins in rats." Drug Metabolism and Disposition **30**(11): 1246-1249.

Cao, X. H., S. T. Gibbs, et al. (2006). "Why is it challenging to predict intestinal drug absorption and oral bioavailability in human using rat model." Pharmaceutical Research **23**(8): 1675-1686.

Chanda, J. and S. Bandyopadhyay (2006). "Perturbation of phospholipid bilayer properties by ethanol at a high concentration." Langmuir **22**(8): 3775-3781.

Cheboyina, S. and C. M. Wyandt (2008). "Wax-based sustained release matrix pellets prepared by a novel freeze pelletization technique - II. In vitro drug release studies and release mechanisms." International Journal of Pharmaceutics **359**(1-2): 167-173.

Chen, X. X., A. Murawski, et al. (2008). "A novel design of artificial membrane for improving the PAMPA model." Pharmaceutical Research **25**(7): 1511-1520.

Chen, Z. Y., Q. Y. Zhu, et al. (2001). "Degradation of green tea catechins in tea drinks." Journal of Agricultural and Food Chemistry **49**(1): 477-482.

Chiou, W. L. and A. Barve (1998). "Linear correlation of the fraction of oral dose absorbed of 64 drugs between humans and rats." Pharmaceutical Research **15**(11): 1792-1795.

Chiou, W. L. and P. W. Buehler (2002). "Comparison of oral absorption and bioavailability of drugs between monkey and human." Pharmaceutical Research **19**(6): 868-874.

Choi, Y. W. and J. A. Rogers (1990). "The liposome as a model membrane in correlations of partitioning with alpha-adrenoceptor agonist activities." Pharmaceutical Research **7**(5): 508-512.

Clark, D. E. (1999). "Rapid calculation of polar molecular surface area and its application to the prediction of transport phenomena. 1. Prediction of intestinal absorption." Journal of Pharmaceutical Sciences **88**(8): 807-814.

Conradi, R. A., A. R. Hilgers, et al. (1991). "The influence of peptide structure on transport across Caco-2 cells." Pharmaceutical Research **8**(12): 1453-1460.

Corti, G., F. Maestrelli, et al. (2006). "Development and evaluation of an in vitro method for prediction of human drug absorption - I. Assessment of artificial membrane composition." European Journal of Pharmaceutical Sciences **27**(4): 346-353.

Corti, G., F. Maestrelli, et al. (2006). "Development and evaluation of an in vitro method for prediction of human drug absorption - II. Demonstration of the method suitability." European Journal of Pharmaceutical Sciences **27**(4): 354-362.

Crank, J. (1979). The mathematics of diffusion, Clarendon Press.

Cyprotex. (2012). "Caco-2 permeability assay." from http://www.cyprotex.com/admepk/in-vitro-permeability/caco-2-permeability/.

Cyprotex (2012). "Parallel artificial membrane permeability assay (PAMPA)." from http://www.cyprotex.com/admepk/in-vitro-permeability/pampa/.

Desai, K. G. H. and H. J. Park (2005). "Recent developments in microencapsulation of food ingredients." Drying Technology **23**(7): 1361-1394.

Dhatfield (2008). "Cell membrane detailed diagram 3."from http://en.wikipedia.org/wiki/File:Cell_membrane_detailed_diagram_3.svg

DiMasi, J. A. (2002). "The value of improving the productivity of the drug development process - Faster times and better decisions." Pharmacoeconomics **20**: 1-10.

Donhowe, I. G. and O. Fennema (1993). "Water-vapor and oxygen permeability of wax films." Journal of the American Oil Chemists Society **70**(9): 867-873.

Dressman, J. B., G. L. Amidon, et al. (1985). "Absorption potential: estimating the fraction absorbed for orally administered drugs." Journal of Pharmaceutical Sciences **74**(5): 588-589.

Dufresne, C. J. and E. R. Farnworth (2001). "A review of latest research findings on the health promotion properties of tea." Journal of Nutritional Biochemistry **12**(7): 404-421.

Dziezak, J. D. (1988). "Microencapsulation and encapsulated ingredients " Food Technology **42**(4): 136-143.

Eltayar, N., R. S. Tsai, et al. (1991). "Partitioning of solutes in different solvent systems-The contribution of hydrogen-bonding capacity and polarity " Journal of Pharmaceutical Sciences **80**(6): 590-598.

Escher, B. I., R. P. Schwarzenbach, et al. (2000). "Evaluation of liposome-water partitioning of organic acids and bases. 1. Development of a sorption model." Environmental Science & Technology **34**(18): 3954-3961.

Fagerholm, U. (2007). "Prediction of human pharmacokinetics - gastrointestinal absorption." Journal of Pharmacy and Pharmacology **59**(7): 905-916.

Fagerholm, U., M. Johansson, et al. (1996). "Comparison between permeability coefficients in rat and human jejunum." Pharmaceutical Research **13**(9): 1336-1342.

Fagerholm, U., A. Lindahl, et al. (1997). "Regional intestinal permeability in rats of compounds with different physicochemical properties and transport mechanisms." Journal of Pharmacy and Pharmacology **49**(7): 687-690.

Fang, J. Y., W. R. Lee, et al. (2006). "Effect of liposome encapsulation of tea catechins on their accumulation in basal cell carcinomas." Journal of Dermatological Science **42**(2): 101-109.

Fang, Z. and B. Bhandari (2010). "Encapsulation of polyphenols - a review." Trends in Food Science & Technology **21**(10): 510-523.

Feldstein, L. (1912). "The refractive index of beeswax." Journal of Industrial and Engineering Chemistry-Us **4**: 498-499.

Fiebich, B. L., K. Lieb, et al. (2000). "Effects of caffeine and paracetamol alone or in combination with acetylsalicylic acid on prostaglandin E-2 synthesis in rat microglial cells." Neuropharmacology **39**(11): 2205-2213.

Field, L. D., S. Sternhell, et al. (2008). Organic Structures from Spectra, John Wiley & Sons.

Finkelstein, A. (1976). "Water and nonelectrolyte permeability of lipid bilayer membranes." Journal of General Physiology **68**(2): 127-135.

Fischer, H., M. Kansy, et al. (2007). "Permeation of permanently positive charged molecules through artificial membranes - Influence of physico-chemical properties." European Journal of Pharmaceutical Sciences **31**(1): 32-42.

Flaten, G. E., H. Bunjes, et al. (2006). "Drug permeability across a phospholipid vesicle-based barrier - 2. Characterization of barrier structure, storage stability and stability towards pH changes." European Journal of Pharmaceutical Sciences **28**(4): 336-343.

Flaten, G. E., A. B. Dhanikula, et al. (2006). "Drug permeability across a phospholipid vesicle based barrier: A novel approach for studying passive diffusion." European Journal of Pharmaceutical Sciences **27**(1): 80-90.

Flaten, G. E., K. Luthman, et al. (2008). "Drug permeability across a phospholipid vesicle-based barrier - 4. The effect of tensides, co-solvents and pH changes on barrier integrity and on drug permeability." European Journal of Pharmaceutical Sciences **34**(2-3): 173-180.

Flaten, G. E., M. Skar, et al. (2007). "Drug permeability across a phospholipid vesicle based barrier: 3. Characterization of drug-membrane interactions and the effect of agitation on the barrier integrity and on the permeability." European Journal of Pharmaceutical Sciences **30**(3-4): 324-332.

Friedman, M., C. E. Levin, et al. (2009). "Stability of Green Tea Catechins in Commercial Tea Leaves during Storage for 6 Months." Journal of Food Science **74**(2): H47-H51.

G. Giebisch, D. C. T., H. H. Ussing, Ed. (1978). Membrane transpot in biology, Springer-Verlag Berlin, Heidelberg, New York.

Garrett, M. D., M. I. Walton, et al. (2003). "The contemporary drug development process: advances and challenges in preclinical and clinical development." Progress in cell cycle research **5**: 145-158.

Gordeliy, V. I., M. A. Kiselev, et al. (1998). "Lipid membrane structure and interactions in dimethyl sulfoxide/water mixtures." Biophysical Journal **75**(5): 2343-2351.

Gowda, D. V., V. Ravi, et al. (2009). "Preparation, evaluation and bioavailability studies of indomethacin-bees wax microspheres." Journal of Materials Science-Materials in Medicine **20**(7): 1447-1456.

Grasset, E., M. Pinto, et al. (1984). "Epithelial properties of human colonic-carcinoma cell-line Caco-2-electrical parameters." American Journal of Physiology **247**(3): C260-C267.

Gurtovenko, A. A. and J. Anwar (2007). "Modulating the structure and properties of cell membranes: The molecular mechanism of action of dimethyl sulfoxide." Journal of Physical Chemistry B **111**(35): 10453-10460.

Gurtovenko, A. A. and J. Anwar (2009). "Interaction of Ethanol with Biological Membranes: The Formation of Non-bilayer Structures within the Membrane Interior and their Significance." Journal of Physical Chemistry B **113**(7): 1983-1992.

Hamza, A. and C. G. Zhan (2006). "How can (-)-epigallocatechin gallate from green tea prevent HIV-1 infection? Mechanistic insights from computational modeling and the implication for rational design of anti-HIV-1 entry inhibitors." Journal of Physical Chemistry B **110**(6): 2910-2917.

Hashimoto, T., S. Kumazawa, et al. (1999). "Interaction of tea catechins with lipid bilayers investigated with liposome systems." Bioscience Biotechnology and Biochemistry **63**(12): 2252-2255.

Hauser, H., M. Stubbs, et al. (1972). "Ion permeability of phospholipid bilayers." Nature **239**(5371): 342-344.

Heaney, R. P. (2001). "Factors influencing the measurement of bioavailability, taking calcium as a model." Journal of Nutrition **131**: 1344S-1348S.

Henning, S. M., C. Fajardo-Lira, et al. (2003). "Catechin content of 18 teas and a green tea extract supplement correlates with the antioxidant capacity." Nutrition and Cancer-an International Journal **45**(2): 226-235.

Henning, S. M., Y. T. Niu, et al. (2004). "Bioavailability and antioxidant activity of tea flavanols after consumption of green tea, black tea, or a green tea extract supplement." American Journal of Clinical Nutrition **80**(6): 1558-1564.

Higdon, J. V. and B. Frei (2003). "Tea catechins and polyphenols: Health effects, metabolism, and antioxidant functions." Critical Reviews in Food Science and Nutrition **43**(1): 89-143.

Higuchi, T. (1963). "Mechanism of sustained-action medication - theoretical analysis of rate of release of solid drugs dispersed in solid matrices." Journal of Pharmaceutical Sciences **52**(12): 1145-1149.

Hilgers, A. R., R. A. Conradi, et al. (1990). "Caco-2 cell monolayers as a model for drug transport across the intestinal mucosa." Pharmaceutical Research **7**(9): 902-910.

Horter, D. and J. B. Dressman (2001). "Influence of physicochemical properties on dissolution of drugs in the gastrointestinal tract." Advanced Drug Delivery Reviews **46**(1-3): 75-87.

Hu, B., C. L. Pan, et al. (2008). "Optimization of fabrication parameters to produce chitosan-tripolyphosphate nanoparticles for delivery of tea catechins." Journal of Agricultural and Food Chemistry **56**(16): 7451-7458.

Inada, H., N. Nakagawa, et al. (1990). "Effect of the binary ethanol water solvent on the in-vitro skin permeation of nifedipine." Yakuzaigaku **50**(1): 35-41.

Inoue, M. B., M. Inoue, et al. (2002). "Potentiometric and (1)H NMR studies of complexation of Al(3+) with (-)-epigallocatechin gallate, a major active constituent of green tea." Journal of Inorganic Biochemistry **88**(1): 7-13.

Irvine, J. D., L. Takahashi, et al. (1999). "MDCK (Madin-Darby canine kidney) cells: A tool for membrane permeability screening." Journal of Pharmaceutical Sciences **88**(1): 28-33.

J. A. Ruell, A. A., C. Du, K. Tsinman. (2002). "A simple PAMPA filter for passively absorbed compounds.", from http://www.pion-inc.com/images/simplePAMPAfilter1.pdf.

Kajiya, K., H. Hojo, et al. (2004). "Relationship between antibacterial activity of (+)-catechin derivatives and their interaction with a model membrane." Journal of Agricultural and Food Chemistry **52**(6): 1514-1519.

Kamp, F. and J. A. Hamilton (2006). "How fatty acids of different chain length enter and leave cells by free diffusion." Prostaglandins Leukotrienes and Essential Fatty Acids **75**(3): 149-159.

Kansy, M., F. Senner, et al. (1998). "Physicochemical high throughput screening: Parallel artificial membrane permeation assay in the description of passive absorption processes." Journal of Medicinal Chemistry **41**(7): 1007-1010.

Kararli, T. T. (1995). "Comparison of the gastrointestinal anatomy, physiology, and biochemistry of humans and commonly used laboratory animals." Biopharmaceutics & Drug Disposition **16**(5): 351-380.

Katiyar, S., C. A. Elmets, et al. (2007). "Green tea and skin cancer: photoimmunology, angiogenesis and DNA repair." Journal of Nutritional Biochemistry **18**(5): 287-296.

Kelder, J., P. D. J. Grootenhuis, et al. (1999). "Polar molecular surface as a dominating determinant for oral absorption and brain penetration of drugs." Pharmaceutical Research **16**(10): 1514-1519.

Kiselev, M. A., P. Lesieur, et al. (1999). "DMSO-induced dehydration of DPPC membranes studied by X-ray diffraction, small-angle neutron scattering, and calorimetry." Journal of Alloys and Compounds **286**(1-2): 195-202.

Knight, C. G., Ed. (1981). Liposomes: From physical structure to therapeutic applications. Research monographs in cell and tissue physiology. Cambridge, Elsevier.

Kobayashi, Y., T. Komatsu, et al. (2004). "In vitro permeation of several drugs through the human nail plate: relationship between physicochemical properties and nail permeability of drugs." European Journal of Pharmaceutical Sciences **21**(4): 471-477.

Koenig, B. W. and K. Gawrisch (2005). "Lipid-ethanol interaction studied by NMR on bicelles." Journal of Physical Chemistry B **109**(15): 7540-7547.

Komatsu, H. and S. Okada (1995). "Ethanol-induced aggregation and fusion of small phosphatidylcholine liposome-participation of interdigitated membrane formation in their processes." Biochimica Et Biophysica Acta-Biomembranes **1235**(2): 270-280.

Kraljevic, S., P. J. Stambrook, et al. (2004). "Accelerating drug discovery - Although the evolution of '-omics' methodologies is still in its infancy, both the pharmaceutical industry and patients could benefit from their implementation in the drug development process." Embo Reports **5**(9): 837-842.

Kuriharabergstrom, T., K. Knutson, et al. (1990). "Percutaneous-absorption enhancement of anionic molecule by ethanol water-systems in human skin." Pharmaceutical Research **7**(7): 762-766.

Kuzuhara, T., M. Suganuma, et al. (2008). "Green tea catechin as a chemical chaperone in cancer prevention." Cancer Letters **261**(1): 12-20.

Lambert, J. D., J. G. Hong, et al. (2004). "Piperine enhances the bioavailability of the tea polyphenol (-)-epigallocatechin-3-gallate in mice." Journal of Nutrition **134**(8): 1948-1952.

Lambert, J. D., S. M. Sang, et al. (2006). "Peracetylation as a means of enhancing in vitro bioactivity and bioavailability of epigallocatechin-3-gallate." Drug Metabolism and Disposition **34**(12): 2111-2116.

Leahy, D. E., P. J. Taylor, et al. (1989). "Model solvent systems for QSAR. 1. Propylene-glycol dipelargonate (PGDP)-a new standard solvent for use in partition-coefficient determination." Quantitative Structure-Activity Relationships **8**(1): 17-31.

Lee, P. H., S. N. Ayyarnpalayarn, et al. (2007). "In silico prediction of ionization constants of drugs." Molecular Pharmaceutics **4**(4): 498-512.

Lennernas, H. (1997). "Human jejunal effective permeability and its correlation with preclinical drug absorption models." Journal of Pharmacy and Pharmacology **49**(7): 627-638.

Lennernas, H. (1998). "Human intestinal permeability." Journal of Pharmaceutical Sciences **87**(4): 403-410.

Liang, X. M., G. Z. Mao, et al. (2004). "Mechanical properties and stability measurement of cholesterol-containing liposome on mica by atomic force microscopy." Journal of Colloid and Interface Science **278**(1): 53-62.

Lipinski, C. A., F. Lombardo, et al. (1997). "Experimental and computational approaches to estimate solubility and permeability in drug discovery and development settings." Advanced Drug Delivery Reviews **23**(1-3): 3-25.

Liu, M. (2010). Understanding the Mechanical strength of Microcapsules and Their Adhesion on Fabric Surfaces. School of Chemical Engieering. Birmingham, University of Birmingham. **Doctor of Philosophy:** 281.

Lombardo, F., M. Y. Shalaeva, et al. (2001). "ElogD(oct): A tool for lipophilicity determination in drug discovery. 2. Basic and neutral compounds." Journal of Medicinal Chemistry **44**(15): 2490-2497.

Lundahl, P. and F. Beigi (1997). "Immobilized liposome chromatography of drugs for model analysis of drug-membrane interactions." Advanced Drug Delivery Reviews **23**(1-3): 221-227.

Ma, Q. H., Q. Xia, et al. (2007). Preparation of tea polyphenols-loaded solid lipid nanoparticles based on the phase behaviors of hot microemulsions. Nanoscience and Technology, Pts 1 and 2. C. Bai, S. Xie and X. Zhu. Stafa-Zurich, Trans Tech Publications Ltd. **121-123:** 705-708.

Madara, J. L. (1998). "Regulation of the movement of solutes across tight junctions." Annual Review of Physiology **60**: 143-159.

Madene, A., M. Jacquot, et al. (2006). "Flavour encapsulation and controlled release - a review." International Journal of Food Science and Technology **41**(1): 1-21.

Malvern. (2012). "Dynamic Light Scattering (DLS) ", from http://www.malvern.com/labeng/technology/dynamic_light_scattering/dynamic_light_scattering.htm.

Mandagere, A. K., T. N. Thompson, et al. (2002). "Graphical model for estimating oral bioavailability of drugs in humans and other species from their caco-2 permeability and in vitro liver enzyme metabolic stability rates." Journal of Medicinal Chemistry **45**(2): 304-311.

Matsson, P., C. A. S. Bergstrom, et al. (2005). "Exploring the role of different drug transport routes in permeability screening." Journal of Medicinal Chemistry **48**(2): 604-613.

Mehta, A. (2011). "Ultraviolet-Visible (UV-Vis) Spectroscopy – Principle." from http://pharmaxchange.info/press/2011/12/ultraviolet-visible-uv-vis-spectroscopy-principle/.

Mellema, M. (2007). Scope and limitations of using wax to encapsulate water-soluble compounds. Food Colloids: Self-Assembly and Material Science. E. Dickinson and M. E. Leser. Cambridge, Royal Soc Chemistry. **302:** 103-115.

Mellema, M., W. A. J. Van Benthum, et al. (2006). "Wax encapsulation of water-soluble compounds for application in foods." Journal of Microencapsulation **23**(7): 729-740.

Moser, K., K. Kriwet, et al. (2001). "Passive skin penetration enhancement and its quantification in vitro." European Journal of Pharmaceutics and Biopharmaceutics **52**(2): 103-112.

Nakagawa, K., S. Okuda, et al. (1997). "Dose-dependent incorporation of tea catechins, (-)-epigallocatechin-3-gallate and (-)-epigallocatechin, into human plasma." Bioscience Biotechnology and Biochemistry **61**(12): 1981-1985.

Nance, C. L. and W. T. Shearer (2003). "Is green tea good for HIV-1 infection?" Journal of Allergy and Clinical Immunology **112**(5): 851-853.

Pagliara, A., M. Reist, et al. (1999). "Evaluation and prediction of drug permeation." Journal of Pharmacy and Pharmacology **51**(12): 1339-1357.

Palm, K., P. Stenberg, et al. (1997). "Polar molecular surface properties predict the intestinal absorption of drugs in humans." Pharmaceutical Research **14**(5): 568-571.

Parrott, N. and T. Lave (2002). "Prediction of intestinal absorption: comparative assessment of GASTROPLUS (TM) and IDEA (TM)." European Journal of Pharmaceutical Sciences **17**(1-2): 51-61.

Patra, M., E. Salonen, et al. (2006). "Under the influence of alcohol: The effect of ethanol and methanol on lipid bilayers." Biophysical Journal **90**(4): 1121-1135.

Paula, S., A. G. Volkov, et al. (1996). "Permeation of protons, potassium ions, and small polar molecules through phospholipid bilayers as a function of membrane thickness." Biophysical Journal **70**(1): 339-348.

Pauletti, G. M. and H. Wunderliallenspach (1994). "Partition-coefficients in-vitro-Artificial membranes as a standardized distribution model." European Journal of Pharmaceutical Sciences **1**(5): 273-282.

Pershing, L. K., B. S. Silver, et al. (1992). "Feasibility of measuring the bioavailability of topical betamethasone dipropionate in commercial formulations using drug content in skin and a skin blanching bioassay" Pharmaceutical Research **9**(1): 45-51.

Petty, H. R. (1993). Molecular biology of membranes: structure and function, Plenum.

Pietta, P. G., P. Simonetti, et al. (1998). "Catechin metabolites after intake of green tea infusions." Biofactors **8**(1-2): 111-118.

Pinto, M., S. Robineleon, et al. (1983). "Enterocyte-like differentiation and polarization of the human-colon carcinoma cell-line Caco-2 in culture." Biology of the Cell **47**(3): 323-330.

Platts, J. A. (2000). "Theoretical prediction of hydrogen bond donor capacity." Physical Chemistry Chemical Physics **2**(5): 973-980.

Potts, R. O. and R. H. Guy (1992). "Predicting skin permeability " Pharmaceutical Research **9**(5): 663-669.

Potts, R. O. and R. H. Guy (1993). "The influence of molecular volume and hydrogen-bonding on peptide-transport across epithelial membranes." Pharmaceutical Research **10**(4): 635-636.

Quorum. (2001). "Cryo-SEM Preparation Techniques and Advantages." from http://www.quorumtech.com/applications/techniques-and-advantages/cryo-sem-techniques-and-advantages.html.

Raghuvanshi, R. S., K. P. Tripathi, et al. (1992). "Release kinetics of salbutamol sulfate from wax coated microcapsules and tabletted microcapsules." Journal of Microencapsulation **9**(4): 449-455.

Ranjha, N. M., H. Khan, et al. (2010). "Encapsulation and characterization of controlled release flurbiprofen loaded microspheres using beeswax as an encapsulating agent." Journal of Materials Science-Materials in Medicine **21**(5): 1621-1630.

Rastogi, S. C. (2007). Cell Biology, New Age International.

Rebecca Notman, M. N., Brendan O'Malley, Jamshed Anwar (2006). "Molecular Basis for Dimethylsulfoxide (DMSO) Action on Lipid Membranes." J. AM. CHEM. SOC(128): 13982-13983.

Sambuy, Y., I. Angelis, et al. (2005). "The Caco-2 cell line as a model of the intestinal barrier: influence of cell and culture-related factors on Caco-2 cell functional characteristics." Cell Biology and Toxicology **21**(1): 1-26.

Semenov, V. V. (1989). Archeological and forensic science biological object search - by using ultraviolet radiation of prescribed energy density and recording phosphorescence signal

on colour reversible film. Derwent Innovations Index. Soviet Union Semenov, V V (SEME-Individual)**:** 5.

Shah, V. P., Y. Tsong, et al. (1998). "In vitro dissolution profile comparison - Statistics and analysis of the similarity factor, f(2)." Pharmaceutical Research **15**(6): 889-896.

Siissalo, S., L. Laine, et al. (2010). "Caco-2 cell monolayers as a tool to study simultaneous phase II metabolism and metabolite efflux of indomethacin, paracetamol and 1-naphthol." International Journal of Pharmaceutics **383**(1-2): 24-29.

Singer, S. J. and G. L. Nicolson (1972). "Fluid mosaic model of structure of cell-membranes." Science **175**(4023): 720-&.

Sirk, T. W., E. F. Brown, et al. (2009). "Molecular Binding of Catechins to Biomembranes: Relationship to Biological Activity." Journal of Agricultural and Food Chemistry **57**(15): 6720-6728.

Sirk, T. W., E. F. Brown, et al. (2008). "Molecular dynamics study on the biophysical interactions of seven green tea catechins with lipid bilayers of cell membranes." Journal of Agricultural and Food Chemistry **56**(17): 7750-7758.

Stegemann, S., F. Leveiller, et al. (2007). "When poor solubility becomes an issue: From early stage to proof of concept." European Journal of Pharmaceutical Sciences **31**(5): 249-261.

Stein, W. D. (1986). Transport and diffusion across cell membranes, Academic press, Inc.

Stewart, B. H., O. H. Chan, et al. (1997). "Discrimination between drug candidates using models for evaluation of intestinal absorption." Advanced Drug Delivery Reviews **23**(1-3): 27-45.

Straube, A., B. Aicher, et al. (2011). "Combined analgesics in (headache) pain therapy: shotgun approach or precise multi-target therapeutics?" Bmc Neurology **11**:43-58.

Su, Y. L., L. K. Leung, et al. (2003). "Stability of tea theaflavins and catechins." Food Chemistry **83**(2): 189-195.

Sugano, K., H. Hamada, et al. (2001). "High throughput prediction of oral absorption: Improvement of the composition of the lipid solution used in parallel artificial membrane permeation assay." Journal of Biomolecular Screening **6**(3): 189-196.

Sugano, K., Y. Nabuchi, et al. (2003). "Prediction of human intestinal permeability using artificial membrane permeability." International Journal of Pharmaceutics **257**(1-2): 245-251.

Sum, A. K. and J. J. de Pablo (2003). "Molecular simulation study on the influence of dimethylsulfoxide on the structure of phospholipid bilayers." Biophysical Journal **85**(6): 3636-3645.

Tavelin, S., J. Taipalensuu, et al. (2003). "Prediction of the oral absorption of low-permeability drugs using small intestine-like 2/4/A1 cell monolayers." Pharmaceutical Research **20**(3): 397-405.

Tester, C. C., R. E. Brock, et al. (2011). "In vitro synthesis and stabilization of amorphous calcium carbonate (ACC) nanoparticles within liposomes." Crystengcomm **13**(12): 3975-3978.

Uekusa, Y., Y. Takeshita, et al. (2008). "Partition Coefficients of Polyphenols for Phosphatidylcholine Investigated by HPLC with an Immobilized Artificial Membrane Column." Bioscience Biotechnology and Biochemistry **72**(12): 3289-3292.

UK, R. C. (2011). "Antibiotic progress for disease that causes half a million deaths a year." from http://www.stfc.ac.uk/News+and+Events/24795.aspx.

Uner, M., U. Gonullu, et al. (2005). "A new approach for preparing a controlled release ketoprofen tablets by using beeswax." Farmaco (Lausanne) **60**(1): 27-31.

Veber, D. F., S. R. Johnson, et al. (2002). "Molecular properties that influence the oral bioavailability of drug candidates." Journal of Medicinal Chemistry **45**(12): 2615-2623.

von Heijne, G. and D. Rees (2008). "Membranes: reading between the lines." Current Opinion in Structural Biology **18**(4): 403-405.

Walter, A. and J. Gutknecht (1986). "Permeability of small nonellectrolytes through lipid bilayer-membranes." Journal of Membrane Biology **90**(3): 207-217.

Watkinson, R. M., C. Herkenne, et al. (2009). "Influence of Ethanol on the Solubility, Ionization and Permeation Characteristics of Ibuprofen in Silicone and Human Skin." Skin Pharmacology and Physiology **22**(1): 15-21.

Williams, A. C. and B. W. Barry (2004). "Penetration enhancers." Advanced Drug Delivery Reviews **56**(5): 603-618.

Williamson, M. P., T. G. McCormick, et al. (2006). "Epigallocatechin gallate, the main polyphenol in green tea, binds to the T-cell receptor, CD4: Potential for HIV-1 therapy." Journal of Allergy and Clinical Immunology **118**(6): 1369-1374.

Wohnsland, F. and B. Faller (2001). "High-throughput permeability pH profile and high-throughput alkane/water log P with artificial membranes." Journal of Medicinal Chemistry **44**(6): 923-930.

Xiang, T. X. and B. D. Anderson (1994). "The relationship between permeant size and permeability in lipid bilayer membranes." Journal of Membrane Biology **140**(2): 111-122.

Xuemei Liang, G. M., K.Y. Simon Ng (2004). "Mechanical properties and stability measurement of cholesterol-containing liposome on mica by atomic force microscopy." Colloid and Interface Science (278): 53-62.

Yamaguchi, K., M. Honda, et al. (2002). "Inhibitory effects of (-)-epigallocatechin gallate on the life cycle of human immunodeficiency virus type 1 (HIV-1)." Antiviral Research **53**(1): 19-34.

Yamashita, S., T. Furubayashi, et al. (2000). "Optimized conditions for prediction of intestinal drug permeability using Caco-2 cells." European Journal of Pharmaceutical Sciences **10**(3): 195-204.

Yang, C. S., J. Y. Chung, et al. (2000). "Tea and tea polyphenols in cancer prevention." Journal of Nutrition **130**(2): 472S-478S.

Yang, C. S. and Z. Y. Wang (1993). "Tea and cancer." Journal of the National Cancer Institute **85**(13): 1038-1049.

Yazdanian, M., S. L. Glynn, et al. (1998). "Correlating partitioning and Caco-2 cell permeability of structurally diverse small molecular weight compounds." Pharmaceutical Research **15**(9): 1490-1494.

Young, R. C., R. C. Mitchell, et al. (1988). "Development of a new physicochemical model for brain penetration and its application to the design of centrally acting H-2-receptor histamine-antagonists." Journal of Medicinal Chemistry **31**(3): 656-671.

Yvon, H. J. "Raman spectroscopy for analysis and monitoring." from http://www.horiba.com/fileadmin/uploads/Scientific/Documents/Raman/bands.pdf.

Zakeri-Milani, P., H. Valizadeh, et al. (2007). "Predicting human intestinal permeability using single-pass intestinal perfusion in rat." Journal of Pharmacy and Pharmaceutical Sciences **10**(3): 368-379.

Zhu, C. Y., L. Jiang, et al. (2002). "A comparative study of artificial membrane permeability assay for high throughput profiling of drug absorption potential." European Journal of Medicinal Chemistry **37**(5): 399-407.